CHARACTERIZATION AND PROCESSING OF LIGNOCELLULOSIC BIOMASS IN IONIC LIQUIDS

By

Michael Anthony FitzPatrick

A thesis submitted to the Department of Chemical Engineering

In conformity with the requirements for the degree of Master of Applied Science

Queen's University

Kingston, Ontario, Canada

(May, 2011)

Abstract

In the last decade there has been increasing research interest in the value of bio-sourced materials from lignocellulosic biomass. The dissolution of cellulose by ionic liquids (ILs) has led to investigations including the dissolution of cellulose, lignin, and complete biomass samples and the *in situ* processing of cellulose. Rapid quantitative measurement of cellulose dissolution in ILs is difficult. In this work, Fourier transform infrared spectroscopy (FTIR) spectra of cellulose dissolved in 1-ethyl-3-methylimidazolium acetate ([emim][OAc]) were subjected to partial least squares (PLS) regression to model dissolved cellulose content. PLS regression was used due to the ease in developing predictive models with this technique in addition to linear regression being ineffectual for modeling when applied to potentially thousands of variables. Applying a normalization data treatment, before regression, generated a model that estimated cellulose content within 0.533 wt%. The methods described provided the basis for a rapid methodology to determine dissolved cellulose content.

Development of rapid and facile screening techniques to determine the effectiveness of various ILs as solvents for cellulose or lignin will aid in the development of lignocellulosic based bioproducts. In this work, optical microscopy with and without the use of cross-polarized lenses, was used to monitor cellulose and lignin dissolution in two imidazolium-based and two phosphonium-based ILs as well as n,n-dimethylacetamide/lithium chloride (DMAc/LiCl), demonstrating that this technique could be applied more broadly than solely for ILs. The described optical microscopy methodology was more rapid and sensitive than more traditional techniques, such as visual inspection.

The viscosity of [emim][OAc] (162 cP) is 100 times that of water at 20°C and could inhibit its use as a solvent for cellulose. There is a need for simple, low-cost and environmentally benign methods to reduce the viscosity of ILs to aid in cellulose dissolution. In this work, 4 wt%

cellulose dissolved in [emim][OAc] was subjected to 50 psi CO_2 and 20 psi N_2, as a control environment, at both 50°C and 75°C. After 24 hours a nearly 2-fold increase in dissolved cellulose over the N_2 control was demonstrated through the application of a 50 psi CO_2 environment for cellulose dissolution in [emim][OAc] at 50°C.

Statement of Co-Authorship

I wrote the first version of all manuscripts presented in this thesis. Dr. Champagne and Dr. Cunningham edited all of manuscripts to improve the writing, organization, content, and to enhance the understanding of the technical findings.

I was responsible for determining the topic and aim of the review paper (Chapter 2) as well as for the creation of Figure 2.1. Dr. Champagne and Dr. Cunningham helped revise the scope of the manuscript to ensure that it addressed the appropriate literature. Additionally, Dr. Whitney edited the manuscript to help improve the writing and offered technical insights.

In Chapter 4 of this thesis, I was responsible for the creation of all calibration and validation standards, conducting all ATR FTIR, PLS regression on the resulting spectra and application of all data preprocessing techniques to the aforementioned spectra.

In Chapter 5 of this thesis, I was responsible for the idea that optical microscopy could be used to screen solvents for biomass dissolution. In addition, I prepared all dissolution experiments and conducted all microscopy. Charlene Falkenburger provided insight into how best to prepare the samples for dissolution experiments and microscopic analysis, as well as guidance in determining the length of time required for the dissolution experiments.

For Chapter 6 of this thesis, I was responsible for suggesting that CO_2 at subcritical pressures be investigated to decrease IL viscosity and for determining which pressures and temperatures would be investigated in this study. I conducted all dissolution experiments, preformed all cellulose regeneration, and carried out all gravimetric and TGA analysis as well as CrI calculations. Mr. Alan Grant prepared samples for and collected all XRD spectra.

Acknowledgements

Firstly, and most importantly, I would like to thank my supervisors, Drs. Michael Cunningham and Pascale Champagne. Their passion and vision for innovative research is an asset to the scientific community and was a real inspiration to myself. I would like to thank them for having the confidence in me to explore a new area and for having the patience and giving me the support needed to complete my thesis. I have been lucky to have had them both as my co-supervisors.

I would like to thank the staff at Queen's University for their help during my thesis. Barb Lawson for always having an answer to the unending stream of questions; Maureen Plunkett for all the chocolates!; and Steve Hodgson, Kelly Sedore, and Dr. Andrea Liskova for their help in setting up lab equipment, experimental procedures, and analytics. I would like to thank Drs. Brian Amsden and Dale Marecak for assistance with the IR spectrometer. I would also like to thank Cytec Canada Inc. and Dr. Serguei Zavorine for providing the phosphonium-based ILs (CYPHOS® 109 and CYPHOS® 441) for the optical microscopy work. I would also like to thank Dr. Andrea Liskova and Alan Grant for their help with conducting TGA and XRD analysis, respectively, for the carbon dioxide study.

I would like to thank my lab mate, Daniel Krasznai, for his support in the lab and insightful discussions. Without his suggestions and help setting up the lab none of this work would have been possible. For this I am truly grateful. I would also like to thank our undergraduate student, Charlene Falkenburger, for her companionship in the lab and for allowing me and trusting me to be involved with her project.

I would like to thank the friends whose friendship was made, or made stronger, in our time at Queen's. Adam Hepburn for the late night and lunchtime lab breaks; Andrew Evans and

iv

Table of Contents

List of Figures

List of Tables

List of Abbreviations

1-Alkyl-3-Methylimidazolium Chloride	[amim]Cl
American Society of Testing and Materials	ASTM
Attenuated Total Reflectance	ATR
Atom-Transfer Radical Polymerization	ATRP
1-Butyl-2,3-Dimethylimidazolium Tetrafluoroborate	[bm$_2$im][BF$_4$]
1-Butyl-3-Methylimidazolium Tetrafluoroborate	[bmim][BF$_4$]
1-Butyl-3-Methylimidazolium Bromide	[bmim]Br
1-Butyl-3-Methylimidazolium Trifluoromethanesulfonate	[bmim][CF3SO3]
1-Butyl-3-Methylimidazolium Chloride	[bmim]Cl
1-Butyl-3-Methylimidazolium Methylsulfate	[bmim][MeSO$_4$]
1-Butyl-3-Methylimidazolium Acetate	[bmim][OAc]
1-Butyl-3-Methylimidazolium Hexafluoroborate	[bmim][PF$_6$]
1-Butyl-3-Methylimidazolium Thiocyanate	[bmim][SCN]
1-Butyl-3-Methylpyridinium Chloride	[bmpy]Cl
1-Butyl-4-Methylpyridinium Hexafluorophosphate	[bmpy][PF$_6$]
1-Methyl-3-Benzylimidazolium Chloride	[bzmim]Cl
1-Methyl-3-Benzylimidazolium Dicyanamide	[bzmim][Dca]
1-Methyl-3-M-Methoxylbenzylimidazolium Chloride	[bz-ome-mim]Cl
Carbon Monoxide	CO
Carbon Dioxide	CO$_2$
Canadian Pulp and Paper Association	CPPA
Chromium (II) Chloride	CrCl$_2$
Crystallinity Index	CrI
Cellulose Solvent-Based Lignocellulosic Fractionation	CSLF
Trihexyl(tetradecyl)phosphonium Bis(trifluoromethylsulfonyl)imide	CYPHOS® 109
Tetrabutylphosphonium Acetate	CYPHOS® 441
N,N-Dimethylacetamide/Lithium Chloride	DMAc/LiCl
Dimethyl Sulfoxide	DMSO
Dinitrosalicylic Acid	DNS
Degree of Polymerization	DP
1,3-Dimethylimidazolium-Dimethylphosphate	ECOENG
1-Ethyl-3-Methylimidazolium Chloride	[emim]Cl

1-Ethyl-3-Methylimidazolium Diethyl Phosphate	[emim][Et$_2$PO$_4$]
1-Ethyl-3-Methylimidazolium Acetate	[emim][OAc]
Fourier Transform Infrared Spectroscopy	FTIR
Gel-Permeation Chromatography	GPC
Sulfuric Acid	H$_2$SO$_4$
Hydrochloric Acid	HCl
5-Hydroxymethyl Furfural	HMF
1-Hexyl-3-Methylimidazolium Trifluoromethanesulfonate	[hmim][CF$_3$SO$_3$]
Nitric Acid	HNO$_3$
High Performance Liquid Chromatography	HPLC
Ionic Liquid	IL
Lateral Order Index	LOI
1,3-Dimethylimidazolium Methylsulfate	[mmim][MeSO$_4$]
Multiplicative Scatter Correction	MSC
Sodium Hydroxide	NaOH
Near Infrared Spectroscopy	NIR
Nuclear Magnetic Resonance Spectroscopy	NMR
Polyethylene Terephthalate	PET
Polyhydroxyalkanoate	PHA
Partial Least Squares	PLS
1-Propyl-3-Methylimidazolium Bromide	[propylmim]Br
Root Mean Squared Error	RMSE
Root Mean Squared Error of Prediction	RMSEP
Size-Exclusion Chromatography	SEC
Steam Exploded Wheat Straw	SEWS
Standard Normal Variate	SNV
Technical Association of the Pulp and Paper Industry	TAPPI
Total Crystallinity Index	TCI
Trifluoroacetic Acid	TFA
Thermogravimetric Analysis	TGA
Thermomechanical Pulp	TMP
Total Reducing Sugar	TRS
Ultraviolet-Visible Spectroscopy	UV- Vis
X-Ray Diffraction	XRD

Chapter 1
Introduction

1.1 Background

In 2004, with the acknowledgement of rising oil prices, the US Department of Energy identified twelve chemicals, derived from the biological conversion of biomass, that could be used as building block chemicals in a bio-based economy (PNNL/NREL, 2004). Canada is primed to take advantage of the burgeoning bio-based economy due to its abundance of biomass. Approximately 35-50 wt% lignocellulosic biomass is comprised of cellulose, making cellulose the most abundant biopolymer on earth (Bhat and Bhat, 1997; Reddy and Yang, 2005; van Haveren et al., 2008; Zhang, 2008). Additionally, lignin may be a potentially valuable source of aromatic compounds due to its complex aromatic structure (FitzPatrick et al., 2010; Mohanty et al., 2000; Zavrel et al., 2009; Zhang and Lynd, 2004). However, lignocellulosic biomass is resistant to hydrolysis due to inter- and intramolecular bonds present between cellulose fibers and the complex three-dimensional structure of lignocellulosic biomass species (Huber and Dumesic, 2006; Mosier et al., 2005; Zhbankov, 1992).

The main stumbling blocks of biomass processing are the high costs and low yields of current hydrolysis and pretreatment processes (Champagne, 2007; da Costa Sousa et al., 2009). As a result, considerable pretreatment research efforts, aimed at developing techniques to enable processing of this valuable resource, have been undertaken (FitzPatrick et al., 2010; Lynd et al., 2002). Novel pretreatment and fractionation methods using ionic liquids (ILs) have made new approaches to biomass utilization possible (Fort et al., 2007).

1.2 Motivation

ILs are considered "alternative solvents" due to their high thermal stability and usually negligible vapor pressure, and can be specifically designed since there is nearly an infinite combination of anions and cations that can be used in their synthesis (Fort et al., 2007; Lee et al., 2008). In general, commercially available ILs are currently produced only on the laboratory scale, thus they are very expensive (sometimes upwards of $1000 per kg of IL) (Joglekar et al., 2007). As demand for ILs increases, commercial-scale production of ILs may begin, reducing the cost of ILs. The economical production of existing and/or novel ILs is imperative to further the use of ILs commercially as solvents (Cao et al., 2009; Zhu et al., 2006).

It has been demonstrated that both cellulose and lignin dissolve in a range of ILs and, perhaps more importantly, can be readily regenerated from these solutions (Fort et al., 2007). ILs have been shown to disrupt the aforementioned hydrogen bonding network in lignocellulosic biomass (Swatloski et al., 2002; Zavrel et al., 2009). Additionally, the π-π electron interactions that occur between the cations of ILs and lignin may also enhance lignocellulose dissolution (Kilpeläinen et al., 2007; Zavrel et al., 2009). In order to assess the potential of a particular IL for biomass dissolution, visual inspection of the IL/cellulose and/or lignin solution has been traditionally employed (Heinze et al., 2005; Kilpeläinen et al., 2007; Köhler et al., 2007; Pu et al., 2007). However, in some cases visual inspection may not be sufficient and optical microscopy offers more sensitivity for evaluating biomass dissolution. Infrared spectroscopy has also been used to analyze biomass samples, including the study of change in crystallinity and structural characteristics between different cellulose sources (Hurtubise and Krassig, 1960; Nelson and O'Connor, 1964a; Nelson and O'Connor, 1964b). Fourier transform infrared spectroscopy (FTIR) has been used for compositional analysis of potential biomass feedstocks (Hames et al., 2003; Moore and Owen, 2001). Moreover, when compared to traditional wet chemical methods for compositional analysis, FTIR has the potential to be far lower in cost (~$10 per sample as opposed to $800-$2000 per sample, even with 100 calibration standards) and much more rapid

(within a day as opposed to results taking days, or even weeks), while still able to determine the composition of corn stover, specifically the cellulose component, within 1.4 wt% (Hames et al., 2003). The quantitative determination of α-D-glucose, the repeating monomer in starch, in an IL has also been studied via FTIR (Kiefer et al., 2008). The screening of novel ILs and IL/cellulose and lignin dissolution approaches, at lower costs than current methods, are paramount to the continuing evolution of value-added lignocellulosic biomass processing research.

The IL, 1-ethyl-3-methylimidazolium acetate ([emim][OAc]), has been shown to dissolve lignin, cellulose and wood flour under relatively mild conditions (temperatures ranging from 40°C to 100°C) (Zavrel et al., 2009). [emim][OAc] has also been used to facilitate the functionalization of cellulose to cellulose acetate, industrially relevant due to its wide commercial appeal, by 2-furoyl chloride (Köhler et al., 2007). However, the viscosity of [emim][OAc] may hinder its use in cellulose processing. The viscosity of [emim][OAc], 162 cP at 20°C (Bonhote et al., 1996), has been shown to increase with cellulose dissolution in the IL (Gericke et al., 2009; Hermanutz et al., 2008; Song et al., 2010).

Aki et al. (2004) showed that, in general, ILs only dissolve moderate amounts of CO_2 (less than 10 mol% at 60°C under an approximately 50 psi CO_2 environment). This resulted in only slight corresponding IL volume expansions (<10% at up to 30 mol% CO_2). Polarity and the accepting and donating of hydrogen-bonds, properties important to cellulose dissolution, are not changed by CO_2 dissolution in ILs (Fredlake et al., 2004; Jessop and Subramaniam, 2007). Additionally, the viscosity of ILs has been shown to change with CO_2 dissolution. For example, Liu et al. (2003) observed that the viscosity of [bmim][PF_6] decreased by nearly 50% upon the dissolution of 30 mol% CO_2 at 50°C. The investigation of subcritical CO_2 as a means to reduce the viscosity of IL/cellulose solutions represents a simple, inexpensive, and environmentally benign method to overcome slow dissolution kinetics associated with high viscosity. Furthermore, this approach to reducing the viscosity of IL/cellulose solutions could potentially

reduce the cost of using ILs for cellulose dissolution through more rapid dissolution times and reducing the dissolution temperature.

1.3 Overview of the Thesis

1.3.1 Objectives

The research conducted for this thesis focused on developing solutions to two key problems that inhibit the use of ILs for the processing of biomass. ILs have frequently been investigated as solvents for the dissolution of cellulose, lignin and lignocellulose in the last ten years (Swatloski et al., 2002; Zavrel et al., 2009; Zhu et al., 2006). Additionally, they have been used in the functionalization of cellulose and production of value-added chemicals from lignin (Cao et al., 2009; Feng and Chen, 2008; Zakzeski et al., 2010). However, research aimed at the discovery of novel ILs and IL/cellulose and lignin dissolution approaches would benefit from simple and reliable characterization and quantitative analytical techniques (Joglekar et al., 2007). Thus, the first goal of this research addressed the need for simple, rapid and inexpensive techniques to screen and quantitatively monitor the dissolution of biomass, with a focus on cellulose and lignin, in ILs. Initial studies focused on the development of a method to quantitatively monitor cellulose dissolution in an IL. For this work up to 4 wt% cellulose was dissolved in [emim][OAc] since cellulose has been shown to readily dissolve in this IL at this loading (Zavrel et al., 2009). Subsequent work focused on the development of a simple and inexpensive method to qualitatively screen for cellulose and lignin dissolution in four ILs, while the robustness of this method was demonstrated by screening using a non-IL solvent.

The viscosity of most ILs may inhibit their use as solvents for cellulose and lignin. This problem is amplified with increasing cellulose dissolution in ILs. Specifically, the IL 1-ethyl-3-methylimidazolium acetate ([emim][OAc]), although less viscous than many ILs at room temperature, has a dynamic viscosity at 20°C that is two orders of magnitude greater than water (Bonhote et al., 1996). To overcome this issue, ILs are typically diluted with an organic solvent

4

that does not dissolve cellulose, often dimethyl sulfoxide (DMSO). However, large volumes of DMSO are necessary ($\geq$15 wt% in 5 wt% biomass dissolutions), which can be combustible and further increase the cost of using ILs to dissolve biomass (Fort et al., 2007). Thus, the second objective of this work was the investigation of a simple, low cost and environmentally benign method using CO_2 to reduce the viscosity of IL/cellulose solutions.

1.3.2 Scope and Organization of Thesis

Chapter 2 and Chapter 3 of this thesis provide an overview of the literature pertinent to the research presented in this thesis. Chapter 2 presents a summary of the literature aimed at developing value-added materials and chemicals from lignocellulosic biomass. The chapter presents advances in lignocellulosic biomass processing and analysis, as well as existing industrial biomass processing applications, within a biorefining context. Chapter 3 provides an outline of the raw materials and characterization techniques available for use in a biorefinery context. In addition ILs, including properties important for biomass dissolution, are discussed.

Chapter 4 focuses on addressing the first objective of this thesis by outlining the development of a facile, rapid and inexpensive method to quantitatively determine cellulose dissolved in an IL. FTIR, operated in attenuated total reflectance (ATR) mode, was employed to generate spectra of 0-4 wt% cellulose dissolved in [emim][OAc]. PLS regression was applied to the spectra to quantitatively determine the amount of cellulose dissolved in [emim][OAc]. Additionally, data preprocessing techniques were applied to enhance the predictive capability of the models. The effect of different data preprocessing techniques on the prediction of cellulose content was explored.

Once a method to quantitatively analyze cellulose content in IL/cellulose solutions was established, a simple and environmentally benign technique to screen ILs for the dissolution of cellulose and lignin was explored. In Chapter 5 an optical microscopy method was used to

monitor cellulose and lignin dissolution in four ILs (2 imidazolium-based and 2 phosphonium-based), as well as non-IL DMAc/LiCl, to establish a facile rapid screening methodology.

Developing a simple, low-cost method to decrease the viscosity of IL/cellulose solutions, without limiting the dissolution of cellulose was the intent of the study presented in Chapter 6. After the characterization techniques were developed, an approach to overcome the high viscosity of IL/cellulose was proposed. The effect of 50 psi CO_2 on the dissolution of 4 wt% cellulose in [emim][OAc] was studied at 50°C and 75°C for up to 24 hours and compared to a 20 psi N_2 control environment.

Finally, Chapter 7 summarizes the findings and recommendations for future work of this thesis.

1.4 References

Aki, S.N.V.K., B.R. Mellein, E.M. Saurer, J.F. Brennecke, 2004. High-pressure phase behavior of carbon dioxide with imidazolium-based ionic liquids, J. Phys. Chem. B. 108, 20355-20365.

Bhat, M.K., S. Bhat, 1997. Cellulose degrading enzymes and their potential industrial applications, Biotechnol. Adv. 15, 583-620.

Bonhote, P., A. Dias, N. Papageorgiou, K. Kalyanasundaram, M. Gratzel, 1996. Hydrophobic, highly conductive ambient-temperature molten salts, Inorg. Chem. 35, 1168-1178.

Cao, Y., J. Wu, J. Zhang, H. Li, Y. Zhang, J. He, 2009. Room temperature ionic liquids (RTILs): A new and versatile platform for cellulose processing and derivatization, Chem.Eng.J. 147, 13-21.

Champagne, P., 2007. Feasibility of producing bio-ethanol from waste residues: A Canadian perspective Feasibility of producing bio-ethanol from waste residues in Canada, Res.Con.&Rec. 50, 211-230.

da Costa Sousa, L., S.P. Chundawat, V. Balan, B.E. Dale, 2009. 'Cradle-to-grave' assessment of existing lignocellulose pretreatment technologies, Curr. Opin. Biotechnol. 20, 339-347.

Feng, L., Z. Chen, 2008. Research progress on dissolution and functional modification of cellulose in ionic liquids, J. Mol. Liq. 142, 1-5.

FitzPatrick, M., P. Champagne, M.F. Cunningham, R.A. Whitney, 2010. A biorefinery processing perspective: Treatment of lignocellulosic materials for the production of value-added products, Bioresour.Technol. 101, 8915-8922.

Fort, D.A., R.C. Remsing, R.P. Swatloski, P. Moyna, G. Moyna, R.D. Rogers, 2007. Can ionic liquids dissolve wood? Processing and analysis of lignocellulosic materials with 1-*n*-butyl-3-methylimidazolium chloride, Green Chem. 9, 63-69.

Fredlake, C.P., M.J. Muldoon, S.N.V.K. Aki, T. Welton, J.F. Brennecke, 2004. Solvent strength of ionic liquid/CO2 mixtures, Phys.Chem.Chem.Phys. 6, 3280-3285.

Gericke, M., K. Schlufter, T. Liebert, T. Heinze, T. Budtova, 2009. Rheological properties of cellulose/ionic liquid solutions: From dilute to concentrated states, Biomacromolecules. 10, 1188-1194.

Hames, B.R., S.R. Thomas, A.D. Sluiter, C.J. Roth, D.W. Templeton, 2003. Rapid biomass analysis, Appl.Biochem.Biotechnol. 105, 5-16.

Heinze, T., K. Schwikal, S. Barthel, 2005. Ionic liquids as reaction medium in cellulose functionalization, Macromol.Biosci. 5, 520-525.

Hermanutz, F., F. Gähr, E. Uerdingen, F. Meister, B. Kosan, 2008. New developments in dissolving and processing of cellulose in ionic liquids, Macromol.Symp. 262, 23-27.

Huber, G.W., J.A. Dumesic, 2006. An overview of aqueous-phase catalytic processes for production of hydrogen and alkanes in a biorefinery, Catalysis Today. 111, 119-132.

Hurtubise, F.G., H. Krassig, 1960. Classification of fine Structural characteristics in cellulose by infared spectroscopy. Use of potassium bromide pellet technique, Anal.Chem. 32, 177-181.

Jessop, P.G., B. Subramaniam, 2007. Gas-expanded liquids, Chem.Rev. 107, 2666-2694.

Joglekar, H., I. Rahman, B. Kulkarni, 2007. The path ahead for ionic liquids, Chem.Eng.Technol. 30, 819-828.

Kiefer, J., K. Obert, A. Bösmann, T. Seeger, P. Wasserscheid, A. Leipertz, 2008. Quantitative analysis of alpha-D-glucose in an ionic liquid by using infrared spectroscopy, ChemPhysChem. 9, 1317-1322.

Kilpeläinen, I., H. Xie, A. King, M. Granstrom, S. Heikkinen, D.S. Argyropoulos, 2007. Dissolution of wood in ionic liquids, J.Agric.Food Chem. 55, 9142-9148.

Köhler, S., T. Liebert, M. Schöbitz, J. Schaller, F. Meister, W. Günther, et al., 2007. Interactions of ionic liquids with polysaccharides 1. Unexpected acetylation of cellulose with 1-ethyl-3-methylimidazolium acetate, Macromol.Rapid Commun. 28, 2311-2317.

Lee, S.H., T.V. Doherty, R.J. Linhardt, J.S. Dordick, 2008. Ionic liquid-mediated selective extraction of lignin from wood leading to enhanced enzymatic cellulose hydrolysis, Biotechnol. Bioeng. 102, 1368-1376.

Liu, Z., W. Wu, B. Han, Z. Dong, G. Zhao, J. Wang, et al., 2003. Study on the phase behaviors, viscosities, and tThermodynamic properties of CO2/[C4mim][PF6]/methanol system at elevated pressures, Chem.Eur.J. 9, 3897-3903.

Lynd, L.R., P.J. Weimer, W.H. van Zyl, I.S. Pretorius, 2002. Microbial cellulose utilization: Fundamentals and biotechnology, Microbiol. Mol. Biol. Rev. 66, 506-577.

Mohanty, A.K., M. Misra, G. Hinrichsen, 2000. Biofibres, biodegradable polymers and biocomposites: An overview, Macromol.Mater.Eng. 276-277, 1-24.

Moore, A., N. Owen, 2001. Infrared spectroscopic studies of solid wood, Appl. Spectrosc. Rev. 36, 65-86.

Mosier, N., C. Wyman, B. Dale, R. Elander, Y.Y. Lee, M. Holtzapple, et al., 2005. Features of promising technologies for pretreatment of lignocellulosic biomass, Bioresour.Technol. 96, 673-686.

Nelson, M.L., R.T. O'Connor, 1964a. Relation of certain infrared bands to cellulose crystallinity and crystal lattice type. Part II. A new infrared ratio for estimation of crystallinity in celluloses I and II, J. Appl. Polym. Sci. 8, 1325-1341.

Nelson, M.L., R.T. O'Connor, 1964b. Relation of certain infrared bands to cellulose crystallinity and crystal latticed type. Part I. Spectra of lattice types I, II, III and of amorphous cellulose, J. Appl. Polym. Sci. 8, 1311-1324.

Pacific Northwest National Laboratory, 2004. Top value added chemicals from biomass: Results of screening for potential candidates from sugars and synthesis gas, Department of Energy, Oak Ridge, TN.

Pu, Y., N. Jiang, A.J. Ragauskas, 2007. Ionic liquid as a green solvent for lignin, J. Wood Chem. Tech. 27, 23-33.

Reddy, N., Y. Yang, 2005. Biofibers from agricultural byproducts for industrial applications, Trends Biotechnol. 23, 22-27.

Song, H., J. Zhang, Y. Niu, Z. Wang, 2010. Phase transition and rheological behaviors of concentrated cellulose/ionic liquid solutions, J. Phys. Chem. B. 114, 6006-6013.

Swatloski, R.P., S.K. Spear, J.D. Holbrey, R.D. Rogers, 2002. Dissolution of cellose with ionic liquids, J.Am.Chem.Soc. 124, 4974-4975.

van Haveren, J., E. Scott, J. Sanders, 2008. Bulk chemicals from biomass, Biofuels, Bioprod. Bioref. 2, 41-57.

Zakzeski, J., P.C.A. Bruijnincx, A.L. Jongerius, B.M. Weckhuysen, 2010. The catalytic valorization of lignin for the production of renewable chemicals, Chem.Rev. 110, 3552-3599.

Zavrel, M., D. Bross, M. Funke, J. Buchs, A.C. Spiess, 2009. High-throughput screening for ionic liquids dissolving (ligno-)cellulose, Bioresour.Technol. 100, 2580-2587.

Zhang, Y.-.P., 2008. Reviving the carbohydrate economy via multi-product lignocellulose biorefineries, J.Ind.Microbiol.Biotechnol. 35, 367-375.

Zhang, Y.P., L.R. Lynd, 2004. Toward an aggregated understanding of enzymatic hydrolysis of cellulose: Noncomplexed cellulase systems, Biotechnol. Bioeng. 88, 797-824.

Zhbankov, R.G., 1992. Hydrogen bonds and structure of carbohydrates, J.Mol.Struct. 270, 523-539.

Zhu, S., Y. Wu, Q. Chen, Z. Yu, C. Wang, S. Jin, et al., 2006. Dissolution of cellulose with ionic liquids and its application: A mini-review, Green Chem. 8, 325-327.

Chapter 2

Literature Review Part A: A Biorefinery Processing Perspective: Treatment of Lignocellulosic Materials for the Production of Value-Added Products

Michael FitzPatrick, Pascale Champagne, Michael F. Cunningham, Ralph A. Whitney

2.1 Abstract

In the last decade, there has been increasing research interest in the value of bio-sourced materials recovered from residual biomass. Research that focuses on the use of extracted, recovered and/or synthesized bioproducts for direct industrial applications is essential for the implementation of sustainable approaches in a forward-looking bio-based economy. The effective use of biomass feedstocks, particularly lignocellulosic materials (plant biomass predominantly comprised of cellulose, hemicellulose, and lignin), in large-scale applications will evolve from innovative research aimed at the development and implementation of biorefineries - multi-step, multi-product facilities established for specific bio-sourced feedstocks. This paper presents recent advances in lignocellulosic biomass processing and analysis from a biorefining perspective. In addition, existing industrial biomass processing applications are discussed and examined within a biorefinery context.

2.2 Introduction

The future energy economy will likely be based on a wide range of alternative energy platforms including wind, water, sun, nuclear fission and fusion, as well as biomass. Similarly, the production of chemicals will increasingly depend on biomass, particularly plant biomass. In 2004, the US Department of Energy (DOE) identified twelve chemicals, derived from the conversion of biomass, which could be used as building block chemicals in a bio-based economy (PNNL/NREL, 2004). The chemical structures of these twelve chemicals are shown in Appendix A, Table A.1. Shifting society's dependence from petroleum-based to renewable biomass-based resources is generally viewed as key to the development of a sustainable industrial society, energy independence, and to the effective management of greenhouse gas emissions (Mabee and Saddler, 2010; PNNL/NREL, 2004; Ragauskas et al., 2006). The topic of processing bio-sourced materials has come to the forefront of sustainable engineering research and, in the last 15 years, a number of critical research reviews have been published that address the topics of lignocellulosic biomass pretreatment (Mosier et al., 2005; Yang and Wyman, 2008), hydrolysis (Sun and Cheng, 2002), enzymatic and microbial conversion (Lynd et al., 2002; Zhang and Lynd, 2004), as well as biomass processing approaches (Dodds and Gross, 2007; Lucia et al., 2006; van Haveren et al., 2007) and future biorefining perspectives (Hatti-Kaul et al., 2007; Ragauskas et al., 2006).

The use of biomass as a resource for energy and fuel production will be limited by maximum production rates and the supply of biomass rather than the demand for energy and fuel. The relatively low energy content, seasonality and discrete geographic availability of biomass feedstocks have been noted as barriers to the large volume demands for energy and fuel (Lipinsky, 1981). In contrast, chemical production requires far lower volumes of biomass to satisfy demand. For example, in the United States, the chemical products segment consumed just over 3% of the total US petroleum consumption in 2007 for a value-added worth (value including capital and labour costs) of $375 billion (USD), whereas the transportation segment accounted for

over 70% of the US petroleum consumption for a value-added worth of $385 billion (USD) (Smith, 2008). The remaining 27% of the US petroleum consumption was allocated to non-transportation energy usage, for a value-added worth of $135 billion (USD). As such, there exists an economic opportunity for the development of bio-sourced chemical products since the value of the chemical industry is comparable to the fuel industry, but requires only a fraction of the biomass.

The cost of using starch as a feedstock is high because grain and sugar crops are expensive. Consequently, there has been an increase in lignocellulosic biomass processing research, focusing particularly on agricultural and forestry residues, since these are low in cost, abundant, readily available and renewable (Claassen et al., 1999; Galbe and Zacchi, 2002; Pan et al., 2005b). However, it is inherently complex and heterogeneous in composition, and can be recalcitrant to conversion reactions.

2.3 The Biorefinery

With emerging research trends in the production of bio-based products, the biorefinery concept will continue to gain momentum. The definition of the term biorefinery has been subject to debate, but the overall goal of the biorefinery production approach is the generation of a variety of goods from different biomass feedstocks, within a particular biorefinery, through a combination of technologies. Ideally, a biorefinery should integrate biomass conversion processes to produce a range of fuels, power, materials, and chemicals from biomass (Fernando et al., 2006; Kaparaju et al., 2009; Laser et al., 2009; Lynd et al., 2009). Conceptually, a biorefinery would apply hybrid technologies from different fields including polymer chemistry, bioengineering and agriculture (Ohara, 2003). Simply, many petrochemicals are produced from crude oil-fed refineries, whereas in the future, it is anticipated that many bio-sourced products will be produced from biorefineries fed with biomass. The term biorefinery is derived both from the raw material

feedstock which is renewable biomass and also from the bioconversion processes often applied in the treatment and processing of the raw materials (Kamm and Kamm, 2004).
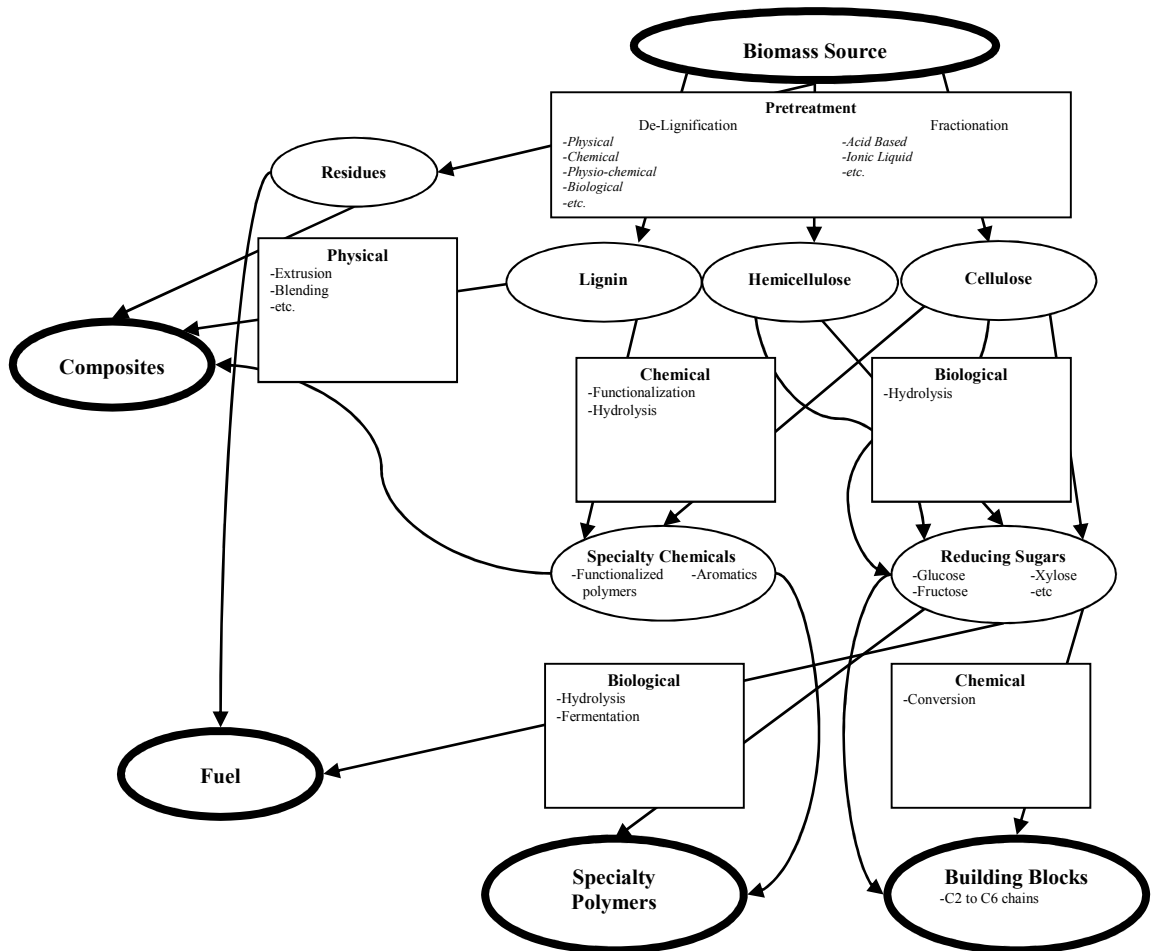
Figure 2.1: Conceptual biorefinery schematic.

This allows for the development of systems that ideally attempt to render the term "waste", in its application to biomass processing, obsolete as each production stream has the potential to be converted into a by-product stream rather than waste streams (Kamm and Kamm, 2007). This concept is illustrated in Figure 2.1 for a lignocellulosic feedstock. A biorefinery approach involves multi-step processes in which the first step, following feedstock selection, typically

involves treating the precursor-containing biomass to make it more amenable for further processing. This step is conventionally referred as pretreatment. Initial implementation of the biorefinery approach into an existing infrastructure will involve either their operation in parallel to or their inclusion at the tail-end of the existing primary industry, such as pulp and paper or wood processing. Thus, a conceptual biorefinery will initially be a separate entity to existing facilities or the existing primary industry will occur prior to the biomass source in concept illustrated in Figure 2.1. The choice of pretreatment technique is especially important for biomass sources coming from existing facilities as these sources of biomass will not only be of lower value, but will also contain impurities and chemicals from the previous processing. Thus, pretreatment in a biorefinery may also include steps to clean and/or prepare the feedstock.

Following pretreatment, the biomass components are subject to a combination of biological and/or chemical treatments. The outputs from this step (specialty chemicals or reducing sugars) could be further converted to chemical building blocks for further processing uses, which have been outlined by the DOE (PNNL/NREL, 2004). Furthermore, thermal processing of biomass, which would be a parallel approach to the potential biorefinery concept illustrated in Figure 2.1, exists as an alternative treatment method (Yang and Wyman, 2008). Thermal processing treatments, including pyrolysis and gasification, typically involve the rapid heating of biomass to produce liquid or gaseous fuels which can be further refined, especially to transportation fuels (Sun and Cheng, 2002; Yang and Wyman, 2008). The conversion to specialty polymers ready for market use, to a fuel/energy source, or use in composite materials are possible processing options, as shown in Figure 2.1. However, these final two uses, in addition to physical and thermal processing, are beyond the scope of this thesis.

Similar to petroleum, biomass has a complex composition and, as such, its primary fractionation into its main components allows for treatment and processing into a wide range of products. However, unlike petroleum feedstocks, biomass feedstocks typically have low thermal stabilities and a high degree of functionality. Consequently, they require unique reaction

15

conditions, such as aqueous-phase processing, in contrast to petroleum feedstocks (Huber and Dumesic, 2006).

There are several potential large-scale industrial biorefinery formats, whose primary difference is their biomass feedstock source. Of these, the lignocellulosic feedstock (LCF) biorefinery scheme has shown significant promise as it has the potential to accommodate a wide range of low cost feedstocks (straw, reeds, grass, wood, paper-waste, etc.) that could yield conversion products in both the existing petrochemical-dominated market and the future bio-based product markets. The concept of fractionating biomass into its core constituents, an important step in the development of biorefining technologies, has the potential to benefit a wide range of bioprocessing industries due to the ease and improved efficiency associated with less variable material feedstocks. However, the development and application of lignocellulosic biomass fractionation technologies that are technically and economically feasible are still in their infancy. Therefore, in the next decade, fundamental and applied research will be critically needed in this area.

For example, most of the hemicellulose encountered in traditional Kraft pulping (one of the most common industrial wood pulping techniques) is dissolved in the black liquor in the form of saccharified mono sugars, along with lignin and inorganic pulping chemicals. This black liquor is traditionally combusted for power generation, however, the fact that hemicellulose has a lower heating value than lignin represents an uneconomical use of this resource. Rather, if the hemicellulose and lignin were separated prior to combustion (fractionation), a more efficient use for hemicellulose could be derived, such as the production of fuels (ethanol) or higher-value chemicals (polyesters) (Huang et al., 2008).

The choice of feedstock and final products are important in biorefinery design due to the large-scale production implications. Initial feedstock availability and its potential use in multiple production streams both need to be considered (Mabee et al., 2005). For example, an existing biorefinery in Pomacle, France produces both ethanol and succinic acid in addition to beet sugar

and glucose from a single facility with many processing streams (Hatti-Kaul et al., 2007; Le Henaff and Huc, 2008). This is accomplished through the use of a robust microorganism (*Escherichia coli K-12*) that uses a variety of feedstocks (glucose, sucrose, glycerine, etc.) in an anaerobic, aqueous process. The importance of the biorefinery approach is also illustrated in the production of biodiesel. Crude glycerol is a co-product of the chemical process used to synthesize biodiesel from biomass feedstocks and had traditionally been considered a waste material due to the relatively low glycerol market value. Recently, chemical companies such as Dow Chemical Company, Huntsman Corporation, Cargill and Archer Daniels Midland Corporation, have begun to use glycerol as a low-cost building block material for conversion to higher-value propylene glycol (McCoy, 2007). Furthermore, Dow Chemical Company and Solvay are exploring the use of glycerol in the production of epichlorohydrin, which can be used in the manufacture of epoxy resins and epichlorohydrin elastomers (Dodds and Gross, 2007). Due to its versatility, it is anticipated that glycerol could become a substitute for many commonly used petrochemicals (Pagliaro and Rossi, 2008). The chemical structure of glycerol is demonstrated in Appendix A, Table A.1.

2.3.1 Biorefinery Processing Strategies

A critical juncture in the area of processing biomass into value-added products is whether or not to take a direct or indirect product substitution approach. In this context, direct product substitution occurs when an existing product on the market is produced through the development of a new processing method. Thus, direct product substitution involves producing commodities with existing market value, but using biomass as a feedstock for their production using new processing approaches. These products would have the advantage of increased likelihood of product acceptance in the marketplace due to their familiarity. However, existing petroleum-based infrastructure and optimized large-scale facilities make it difficult for biomass-derived products to compete with these established products on an economic basis (Lipinsky, 1981).

Indirect product substitution occurs when a new product is developed that is unique to the market, but serves a similar function as an existing product. Indirect product substitution involves the use of new chemicals to perform similar functions as existing chemicals, without duplicating their molecular structures. The complex chemical diversity of biomass feedstocks offers the opportunity to generate a wide-range of new polymers and reaction intermediates (Carole et al., 2004; Clark et al., 2006; Fengel and Wegener, 1984; Fernando et al., 2006; Lipinsky, 1981; PNNL/NREL, 2004). Indirectly substituted products do not differ from existing products solely on their production feedstock (i.e. lignocellulose instead of petroleum). For indirect product substitution to be successful, these products would have to perform similar functions as existing chemicals at a lower cost, or have unique properties that cannot be obtained with existing chemicals, in addition to performing similar functions.

Perhaps one of the most promising and realistic approaches, with a higher likelihood of acceptance by established chemical producers, is the development of processes to make bio-sourced intermediate chemicals. These intermediates (e.g. acrylic acid) could be used as "drop in" components to existing chemical production facilities to make higher value-added chemicals (e.g. acrylic esters), without requiring additional capital investment or expensive changes to an optimized chemical manufacturing process. In terms of bulk chemical production on an industrial scale, a feedstock that is inexpensive and readily available is required. These requirements are met by lignocellulosic biomass.

2.4 Lignocellulosic Pretreatment Techniques

Typically, pretreatment aims to convert native lignocellulosic biomass, in which cellulose is recalcitrant to hydrolysis, into a form where hydrolysis is effectively achieved. Pretreatment of lignocellulosic biomass yields materials that can be characterized by cellulose substrate redistribution either as an increase in the accessible cellulose surface area and/or the solubilisation of lignin (Lynd et al., 2002). A brief review of the traditional categories of pretreatment is

presented in this section. Additionally fractionation, a newer class of pretreatment which aims to not only improve hydrolysis, but also separate the core constituents of lignocellulosic biomass, will be discussed.

2.4.1 Physical and Chemical Structure Modification

The structure of cellulose favours ordering of the polymer chains into tightly packed arrangements that are water insoluble and resistant to depolymerisation (Mosier et al., 2005). Thus, it is imperative that a pretreatment regime alter the structure of biomass to make the cellulose more accessible to hydrolysis. Crystallinity, accessible specific surface area, particle size, degree of polymerization of the cellulose, coating of cellulose by both lignin and hemicellulose and the heterogeneous nature of biomass all have been proclaimed to contribute to the recalcitrance of lignocellulosic materials to hydrolysis (Chandra et al., 2007; Mosier et al., 2005; Puri, 1984). However, the economics of pretreatment must be balanced against the costs of downstream processing, and there is a need to elucidate the trade-off between operating costs, capital costs, and input (biomass) costs when investigating a pretreatment regime for a biorefineries (Sousa et al., 2009; Yang and Wyman, 2008).

However, it should be noted that there can be difficulties in interpreting the effects of pretreatment. When a substrate is exposed to conditions that alter one of the factors influencing reactivity, other factors that influence reactivity may also change (Chandra et al., 2007; Kumar et al., 2009; Zhang and Lynd, 2004). Decoupling these effects remains a challenge. For example, removal of hemicellulose can increase cellulose yields from enzymatic hydrolysis, and often the rate and yield of cellulose will further increase with the additional removal of lignin. Also, hydrolysis of hemicellulose at high temperatures can lead to a change in the nature of lignin, affecting enzymatic digestibility, though the lignin still remains in the solid substrate (Lynd et al., 1999).

19

In general, pretreatment approaches can be classified into four categories: 1) physical; 2) chemical; 3) physiochemical; and 4) biological. Ordinarily, physical pretreatments exhibit comparatively lower performance and higher cost (Yang and Wyman, 2008). Physical pretreatment techniques include mechanical comminution and ultrasound (Khanal et al., 2007; Sun and Cheng, 2002; Teramoto et al., 2008).

In general, chemical pretreatment regimes show a high degree of selectivity for the biomass component they degrade, but also involve relatively harsh reaction conditions, which may not be ideal in a biorefinery scheme due to possible effects on downstream biological processing. Chemical pretreatment processes include ozonolysis, dilute and concentrated acid, alkaline, oxidative H_2O_2 delignification and organosolv (an organic or aqueous organic solvent mixed with an inorganic acid catalyst) (Mosier et al., 2005; Sun and Cheng, 2002).

Physiochemical pretreatment combines chemical and physical treatment options. Often, milder chemical conditions are used, but under more extreme operational conditions, typically involving elevated pressures and temperatures, adding to the cost of implementing these techniques in a biorefinery scheme. Different physiochemical pretreatment techniques include liquid hot water (hydrothermolysis, aqueous or steam/aqueous, uncatalyzed solvolysis aquasolv), steam explosion (autohydrolysis with and without chemical addition), ammonia fibre explosion (AFEX), and CO_2 explosion (Mosier et al., 2005; Pan et al., 2005).

Finally, the biological pretreatment route offers important advantages such as low chemical and energy use, in addition to mild operational conditions and likely ease of integration into a consolidating bioprocessing set-up. However, a controllable, and more importantly, rapid system has not been developed to date (Sun and Cheng, 2002; Yang and Wyman, 2008).

2.4.2 Lignocellulose Fractionation

Fractionation is a specific class of pretreatment where the biomass feedstock is separated into its core components (cellulose, hemicelluloses, and lignin) such that each individual

component may be more readily processed or functionalized. The largest obstacle to be overcome, in terms of technological and economic barriers, to make biomass biorefineries a reality is the implementation of cost-effective methods to release soluble sugars from lignocellulosic biomass at an industrial scale (Moxley et al., 2008). It has been argued that the conversion of lignocellulosic biomass to higher-value products also requires fractionation (Huang et al., 2008).

2.4.2.1 *Acid Based Fractionation*

It has been shown that cellulose solvents such as concentrated phosphoric acid can completely dissolve cellulose fibres and disrupt the hydrogen bonds that hold together crystalline cellulose, which in turn increase the accessibility of cellulose to cellulase enzymes. Zhang et al. (2007) presented a cellulose solvent-based lignocellulosic fractionation (CSLF) technique using a cellulose solvent, volatile organic solvent, and water to separate lignocellulose at relatively low temperatures and pressures (50°C and atmospheric). The process fractionated lignocellulosic biomass components based on the difference in solubility of cellulose, hemicellulose, and lignin in the cellulose solvent, organic solvent and water, respectively (Zhang et al., 2007). The cellulose solvent was also recycled in the process as a result of the difference in volatility between the cellulose (phosphoric acid) and the organic (acetone) solvents (Moxley et al., 2008). The aim of the CSLF technique is the 1) decrystallization of cellulose fibres; 2) partial removal of lignin and hemicellulose from the cellulose fraction; and 3) relatively modest reaction conditions. Additionally, the CSLF approach has been reported to work independently of biomass type, which would make it a relatively generic and powerful fractionation technique. Studies under various CSLF conditions have demonstrated that the acid concentration is the most important factor, while temperature is the least important in terms of efficiency. It should be noted, however, that these technologies are very capital intensive.

2.4.2.2 *Ionic Liquid Based Fractionation*

Ionic liquids (ILs) are organic salts that exist as liquids at relatively low temperatures; often well below 100°C. They have tuneable physiochemical properties, negligible (or very low) vapour pressures, generally good thermal stability and there is nearly a limitless combination of anions and cations that can be used to synthesize ILs (Fort et al., 2007; Lee et al., 2008). Recent studies of particular interest have indicated that both cellulose and lignin can be dissolved in a variety of ionic liquids, and, perhaps more importantly, easily regenerated from these solutions (Fort et al., 2007; Zhu, 2008).

In terms of dissolution of cellulose, one of the most prominent studies involved the treatment of cellulose with 1-butyl-3-methylimidazolium chloride ([bmim]Cl), where pulp cellulose was dissolved in concentrations of up to 300 g/L without prior treatment (Fort et al., 2007; Swatloski et al., 2002). The structural form of the regenerated cellulose can be altered to include powders, tubes, fibres, and films by altering the regeneration process. The regenerated cellulose microstructure can range from amorphous to crystalline based on the regeneration process (Zhu et al., 2006). However, it should be noted that the regenerated cellulose has essentially the same degree of polymerization and polydispersity as the original cellulose (Zhu, 2008). Typically, regeneration of the solute is achieved by precipitation in the presence of an anti-solvent (water or methanol) due to preferential solute-displacement. This anti-solvent can then be stripped from the IL (for example through flash distillation, evaporation, reverse osmosis or salting out) and the IL recovered for reuse (Dadi et al., 2006; Zhu et al., 2006). Furthermore, 1-butyl-3-methylimidazolium chloride ([bmim]Cl) has been employed under microwave irradiation and/or pressure to dissolve lignocellulosic materials (Zhu et al., 2006). 1-Ethyl-3-methylimidazolium acetate ([emim][OAc]) has been used to dissolve lignin from lignocellulosic biomass with minimal cellulose dissolution. It was observed that the removal of 40% of the original lignin resulted in cellulose digestibility, through enzyme hydrolysis, of greater than 90% of the theoretical maximum (Lee et al., 2008). Thus, ILs have the potential to be used beyond a

lignocellulose fractionation regime for the more environmentally benign pretreatment of lignocellulosic biomass. Preliminary studies have shown that conversion of IL-extracted cellulose to both ethanol and lactic acid was higher than in samples pretreated by steam explosion and chemical pretreatment technologies (Zhu et al., 2006; Zhu, 2008). Regenerated cellulose exhibited a significant improvement, in terms of hydrolysis rate and glucose formation, over untreated cellulose (Dadi et al., 2006). The improvement in hydrolysis rates was attributed to the slight decrease in the degree of polymerization of both cellulose and hemicellulose, the decrease in the crystallinity of the cellulose, and an increase in accessibility due to lignin separation (Liu and Chen, 2006).

2.5 Bio-Based Chemical Production

The biological production of chemicals is not a new technology, though it is one that is central to the sustained development of biorefining technologies due to the high-value and relatively low material demands of this industry. In the first half of the 20th century, several commodity products were produced by fermentation including acetic acid, citric acid, lactic acid, and itaconic acid (Dodds and Gross, 2007; Lipinsky, 1981). Between 1945 and 1950, one tenth of the acetone and two-thirds of the n-butanol in the United States were produced through the fermentation of molasses and starch, respectively (Dodds and Gross, 2007). There is also a long history of bio-based chemical production in the automotive industry. Henry Ford's original manufacturing plan involved production of cars that included plant materials and vegetable oils for fuel, car tires fabricated from Goldenrod based latex, and a car body that included flax, soybean meal, and resin (McLaughlin, 2008). The trend in using biomass as a feedstock in automotive parts manufacturing continues. For instance The Woodbridge Group uses bio-derived polyol foams as key components in the manufacturing of a range of interior automotive parts including sunshades, seat cushions, structural foams, energy absorbance, carpet backing, and armrests (Khalil, 2008).

2.5.1 Classical Chemical Methods

A variety of building block polymers have been processed from biomass sources using more classical chemical approaches and as such these classical technologies will play a role in the development of future biorefineries. One of the more commonly known classical chemical methods to derive polymers from biomass involves the conversion of biological fatty acids to polymer building blocks. Currently this is being accomplished by Cargill, working in conjunction with the Kansas Polymer Research Centre, where they have chemically converted triglyceride carbon-carbon double bonds to alcohol and methoxy groups, leading to a bio-derived polyol (BiOH). These polyols can then be further processed into a range of polyurethane products (Dodds and Gross, 2007).

Levulinic acid is industrially prepared from biotechnology-based routes, using wood processing and agricultural wastes via conversion of hexose sugars in acid (Farone and Cuzens, 2000; Lucia et al., 2006). The chemical structure of levulinic acid is shown in Appendix A, Table A.1. It can be used as a building block for other specialty chemicals or directly in a range of products including resins, plasticizers, and textiles (Lucia et al., 2006). Also, lignin, due to its chemical nature and aromatic structure, can be converted to xylene, benzene, toluene, or other aromatic compounds (van Haveren et al., 2007).

2.5.1.1 *Catalysis*

Catalysts have been employed to enable the transformation of biomass and their range of use from fuels to high-value chemicals make them well suited to maximizing the value of a chosen biorefinery feedstock. One of the better known processes involves the use of Fischer-Tropsch chemistry (Dodds and Gross, 2007). For instance, catalysts, including Fischer-Tropsch synthesis, have been used in the production of biofuels from palm (Chew and Bhatia, 2008). Additionally, platinum catalyzed aqueous phase reforming of glycerol has demonstrated high yields of hydrogen fuel, with low CO content, for use in fuel cells (Pagliaro and Rossi, 2008).

Biocatalysis has also been widely used in the production of high-value products such as fine chemicals and pharmaceutical products (Hatti-Kaul et al., 2007; Thomas et al., 2002). Biocatalysts often selectively catalyze reactions to ensure the desired products are formed and to reduce energy consumption and waste generation, as well as synthesize products that are not possible via chemical reactions alone which are of particular interest for the development of novel specialty chemicals in biorefineries (Hatti-Kaul et al., 2007).

2.5.1.2 *Condensation Polymerization*

Immobilized enzyme catalysts have been used to polymerize bio-derived monomers through condensation polymerizations. This has been performed through the use of a commercially available lipase catalyst to achieve direct polycondensations on sorbitol or glycerol with diacids that can be either chemically or biologically derived (Kumar et al., 2003). This technique has been demonstrated to reduce reaction temperatures and energy consumption, relative to traditional chemical polymerization processing, while also controlling branching during polymerization (Dodds and Gross, 2007). The reduction in temperature and increase in control are especially important in the development of biorefining technologies aimed at competing with traditional petroleum refineries.

2.5.2 Fermentation

Fermentation has been widely used; both in academic and industrial settings, to produce some of the most highly sought after building block chemicals. As such its integration into biorefinery schemes is essential in moving this technology forward. For example, succinic acid, one of the most sought-after chemicals highlighted by the United States Department of Energy as a potential building block, can be produced through fermentation (PNNL/NREL, 2004). The chemical structure of succinic acid is demonstrated in Appendix A, Table A.1. Salts of succinic acid can be derived through the fermentation of glucose, which fixes CO_2 and is thus a green technology (Carole et al., 2004; Lucia et al., 2006). Since most microorganisms used in industrial

fermentation are not tolerant of acidic conditions, the process is neutralized. These salts then undergo more conventional chemical processing such as separation and recovery where they are separated from the microorganisms and then dissolved in an acid solution to form succinic acid (Carole et al., 2004).

In nature, 1,3-propanediol is produced through the fermentation of glycerol (Nakamura and Whited, 2003). Industrially, DuPont, working with Genencor, has developed a low-cost route of producing 1,3-propanediol (1,3PDO) by modifying natural routes. 1,3-Propanediol is a key building block for polypropylene terephthalate, which is not available from petrochemical sources, in addition to being used as fibre in the apparel and carpet industries. Itaconic acid, another DOE top twelve building block chemical, is currently an expensive specialty product with many uses and is industrially produced from the fermentation of carbohydrates by fungi in small quantities. The chemical structure of itaconic acid is shown in Appendix A, Table A.1. Polymerized esters (methyl, ethyl, and vinyl) are used in adhesives and coatings. Itaconic acid is often found in emulsion paints to aid in polymer adhesion and as a hardening agent for organosiloxanes which are used in contact lenses. In addition, due to its two reactive carboxyl groups, itaconic acid has the potential to be incorporated into polymers. Currently, it is being assessed as a biofriendly substitute for acrylic and methacrylic acid in polymers and in styrene-butadiene systems (Lucia et al., 2006; PNNL/NREL, 2004).

Lactic acid, which can be chemically converted to several important chemicals including methyl lactate, lactide, and polylactic acid (a biodegradable replacement for polyethylene terephthalates (PETs)), can be produced through fermentation. Research is being conducted to convert lactic to acrylic acids, major commodity monomers with an international volume demand approximately 1.6 billion kg/year in 2007 (Dodds and Gross, 2007). The hydroxyl and carboxyl groups present in lactic acid make it amenable for conversion into a wide range of value-added products.

Recent research suggests that some organisms express acrylic acid pathways, thus direct fermentation of biomass to acrylic acid is a possibility (Xu et al., 2006). Acrylic acid and its amide and ester derivatives are key components in polymer manufacturing, appearing in a wide-range of products including surface coatings, textiles, detergents, and absorbent materials. Ethylene, which can be polymerized into widely used polyethylene, has been shown to be synthesized directly from biomass hydrolysates using naturally occurring bacteria in soil and the surface of fruits (Danner and Braun, 1999). Although the possibility of ethylene production exists from biomass sources, essentially all production of ethylene is derived from steam cracking in the petrochemical industry, currently resulting in a negligible contribution of biological production of ethylene in industry. The widespread potential of fermentation technologies to add value to lignocellulosic biomass sources makes them integral to development of biorefineries.

2.5.3 Ionic Liquid Phase Reaction

Ionic liquids phase biomass processing has the potential for functional additives to be incorporated directly in solution via dissolution or dispersion before or after cellulose dissolution (Zhu et al., 2006). For this reason, the implantation of this technology into biorefinery designs may serve to decrease the number of processing steps and the corresponding cost and power requirements. For example, it has been shown that ionic liquids (specifically ([bmim]Cl) can be mixed with catalytic amounts of acid (including HCl, H_2SO_4, HNO_3) to effectively combine pretreatment and hydrolysis in one step, resulting in a total reducing sugar yield of up to 81% of the theoretical maximum (Li et al., 2008). Additionally, the combination of pretreatment and hydrolysis has been demonstrated through the careful addition of water to ionic liquids ([bmim]Cl and 1-ethyl-3-methylimidazolium chloride ([emim]Cl)) resulting the conversion of up to 97% of fibrous cellulose to reducing sugars (Zhang et al., 2010). If enzymatic hydrolysis is preferred, however, the cellulose must generally be separated from the IL, because the salinity of ILs has been shown to reduce the activity of many enzymes through denaturing (Turner et al., 2003). To

overcome the salinity of ILs and still maintain enzymatic activity in solution, poly(ethylene glycol) has been used to stabilize enzymes in IL solution and allow them to retain their activity (Turner et al., 2003).

The ionic liquid phase has also been used to stabilize catalysts during reaction. For example, chromium (II) chloride ($CrCl_2$) has been stabilized in both [emim]Cl and 1-alkyl-3-methylimidazolium chloride ([amim]Cl) to catalyze the conversion of biomass into 5-hydroxymethyl furfural (HMF), a top value-added platform chemical (PNNL/NREL, 2004; Zhang et al., 2010; Zhao et al., 2007). Additionally, polymerization reactions involving cellulose and ionic liquids have been reported in recent literature. The ionic liquid has served both as a means to prepare a cellulose derived initiator for atom-transfer radical polymerization (ATRP), as a medium for cellulose polymerization reactions, and as a polymerizable composite (with cellulose) in radical polymerization (Meng et al., 2009; Murakami et al., 2007).

Finally, there exist opportunities for the use of novel ILs, such as switchable ILs, for product separation, as well as investigations in the activities of microbial enzymes derived from extremophiles, such as halophilic organisms, for conversion of reducing sugars in solution (Oren, 2002; Phan et al., 2009). Research in this area would serve not only to further the development of lignocellulosic biomass fractionation techniques, but also advance increasingly environmentally benign pretreatment technologies, as well as have the potential to streamline lignocellulosic biomass processing.

2.5.4 Direct Biological Conversion

2.5.4.1 *Extraction*

Value-added products have been synthesized within biological species, both plant matter and microorganisms. In order to benefit from their production, efficient extraction technologies need to be implemented into biorefineries in the initial processing steps to allow for extraction before further processing. For example, commodity chemicals have been directly extracted from

biomass via conventional chemical extraction techniques. One of the most notable chemicals derived in this manner is ferulic acid, extracted in high percentage yields from corn fibre. Ferulic acid is a chemical feedstock used in the production of fine chemicals such as vanillin and guaiacol. DuPont has been able to extract a monomer from tulips, A-α-methylenebutyrolactone or tulipalin A, which polymerizes in a manner similar to methyl methacrylate and also has favourable durability and refractive index (Lucia et al., 2006; Mullin, 2004). This monomer could replace some petroleum-based methacrylate monomers for products such as mouldings. Thus, a market for value-added product extraction for specialty chemicals exists and biorefinery designs should make the most of this opportunity.

2.5.4.2 *Enzymatic Transformation*

In one of the best illustrations of direct biological conversion, polymers have been produced completely within microbial cells, most notably the family of polyhydroxyalkanoates (PHAs). This technology can be incorporated into a biorefinery as a separate processing stream since the bacteria that produce PHAs have been shown to be amenable to feeding from a wide range of carbon sources. PHAs are a family of natural polymers, comprised of over 150 different hydroxyalkanoates, produced by a range of bacteria (at least 75 genera) for carbon and energy storage (Carole et al., 2004; Munoz and Riley, 2008; Sun et al., 2007b). PHAs are formed as intracellular granules that have been reported at upwards of 90% of dry cell weight (Lee, 2006). They exhibit a wide range of properties, enabling them to be viable in a large fraction of the plastics industry. Typically bacteria synthesize PHA when carbon is abundant in excess, while one essential growth nutrient such as nitrogen or phosphorous is limited. It has also been shown that in some organisms, a carbon-limited feeding strategy can be employed for the production of PHA, with no limiting of essential growth nutrients (Sun et al., 2007a).

Researchers have also been working on genetically modifying plants for direct PHA production (Carole et al., 2004). Advances in genome sequencing provide the foundation for

optimizing PHA synthesis and for developing the ability to produce PHA polymers with a range of properties. PHAs are unique in the field of bio-based polymers in that they are synthesized directly as polymers, leading to the potential use of metabolic and genetic engineering tools to generate new polymers with tailored properties (Lee, 2006). A wide range of carbon sources have been used to synthesize both short-chain-length and medium-chain-length PHAs, which has been summarized in several review papers on the topic (Sun et al., 2007b; Suriyamongkol et al., 2007). Recently, it has been reported that PHAs can be synthesized using a forestry-based biorefinery approach with lignocellulosic process streams, including hemicelluloses hydrolysates, levulinic acid derived from cellulose, and tall oil fatty acids from Kraft pulping, being employed as the carbon sources for the bacteria *Burkholderia cepacia* (Keenan et al., 2006). Other sources of lignocellulosic by-products have been investigated for PHA production, including the use of tequila manufacturing bagasse (the rind and fibrovascular bundles dispersed in the *Agave tequilana* stalk) (Munoz and Riley, 2008). The bacteria used in this study were shown to not only produce PHAs, but also degraded insoluble cellulose under similar conditions, reducing the amount of required pretreatment.

Alternatively, instead of using one particular "super" bacteria, other research has been focused on the use of microbial consortia to produce PHAs from different carbon sources. Industrial wastewaters from methanol-enriched pulp and paper mill foul condensate, fermented municipal primary solids, and biodiesel have been shown to yield PHAs when passed through batch bioreactors containing a mixed microbial consortium from municipal activated sludge (Coats et al., 2007). Analysis of the system revealed different microbial communities present, but functional stability was maintained in spite of the contrasting populations. The wide range of potential carbon sources for PHA production lends itself to the inclusion of this technology in biorefinery designs.

2.6 Conclusion

With the abundance of biomass waste available, the development of new technologies that will make use of biomass for materials production beyond biofuels represents an important opportunity to fully utilize our resources. Development of efficient techniques to fractionate lignocellulosic biomass into its core components will facilitate research on the production of specific biomass derived sugars, building block chemicals and ultimately value-added commodity chemicals while preserving the concept of the biorefinery approach by promoting effective utilization all feedstock fractions.

2.7 References

Carole, T.M., Pellegrino, J., Paster, M.D., 2004. Opportunities in the industrial biobased products industry. Appl. Biochem. Biotechnol. 115, 871-885.

Chandra, R., Bura, R., Mabee, W., Berlin, A., Pan, X., Saddler, J., 2007. Substrate pretreatment: The key to effective enzymatic hydrolysis of lignocellulosics?. Biofuels. Adv. Biochem. Eng. Biotechnol. Springer, pp. 67-93.

Chew, T.L., Bhatia, S., 2008. Catalytic processes towards the production of biofuels in a palm oil and oil palm biomass-based biorefinery. Bioresour. Technol. 99, 7911-7922.

Claassen, P.A.M., van Lier, J.B., Lopez Contreras, A.M., van Niel, E.W.J. Sijtsma, L., Stams, A.J.M., de Vries, S.S., Weusthuis, R.A., 1999. Utilisation of biomass for the supply of energy carriers. Appl. Microbiol. Biotechnol. 52, 0741-0755.

Clark, J.H., Budarin, V., Deswarte, F.E.I., Hardy, J.J.E., Kerton, F.M., Hunt, A.J., Luque, R., Macquarrie, D.J., Milkowski, K., Rodriguez, A., Samuel, O., Tavener, S.J., White, R.J., Wilson, A.J., 2006. Green chemistry and the biorefinery: a partnership for a sustainable future. Green Chem. 8, 853-860.

Coats, E.R., Loge, F.J., Smith, W.A., Thompson, D.N., Wolcott, M.P., 2007. Functional stability of a mixed microbial consortium producing PHA from waste carbon sources. Appl. Biochem. Biotechnol. 137, 909-925.

da Costa Sousa, L., S.P. Chundawat, V. Balan, B.E. Dale, 2009. 'Cradle-to-grave' assessment of existing lignocellulose pretreatment technologies. Curr. Opin. Biotechnol. 20, 339-347.

Dadi, A.P., Varanasi, S., Schall, C.A., 2006. Enhancement of cellulose saccharification kinetics using an ionic liquid pretreatment step. Biotechnol. Bioeng. 95, 904-910.

Danner, H., Braun, R., 1999. Biotechnology for the production of commodity chemicals from biomass. Chem. Soc. Rev. 28, 395-405.

Dodds, D.R., Gross, R.A., 2007. CHEMISTRY: hemicals from biomass. Science 318, 1250-1251.

Farone,W.A., Cuzens, J.E., 2000. Method for the production of levulinic acid and its derivatives. US Patent: 6,054,611.

Fengel, D., Wegener, G., 1984. Wood: Chemistry, ultrastructure, reactions. de Gruyter, Berlin.

Fernando, S., Adhikari, S., Chandrapal, C., Murali, N., 2006. Biorefineries: Current status, challenges, and future direction. Energy Fuels 20, 1727-1737.

Fort, D.A., Remsing, R.C., Swatloski, R.P., Moyna, P., Moyna, G., Rogers, R.D., 2007. Can ionic liquids dissolve wood? Processing and analysis of lignocellulosic materials with 1-n-butyl-3-methylimidazolium chloride. Green Chem. 9, 63-69.

Galbe, M., Zacchi, G., 2002. A review of the production of ethanol from softwood. Appl. Microbiol. Biotechnol. 59, 618-628.

Hatti-Kaul, R., Tornvall, U., Gustafsson, L., Borjesson, P., 2007. Industrial biotechnology for the production of bio-based chemicals - a cradle-to-grave perspective. Trends Biotechnol. 25, 119-124.

Huang, H.J., Ramaswamy, S., Tschirner, U.W., Ramarao, B.V., 2008. A review of separation technologies in current and future biorefineries. Sep. Purif. Technol. 62, 1-21.

Huber, G.W., Dumesic, J.A., 2006. An overview of aqueous-phase catalytic processes for production of hydrogen and alkanes in a biorefinery. Catalysis Today 111, 119-132.

Kamm, B., Kamm, M., 2007. Biorefineries - Multi Product Processes. White Biotechnology. Adv. Biochem. Eng. Biotechnol. Springer, pp. 175-204.

Kamm, B., Kamm, M., 2004. Principles of biorefineries. Appl. Microbiol. Biotechnol. 64, 137-145.

Kaparaju, P., Serrano, M., Thomsen, A.B., Kongjan, P., Angelidaki, I., 2009. Bioethanol, biohydrogen and biogas production from wheat straw in a biorefinery concept. Bioresour. Technol. 100, 2562-2568.

Keenan, T.M., Nakas, J.P., Tanenbaum, S.W., 2006. Polyhydroxyalkanoate copolymers from forest biomass. J. Ind. Microbiol. Biotechnol. 33, 616-626.

Khalil, H., 2008. The use of biomaterials in automotive parts manufacturing. The Canadian Conference on Industrial Bioproduct Innovation. November 5-6, Montreal.

Khanal, S.K., Montalbo, M., van Leeuwen, J.H., Srinivasan, G., Grewell, D., 2007. Ultrasound enhanced glucose release from corn in ethanol plants. Biotechnol. Bioeng. 98, 978-985.

Kumar, A., Kulshrestha, A.S., Gao, W., Gross, R.A., 2003. Versatile route to polyol polyesters by lipase catalysis. Macromolecules 36, 8219-8221.

Kumar, R., Mago, G., Balan, V., Wyman, C.E., 2009. Physical and chemical characterizations of corn stover and poplar solids resulting from leading pretreatment technologies. Bioresour. Technol. 100, 3948-3962.

Laser, M., Jin, H., Jayawardhana, K., Lynd, L.R., 2009. Coproduction of ethanol and power from switchgrass. Biofuels, Bioprod. Biorefin. 3, 195-218.

Le Henaff, Y., Huc, J.-F., 2008. BIO-AMBER: From the patent to industrial demonstration, The Canadian Conference on Industrial Bioproduct Innovation. November 5-6, 2008, Montreal.

Lee, S.H., Doherty, T.V., Linhardt, R.J., Dordick, J.S., 2008. Ionic liquid-mediated selective extraction of lignin from wood leading to enhanced enzymatic cellulose hydrolysis. Biotechnol. Bioeng. 102, 1368-1376.

Lee, S.Y., 2006. Deciphering bioplastic production. Nat. Biotechnol. 24, 1227-1229.

Li, C., Wang, Q., Zhao, Z.K., 2008. Acid in ionic liquid: An efficient system for hydrolysis of lignocellulose. Green Chem. 10, 177-182.

Lipinsky, E.S., 1981. Chemicals from biomass: Petrochemical substitution options. Science 212, 1465-1471.

Liu, L., Chen, H., 2006. Enzymatic hydrolysis of cellulose materials treated with ionic liquid [BMIM] Cl. Chinese Science Bulletin 51, 2432-2436.

Lucia, L.A., Argyropoulos, D.S., Adamopoulos, L., Gaspar, A.R., 2006. Chemicals and energy from biomass. Can. J. Chem. 84, 960-970.

Lynd, L.R., Wyman, C.E., Gerngross, T.U., 1999. Biocommodity engineering. Biotechnol. Prog. 15, 777-793.

Lynd, L.R., Weimer, P.J., van Zyl, W.H., Pretorius, I.S., 2002. Microbial cellulose utilization: Fundamentals and biotechnology. Microbiol. Mol. Biol. Rev. 66, 506-577.

Lynd, L.R., Larson, E., Greene, N., Laser, M., Sheehan, J., Dale, B.E., McLaughlin, S., Wang, M., 2009. The role of biomass in America's energy future: framing the analysis. Biofuels, Bioprod. Biorefin. 3, 113-123.

Mabee, W., Gregg, D., Saddler, J., 2005. Assessing the emerging biorefinery sector in Canada. Appl. Biochem. Biotechnol. 121-124, 765-778.

Mabee, W.E., Saddler, J.N., 2010. Bioethanol from lignocellulosics: Status and perspectives in Canada. Bioresour. Technol. 101, 4806-4813.

McCoy, M., 2007. Biofuels center grows in west. Chemical & Engineering News 85, 12.

McLaughlin, M., 2008. Bioproducts: Significant stakes for the 21st century. The Canadian Conference on Industrial Bioproduct Innovation. November 5-6, Montreal.

Meng, T., Gao, X., Zhang, J. Yuan, J., Zhang, Y., He, J., 2009. Graft copolymers prepared by atom transfer radical polymerization (ATRP) from cellulose. Polymer 50, 447-454.

Mosier, N., Wyman, C., Dale, B., Elander, R., Lee, Y.Y., Holtzapple, M., 2005. Features of promising technologies for pretreatment of lignocellulosic biomass. Bioresour. Technol. 96, 673-686.

Moxley, G., Zhu, Z., Zhang, Y-H.P, 2008. Efficient sugar release by the cellulose solvent-based lignocellulose fractionation technology and enzymatic cellulose hydrolysis. J. Agric. Food Chem. 56, 7885-7890.

Mullin, R., 2004. Sustainable specialties. Chemical & Engineering News 82, 29-37.

Munoz, L.E.A., Riley, M.R., 2008. Utilization of cellulosic waste from tequila bagasse and production of polyhydroxyalkanoate (PHA) bioplastics by Saccharophagus degradans. Biotechnol. Bioeng. 100, 882-888.

Murakami, M., Kaneko, Y., Kadokawa, J., 2007. Preparation of cellulose-polymerized ionic liquid composite by in-situ polymerization of polymerizable ionic liquid in cellulose-dissolving solution. Carbohydr. Polym. 69, 378-381.

Nakamura, C.E., Whited, G.M., 2003. Metabolic engineering for the microbial production of 1,3-propanediol. Curr. Opin. Biotechnol. 14, 454-459.

Ohara, H., 2003. Biorefinery. Appl. Microbiol. Biotechnol. 62, 474-477.

Oren, A., 2002. Diversity of halophilic microorganisms: Environments, phylogeny, physiology, and applications. J. Ind. Microbiol. Biotechnol. 28, 56-63.

Pacific Northwest National Laboratory, National Renewable Energy Laboratory, 2004. Top value added chemicals from biomass: Results of screening for potential candidates from sugars and synthesis gas. Department of Energy, Oak Ridge, TN.

Pagliaro, M., Rossi, M., 2008. The future of glycerol: new uses of a versatile raw material, Royal Society of Chemistry, Cambridge.

Pan, X., Xie,D., Gilkes, N., Gregg, D.J., Saddler, J.N., 2005. Strategies to enhance the enzymatic hydrolysis of pretreated softwood with high residual lignin content. Appl. Biochem. Biotechnol. 124, 1069-1079.

Pan, X., C. Arato, N. Gilkes, D. Gregg, W. Mabee, K. Pye, et al., 2005b. Biorefining of softwoods using ethanol organosolv pulping: Preliminary evaluation of process streams for manufacture of fuel-grade ethanol and co-products. Biotechnol. Bioeng. 90, 473-481.

Phan, L., Brown, H., White, J., Hodgson, A., Jessop, P.G., 2009. Soybean oil extraction and separation using switchable or expanded solvents. Green Chem. 11, 53-59.

Puri, V.P., 1984. Effect of crystallinity and degree of polymerization of cellulose on enzymatic saccharification, Biotechnol. Bioeng. 26, 1219-1222.

Ragauskas, A.J., Williams, C.K., Davison, B.H., Britovsek, G., Cairney, J., C.A. Eckert, et al., 2006. The path forward for biofuels and biomaterials. Science 311, 484-489.

Smith, P. , 2008. ADM: Building a future in renewable industrial chemicals. The Canadian Conference on Industrial Bioproduct Innovation. November 5-6, Montreal.

Sun, Y., Cheng, J., 2002. Hydrolysis of lignocellulosic materials for ethanol production: a review. Bioresour. Technol. 83, 1-11.

Sun, Z., Ramsay, J.A., Guay, M., Ramsay, B.A., 2007a. Carbon-limited fed-batch production of medium-chain-length polyhydroxyalkanoates from nonanoic acid by Pseudomonas putida KT2440. Appl. Microbiol. Biotechnol. 74, 69-77.

Sun, Z., Ramsay, J.A., Guay, M., Ramsay, B.A., 2007b. Fermentation process development for the production of medium-chain-length poly-3-hyroxyalkanoates. Appl. Microbiol. Biotechnol. 75, 475-485.

Suriyamongkol, P., Weselake, R., Narine, S., Moloney, M., Shah, S., 2007. Biotechnological approaches for the production of polyhydroxyalkanoates in microorganisms and plants - A review. Biotechnology Advances 25, 148-175.

Swatloski, R.P., Spear, S.K., Holbrey, J.D., Rogers, R.D., 2002. Dissolution of cellulose with ionic liquids. J. Am. Chem. Soc. 124, 4974-4975.

Teramoto, Y., Tanaka, N., Lee, S., Endo, T., 2008. Pretreatment of eucalyptus wood chips for enzymatic saccharification using combined sulfuric acid-free ethanol cooking and ball milling. Biotechnol. Bioeng. 99, 75-85.

Thomas, S.M., DiCosimo, R., Nagarajan, V., 2002. Biocatalysis: applications and potentials for the chemical industry. Trends Biotechnol. 20, 238-242.

Turner, M.B., Spear, S.K., Huddleston, J.G., Holbrey, J.D., Rogers, R.D., 2003. Ionic liquid salt-induced inactivation and unfolding of cellulase from Trichoderma reesei. Green Chem. 5, 443-447.

van Haveren, J., Scott, E.L., Sanders, J., 2007. Bulk chemicals from biomass. Biofuels, Bioprod. Biorefin. 2, 41-57.

Xu, X., Lin, J., Cen, P., 2006. Advances in the research and development of acrylic acid production from biomass. Chin. J. Chem. Eng. 14, 419-427.

Yang, B.,Wyman, C. 2008. Pretreatment: The key to unlocking low-cost cellulosic ethanol. Biofuels, Bioprod. Biorefin. 2, 26-40.

Zhang, Y.P., Lynd, L.R., 2004. Toward an aggregated understanding of enzymatic hydrolysis of cellulose: Noncomplexed cellulase systems. Biotechnol. Bioeng. 88, 797-824.

Zhang, Y.P., Ding, S., Mielenz, J.R. Cui, J., Elander, R.T., Laser, M., 2007. Fractionating recalcitrant lignocellulose at modest reaction conditions. Biotechnol. Bioeng. 97, 214-223.

Zhang, Y., Du, H., Qian, X., Chen, E.Y.-X., 2010. Ionic liquid−water mixtures: Enhanced Kw for efficient cellulosic biomass conversion. Energy Fuels 4, 2410-2417.

Zhao, H., Holladay, J.E., Brown, H., Zhang, Z.C., 2007. Metal chlorides in ionic liquid solvents convert sugars to 5-hydroxymethylfurfural. Science 316, 1597-1600.

Zhu, S., 2008. Use of ionic liquids for the efficient utilization of lignocellulosic materials. J. Chem. Technol. Biotechnol. 83, 777-779.

Zhu, S., Wu, Y., Chen, Q., Yu, Z., Jin, S., 2006. Dissolution of cellulose with ionic liquids and its application: A mini-review. Green Chem. 8, 325-327.

Chapter 3

Literature Review Part B: Materials and Characterization in a Biorefinery

Michael FitzPatrick

3.1 Abstract

There have been a wide range of lignocellulosic materials that have been studied for potential use as feedstocks in different biorefining configurations. Though the composition of feedstocks differ, they all have the same three common primary constituents: cellulose, hemicellulose and lignin. Due to the variable nature of lignocellulosic feedstocks and the importance of precise characterization to advance biorefining research, a summary of numerous techniques, including limitations and advances of each approach, are presented in this thesis. In addition, how existing characterization techniques, as well as the use of ionic liquids as novel solvents for lignocellulosic biomass, are discussed in the context of a biorefinery concept. Finally, current technological barriers to advancing research in this area are addressed.

3.2 Raw Materials for Use in Biorefining

There exist both seasonal and geographic constraints on any potential biomass feedstock for use in a biorefinery (Lipinsky, 1981). A wide range of materials can and have been investigated for their potential use as feedstocks in a variety of biorefinery configurations. A list of some of the potential biomass feedstocks that could be used in biorefining schemes is shown in Table 3.1 (Lynd et al., 1999, Wiselogel et al., 1996).

Table 3.1: Composition of several representative biomass feedstocks for potential use biorefineries.

Feedstock	Cellulose	Hemicelluloses					Lignin	Extractives and Ashes
		Glucan	*Xylan*	*Galactan*	*Arabinan*	*Mannan*		
Hardwoods[†]	43-53%	13-21%	Up to 1%	1-13%	1-5%	18-29%	1-9%
Softwoods[†]	42-46%	5-9%	Up to 3%	1-3%	~11%	27-30%	Up to 3%
Corn Stover[†]	36-40%	18-22%	~1%	1-3%	~1%	~16%	6-17%
Switchgrass[‡]	40-45%	31-35%					6-12%	9-12%

[†] *Cellulose and glucose reported together as glucan.*
[‡] *Hemicelluloses reported together.*

The most common of these feedstocks are the hard- and softwoods. Wood is a polymeric composite whose properties (both biological and mechanical) are generally determined by the composition of the cell wall. Wood cell walls are primarily made up of three components; cellulose, hemicellulose and lignin (Mai et al., 2004). Overall, cellulose forms a support system that is surrounded by other substances functioning as matrix (hemicellulose) and encrusting (lignin) materials (Sjöström, 1981; Zhang and Lynd, 2004). The tensile strength of wood fibres is derived from the cellulose and hemicellulose, whereas the role of lignin is to facilitate adhesion between fibres. Along with these cell wall polymers, properties of wood are attributed to extractives, additional compounds easily extractable from wood by solvents (Fengel and Wegener, 1984).

3.2.1 Cellulose

Cellulose is the major component in wood, comprising nearly half of both softwoods and hardwoods. It is a high molecular weight homopolymer, comprised of β-D-glucopyranose units which are linked together by (1→4)-glycosidic bonds; the chemical structure of cellulose is shown in Figure 3.1. It is these glycosidic bonds that allow cellulose to arrange in its crystalline form, which is also responsible for its low surface area. In nature, individual linear glucosyl chains undergo self-assembly at the site of biosynthesis (Brown Jr. and Saxena, 2000). An important feature of cellulose, unusual for a polysaccharide, is its crystalline structure. Also, the crystallinity of cellulose varies according to its source. For example, microcrystalline cellulose is nearly 60% crystalline, whereas the crystallinity of Scots pine and Norway spruce varied between 24%-31% and 23%-32%, respectively. The difference in crystallinity in pine and spruce samples is attributed to the location of the sample in the tree, with the higher crystallinity corresponding to older year rings (Andersson et al., 2004).
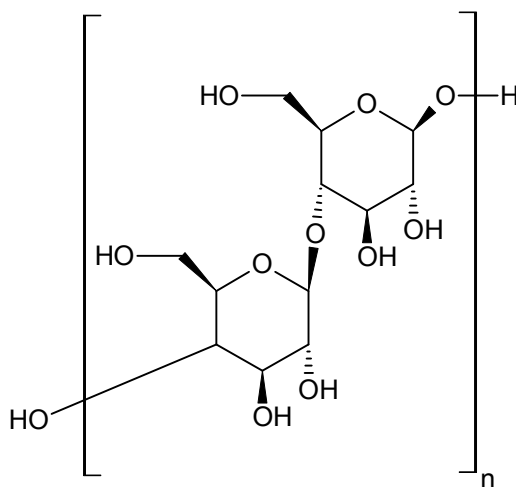
Figure 3.1: Chemical structure of cellulose.

Bundles of cellulose molecules aggregate together in the form of microfibrils with alternating highly ordered crystalline and disordered amorphous regions (Sjöström, 1981). The

crystalline nature of cellulose dictates that the component molecules of each microfibril are packed tightly enough to prevent the penetration of other molecules even as small as water, thereby impeding hydrolysis and making the dissolution and subsequent treatment of cellulose difficult (Lynd et al., 2002).

3.2.2 Hemicellulose

Hemicellulose is classified as a heterogeneous polysaccharide; it is an amorphous polymer that primarily contains five different sugar groups (Sjöström, 1981); more specifically: hexoses (glucose, mannose and galactose) and pentoses (xylose, arabinose). The structure of these primary sugar groups is shown in Figure 3.2. Hemicellulose chains are shorter than the chains in simpler cellulose, can be branched, and often have side groups, such as monosaccharides and acetyl groups (Mai et al., 2004). The general composition of hemicellulose differs between hardwoods and softwoods, with the hemicellulose in hardwoods primarily consisting of the pentoses, whereas the hemicellulose in softwoods includes hexoses (Phaiboonsilpa et al., 2010).
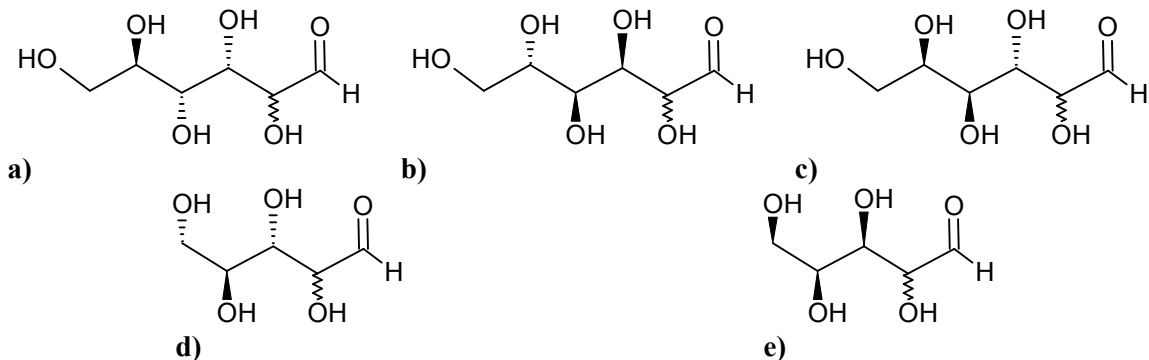
Figure 3.2: Structure of the primary sugar groups in hemicellulose. Hexoses: a) glucose, b) mannose, c) galactose and pentoses: d) xylose and e) arabinose.

Hemicellulose functions as a supporting material in cell walls and is, when compared to cellulose, more readily hydrolyzed to its individual monomeric units. Typically, hemicellulose accounts for 20 to 30% of the mass of dried wood and it is important to note that the composition

and structure of hemicellulose differs between not only hardwoods and softwoods, but also between the stem, branches, roots and bark of a given tree. This makes recovery of exact quantities of reducing sugars difficult (Sjöström, 1981).

3.2.3 Lignin

Lignin is a polymer made up of phenylpropane monomers, which are polymerized by peroxidases or phenoloxidases during biosynthesis and are derived from coniferyl, coumaryl and sinapyl alcohols (Mai et al., 2004; Ragauskas et al., 2006). The structure of lignin, like hemicellulose, depends both on the wood species and on where the lignin is located in the plant. In general, softwoods have higher lignin content than hardwoods (Pandey, 1999). Additionally, softwood lignin is largely based on a coniferyl alcohol unit (shown in Figure 3.3), whereas hardwood lignin is comprised of different base units, including coniferyl alcohol, in varying proportions (Pandey, 1999). A schematic of a representative section of the molecular structure of softwood lignin, as well as the coniferyl alcohol unit, is shown in Figure 3.4 (Pandey, 1999).
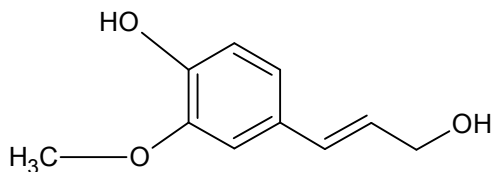
Figure 3.3: Structure of coniferyl alcohol.

The chemical structure of the phenylpropane monomers and their network linkages vary based on morphological regions (middle lamella or secondary wall), cell types and type of wood (hardwood or softwood) (Glasser and Sarkanen, 1989). In the middle lamella of wood lignin is a random three-dimensional network polymer; its most common form. Additionally, lignin is present in the secondary cell wall as a two-dimensional network polymer (Glasser and Sarkanen, 1989).
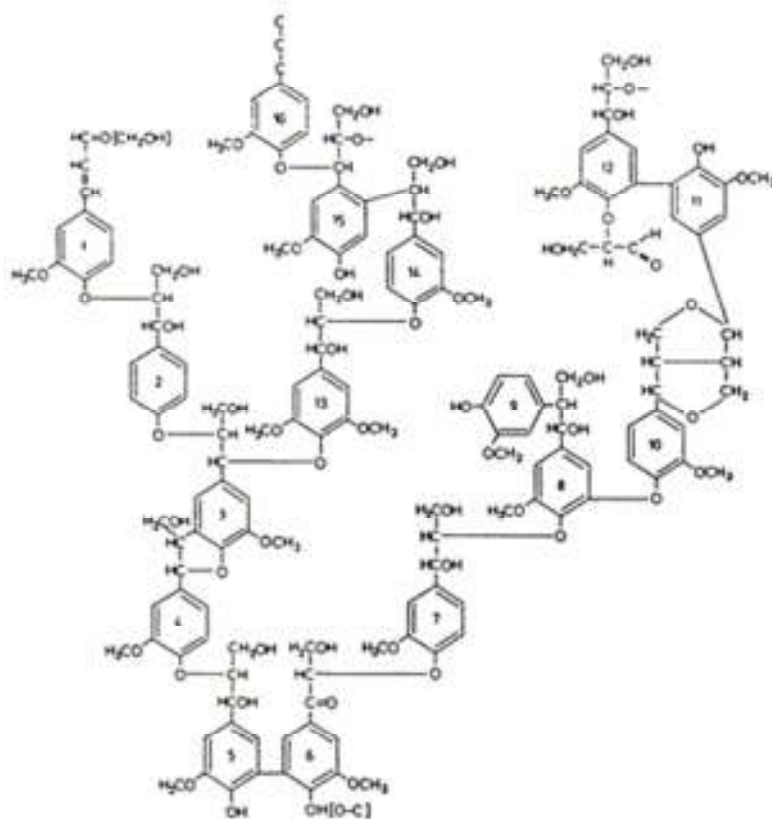
Figure 3.4: Representative chemical structure of a section of softwood lignin (Pandey, 1999).

3.3 Characterization in Biorefineries

Precise characterization of the inputs and outputs of industrial biorefineries is required in order to advance research in this area. As such, an understanding of how characterization has been conducted to date and the challenges, limitations and advances of these approaches, as well as how these pertain to the biorefinery concept and its future research and development will be presented herein. A wide range of procedures exist for lignocellulose analysis that generally fall into either the realm of classical, wet chemical approaches or instrumental techniques, each with their own advantages and limitations (Baeza and Freer, 2001).

The interdependence of the physical characteristics of cellulose makes distinguishing effects that are correlated to a pretreatment technique from the direct cause and effect of that

pretreatment technique essential. This is especially important when trying to understand and assess the effectiveness of different cellulose pretreatment methods. For example, pretreatment methodologies that decrease cellulose crystallinity often increase surface area, and thus a decoupling of the effect of the pretreatment technique on these two properties is required for evaluation of the end goal of a pretreatment method, which typically involves an improvement in cellulose hydrolysis (Zhang and Lynd, 2004). Well defined testing methods, including sampling procedures and analytical techniques, for wood (lignocellulosic biomass) have been published by the Canadian Pulp and Paper Association (CPPA), Technical Association of the Pulp and Paper Industry (TAPPI) and the American Society of Testing and Materials (ASTM) (Baeza and Freer, 2001; Morohoshi, 1991). The following section describes common analytical approaches applicable to biorefineries, however, it should not be considered exhaustive as novel approaches are continually being developed. The analytical techniques outlined here are presented individually to best outline the value and limitations of each methodology. However, it should be noted that many techniques can be used in conjunction with one another to enhance characterization.

3.3.1 Crystallinity Index

Hydrolysis rates for amorphous cellulose are typically much faster than for crystalline cellulose. Therefore, the crystallinity index, CrI, of a sample can be helpful in assessing amenability to hydrolysis (Lynd et al., 2002; Zhang and Lynd, 2004). This crystallinity index, which is a measure of the relative degree of crystallinity, can be determined through the use of X-ray diffraction (XRD) using the following relationship (Segal et al., 1959):

$$CrI = \left(\frac{I_{Cr} - I_{Am}}{I_{Cr}}\right) \times 100$$

Where I_{Cr} is the maximum intensity of the crystalline region (using the 002 reflection measured at $2\theta = 22.5°$ for cellulose I, or the 101 reflection measured at $2\theta = 19.8°$ for cellulose II). I_{Am} is the

maximum intensity of the amorphous region (where $2\theta=18°$ for cellulose I and $2\theta=16°$ for cellulose II) (Oh et al., 2005; Segal et al., 1959).

The CrI of cellulose can also be measured using Fourier Transform Infrared Spectroscopy (FTIR). The ratio of certain infrared bands that appear in FTIR spectra can be related to the crystallinity and type of cellulose present in the sample. Specifically, two well-established indices exist that are a measure of cellulose crystallinity. First, the lateral order index (LOI), defined as $\frac{a_{1429cm^{-1}}}{a_{898cm^{-1}}}$, where the band at 1429 cm^{-1} is attributed to the CH$_2$ scissoring or symmetric bend in cellulose I (this band is shifted to 1420 cm^{-1} in cellulose II) and the band at 893 cm^{-1} is attributed to the C$_1$ group (Hurtubise and Krassig, 1960; Morohoshi, 1991; Nelson and O'Connor, 1964b). The second index, known as the total crystallinity index (TCI) is defined as $\frac{a_{1872cm^{-1}}}{a_{2900cm^{-1}}}$, where the band at 1372 cm^{-1} is attributed to C-H deformation (bending) and the band at 2900 cm^{-1} is attributed to C-H and CH$_2$ stretching. The suitability of FTIR analysis to measure cellulose crystallinity has been compared to XRD measurements and a linear relationship between the results of the two techniques was shown to exist (Marson and El Seoud, 1999). Additionally, it has been shown that the LOI is a better indicator of changes in crystallinity than the TCI for lignocellulose-based cellulose samples (Nelson and O'Connor, 1964a; Zhao et al., 2009).

Nuclear magnetic resonance spectroscopy (NMR) has also been used to measure the CrI of cellulose. Both curve fitting and partial least-squares (PLS) regression have been employed to measure CrI (Lennholm et al., 1994; Teeäär et al., 1987). As with FTIR analysis, the suitability of NMR to measure cellulose crystallinity has been compared to XRD and again a linear relationship between the results of the two techniques was demonstrated. NMR can also be employed to determine the composition of lignocellulosic materials, discussed in Section 3.3.4.2 Non-invasive Techniques.

Optical microscopy has been used to monitor cellulose dissolution in hot water (Deguchi and Tsujii, 2002; Deguchi et al., 2006; Deguchi et al., 2008) and in ionic liquids (Wu et al., 2009;

Zavrel et al., 2009). Crystalline dissolving cellulose can be observed when cross-polarized lenses are used in the optical microscope due to the birefringent nature of crystalline cellulose. This technique represents an interesting breakthrough in cellulose crystallinity measurement as changes in the crystallinity of cellulose can be observed in real time, providing immediate feedback. However, to date this method has only been used qualitatively with no quantitative crystalline cellulose or CrI measurement techniques reported. However, it may be possible to use optical microscopy as a rapid screening technique to evaluate the effectiveness of a solvent in dissolving cellulose that may be overlooked by the more common optical inspection technique.

Measurement of the CrI of lignocellulosic materials is more difficult than with cellulosic materials. Because the crystallinity index of lignocellulose is impacted by the presence of both lignin and hemicellulose comparison of the CrI of lignocellulosic feedstocks to the CrI of pure cellulosic feedstocks may be misleading (Kumar et al., 2009). In addition, as a number of pretreatment techniques alter the physical structure of the feedstock, direct comparison of the CrI of pretreated lignocellulosic materials to non-pretreated materials may not be straightforward and require additional calibration data.

3.3.2 Degree of Polymerization (DP)

There are three different ways in which DP may be defined; number average DP (DP_N), weight average DP (DP_W), or DP inferred from viscosity (DP_V). DP_N values are typically adequate when analyzing cellulose for hydrolysis experiments, while DP_W and DP_V values are used to estimate cellulose properties (Zhang and Lynd, 2004). DP_N can be measured from membrane or vapour pressure osmometry, cryoscopy, ebullioscopy, determination of reducing end concentration, and/or electron microscopy. DP_W can be measured from light scattering, sedimentation equilibrium, and X-ray small angle scattering. DP_V can be calculated from viscosity measurements, obtained from dissolved cellulose solutions (Zhang and Lynd, 2004). The relative solubility of cellulose can be approximated from the DP value, as solubility

drastically decreases with increasing DP due to a corresponding increase in intermolecular hydrogen bonds. However, these DP measures are better suited to model biomass compounds due to the complexity of lignocellulosic biomass (Zhang and Lynd, 2004).

The distribution of DPs for a sample of cellulose (before and after pretreatment) can also be measured through the use of chromatographic techniques including gel-permeation chromatography (GPC)/size-exclusion chromatography (SEC) (Rinaldi et al., 2008; Zhang and Lynd, 2004). However, to use this analytical technique, the cellulose must be derivatized (e.g. using the tricarbanilate form). Similarly, the molecular weight of lignin (number average (M_n) and weight average (M_w) molecular weights) can be determined using gel-permeation chromatography on native and derivatized (lignin acetate) samples (Pan et al., 2005).

3.3.3 Surface Area

Cellulosic particles have both external and internal surface areas, with the internal surface area being much larger than the external surface area (Goering and Van Soest, 1970; Zhang and Lynd, 2004). In general, techniques used to estimate internal surface area cannot be used to estimate external surface area and vice versa. Internal surface areas can be measured by small angle X-ray scattering, mercury porisometry and water vapour sorption. External surface areas, being related to particle shape and size, can be measured from microscopy (both light and electron). The morphology of the cellulose can be determined using field emission scanning electron microscopy, as well as via scanning electron microscopy (Khanal et al., 2007; Teramoto et al., 2008).

3.3.4 Composition

Methods for determining the composition of lignocellulosic biomass, particularly lignin content, can be classified into two categories: invasive and non-invasive methods (Hatfield and Fukushima, 2005).

3.3.4.1 *Invasive Techniques*

The main approaches for invasive techniques are based on the chemical nature of lignin and lignocellulosic materials. Some analytical techniques for the determination of lignin composition rely on the premise that the consumption of oxidants by lignin will occur more readily than by other lignocellulose components. The amount of oxidant consumed (typically chlorine or potassium permanganate) can be used as an approximate measure of the lignin quantity (Hatfield and Fukushima, 2005). There are also procedures available whereby lignin in solution is measured, requiring complete solubilisation of lignin. The thioglycolate lignin method chemically modifies lignin to make the lignin soluble under alkali conditions. Quantification is based on absorbance values obtained from a known quantity of synthetic dehydrogenation lignin polymer (DHP). However, difficulties have been noted with acid soluble lignin, such as lignin obtained from grasses, which may remain in solution during the acid precipitation steps of this process, underestimating the total lignin content (Hatfield and Fukushima, 2005). Another solubilisation technique is the acetyl bromide method, in which the sample is digested by an acetyl bromide in acetic acid solution and UV absorption is conducted on the resulting solution (Johnson et al., 1961). One challenge common to both lignin solubilisation techniques is the need for well-defined lignin calibration standards due to the variable nature of lignin.

Gravimetric measurements can be conducted on lignin residue formed when mineral acids are used to solubilize and hydrolyze cell wall carbohydrates. The most common gravimetric technique is the Klason H_2SO_4 acid procedure, which uses H_2SO_4 to dissolve the polysaccharides in a sample leaving insoluble lignin, which is then rinsed, dried and measured (Sluiter et al., 2008). To remove insoluble materials such as waxes, a variety of preprocessing methods have been developed (Hatfield and Fukushima, 2005). Modifications to this procedure have been reported, including the modification involving acid detergent extraction, leaving a mixture of cellulose and lignin referred to as acid detergent fibre (Hatfield and Fukushima, 2005; Van Soest and McQueen, 1973).

To estimate the quantity of reducing sugars, high performance liquid chromatography (HPLC) can be employed to analyze hydrolysate for sugar content and composition. Additionally, colorimetric assays, such as the dinitrosalicylic acid (DNS) assay, are well-established methods. The DNS assay measures the percent transmittance of the sample at 540 nm using a colorimeter (Miller, 1959). It is non-specific and will measure any reducing sugar and be reported in glucose equivalents. However, conversion to specific reducing sugar estimates can be obtained (Ghose, 1987). For instance if glucose is used as a standard, the percent transmittance for cellobiose will be 15% lower and for xylose will be 15% higher compared to the glucose standard on a weight basis (Ghose, 1987). Other reducing sugar estimation assays have been presented including, but not limited to, the anthrone assay and the Nelson-Somogyi methods. The anthrone assay uses a colormetric technique that incorporates a combination of anthrone and concentrated sulphuric acid to measure reducing sugar content via Ultraviolet-visible spectroscopy (UV-Vis). However, unlike the DNS assay, the anthrone assay is reducing sugar specific, thus the reducing sugar measured depends on the reducing sugar used for calibration (Yemm and Willis, 1954). The Nelson-Somogyi method is also a colormetric technique that measures the reduction of Nelson's copper reagent at 500 nm on a UV-Vis spectrophotometer. This technique can also be used to measure cellulase activity and has the capacity to determine lower sugar concentrations than the DNS assay (Somogyi, 1952).

Additionally, lignin content in lignocellulosic samples can be determined by first hydrolyzing the sample and then applying the Beer-Lambert Law to corresponding UV-microspectrophotometry spectra (Hatfield and Fukushima, 2005):

$$A = -\log\left(\frac{I}{I_0}\right)$$

Here, A is the absorbance of the sample and I and I_0 are the intensities of the transmitted (after passing through the sample) and incident (before reaching the sample) light, respectively. The aim of this technique is to exploit the unique UV absorption spectrum of lignin allowing for the

quantification of lignin content. Hansmann et al. (2004) used UV-microscopy to analyze spruce and birch wood subjected to three different acetylation procedures (acetic anhydride in a non-catalyzed process, isopropenylacetate, and liquid phase acetylation with acetic anhydride). The resulting spectra showed a tendency for characteristic lignin absorbance to shift from 280 nm to shorter wavelengths with acetylation. Moreover, a relationship between weight percent gain through acetylation and the observed spectral shift was established (Hansmann et al., 2004). The use of UV-Vis spectroscopy to determine acid soluble lignin concentration in biomass has also been reported (Hyman et al., 2008).

3.3.4.2 *Non-invasive Techniques*

Here, the term non-invasive refers to the fact that the following techniques leave the sample chemically unaltered, though they may be physically damaging. This may be of considerable interest for biorefinery development as analyses could be conducted *in situ*. However, as with invasive techniques, non-invasive methods require a standard calibration sample and thus often depend on the accuracy of the standard (Hatfield and Fukushima, 2005).

Infrared spectroscopy can be used to characterize phenolics in cell wall samples and quantify the lignin content. Since this technique measures the vibrational energy of different bond types, a single sample can yield considerable information, though an overlap of peak intensities can occur in certain regions of the spectra. This technique allows for the determination of structural and compositional similarities between samples, however, determining total lignin content in the cell wall is difficult. FTIR has been used in plant cell wall analysis where the different polysaccharide structures and compositions were identified based on unique spectral band positions (Kačuráková et al., 2000). Recent developments in FTIR analytical techniques have led to its use in determining the composition of biomass feedstocks, such as corn stover and wood, as well as the lignin and sugar contents of hydrolysates from dilute acid pretreatment (Hames et al., 2003; Moore and Owen, 2001; Tucker et al., 2001). In 2001, Moore and Owen

reviewed the use of FTIR in wood taxonomy to study the mechanisms of weathering and fungal decay of wood and to investigate chemically modified wood (Moore and Owen, 2001). Developments in the use of real time FTIR for process monitoring have enabled *in situ* monitoring of liquid phase sucrose hydrolysis and the online monitoring of ethanol fermentation (Pintar et al., 2002; Veale et al., 2007).

Near infrared spectroscopy (NIR) has also been utilized as a means to quantify lignin through the use of the electromagnetic radiation between visible and conventional infrared wavelengths. In addition to its use to measure lignin, NIR has been used to quantify other plant components (such as fats, oils, proteins, total fibre, etc.) by correlating spectral changes to specific concentrations of the component being measured through reference wet chemistry methods (Hatfield and Fukushima, 2005). ASTM has issued a document that outlines procedures to develop a quantitative infrared analytical technique (ASTM Committee E13 on Molecular Spectroscopy and Chromatography, 2005).

NMR has also been used to provide both characterization of composition and structural features of lignin, especially when the lignin can be dissolved in an appropriate solvent. However, this is not always feasible and severely limits the usefulness of NMR. Although it has been demonstrated that solid state NMR can be used, due to the difficulty in obtaining clean peaks coupled with the cost of instrumentation, solid state NMR has not been widely used to characterize lignocellulosic materials. Quantitative estimates of cellulosic material and lignin extraction of a fractionation technique via NMR were employed by Fort et al. (2007), but the authors acknowledged that the poor signal-to-noise ratio observed in NMR spectra of the biomass extracts led to large integration errors and, consequently, high uncertainty in their measurements.

3.4 Ionic Liquids in a Biorefining Context

3.4.1 Properties

As has been previously discussed, ionic liquids (ILs) are a class of organic salts that are liquid at low (often ambient) temperatures (Fort et al., 2007; Lee et al., 2008; Yang and Pan, 2005). The basis for the formation of the liquid phase in ILs is analogous to that seen in more classical ionic compounds. As the size of the ion increases and its charge decreases, less energy is required to break the bond between ions. Thus large cations (including imidazolium based ions) have a greater difficulty fitting into the favourable lattice structure. This results in lower lattice energy and a depression in the melting point, allowing these ionic compounds to exist as liquids at low temperatures (Dupont and Suarez, 2006). Ionic liquids are composed of ions, unlike traditional solvents that can be described as molecular liquids (Yang and Pan, 2005). Furthermore, their unique properties including very low (often negligible) vapour pressures, good chemical and thermal stability, and non-flammability in some cases, have allowed them to be investigated as alternatives to a number of common solvents (Fort et al., 2007; Lee et al., 2008; Yang and Pan, 2005). However, ILs need to be cost effective in order to be commercially used for cellulose dissolution processes (Hermanutz et al., 2008). Other IL properties of interest in lignocellulosic biomass dissolution, namely viscosity and the hydrogen bonding network, will be discussed in the following sections.

Typically characterization of the physical properties of ILs is conducted under inert environments (such as argon) (Bonhote et al., 1996; Okoturo and VanderNoot, 2004). Though this approach is useful in determining the physical properties of ILs and for furthering the development of tailor-made ILs, these measurements are often not indicative of the conditions under which the IL would be used in industry.

3.4.1.1 *Viscosity*

One potential drawback in using ILs as solvents is their viscosity, as high viscosity can limit mass transfer. Generally, ILs have a higher viscosity than common solvents, with viscosities typically ranging from 10 mPa·s to 500 mPa·s (Endres and Abedin, 2006). The viscosity of ILs is due both to van der Waals forces and hydrogen bonding, which are equally important (Bonhote et al., 1996; Endres and Abedin, 2006; Okoturo and VanderNoot, 2004). For example, Bonhote et al. (1996) demonstrated that although a change in IL anion suppressed hydrogen bonding, the increase in size of the anion and subsequent increase in van der Waals attraction, led to an increase in viscosity. However, a different set of anions achieved sufficient hydrogen bond suppression to overcome the increase in van der Waals attraction and decreased the viscosity (Bonhote et al., 1996). The cations also play a role in the viscosity of the IL as an increase in alkyl chain length will increase the viscosity of the IL due to an increase in van der Waals interactions (Bonhote et al., 1996; Endres and Abedin, 2006). It has, however, been demonstrated that the viscosity of ILs will decrease with increasing temperature, which may also increase mass transfer in the IL phase (Endres and Abedin, 2006; Okoturo and VanderNoot, 2004).

3.4.1.2 *Hydrogen Bonding Network*

The hydrogen bonding network of ILs is believed to be the most important factor in not only the dissolution of cellulose, but also the dissolution of lignocellulosic biomass as a whole. The exact mechanism by which dissolution occurs is not fully understood, but it is believed to be two-fold. Firstly, the role of the anion in the dissolution of biomass is important. Anions which can deprotonate cellulose (via free hydroxyl groups) interfere with the internal hydrogen bonding networks present and act as non-derivatizing solvents for cellulose and lignocellulosic biomass (Dadi et al., 2006; Dupont and Suarez, 2006; Kilpeläinen et al., 2007; Liu and Chen, 2006; Moulthrop et al., 2005; Remsing et al., 2006; Swatloski et al., 2002; Youngs et al., 2007; Zavrel et al., 2009). This is due to anion interaction with the proton in the cellulose hydroxyl group,

disrupting the hydrogen bonding network (Dadi et al., 2006). It has also been suggested that cations can play a role in the dissolution of biomass in ILs (Dadi et al., 2007; Dadi et al., 2006; Youngs et al., 2007; Zavrel et al., 2009). Zhang et al. (2005) suggested that the cation can interact with the oxygen in the cellulose hydroxyl group and thus disrupt the hydrogen bonding network (Zhang et al., 2005). It is the competition of the cation and anion in ILs with lignocellulosic components that causes the dissolution of these components (Kilpeläinen et al., 2007; Moulthrop et al., 2005; Remsing et al., 2006). Kilpeläinen et al. (2007) also suggested that the π-π interactions present in the cations of ILs may interact with the π-π bonds in lignin, further aiding in the dissolution process (Anderson et al., 2002; Kilpeläinen et al., 2007; Zavrel et al., 2009).

3.4.2 Biomass Processing

With the increase in the use of ILs in lignocellulosic biomass dissolution, research into this area has seen a significant increase in the last decade, culminating in several review papers including the dissolution of cellulose in ILs (Feng and Chen, 2008; Zhu et al., 2006), cellulose processing and modification (Cao et al., 2009; Feng and Chen, 2008), the role of ILs in the dissolution and utilization of lignocellulosic materials (Han et al., 2009; Tan and MacFarlane, 2009; Xie et al., 2010; Zhu, 2008), and the role of ILs in the production of value-added chemicals from lignin (Zakzeski et al., 2010). The following section will briefly survey the use of ILs for biomass processing, specifically their use with cellulose, lignin and lignocellulosic materials.

3.4.2.1 *Cellulose*

Cellulose dissolution and/or reaction in ILs has been increasingly studied in the last decade. A brief survey of examples of cellulose dissolution in ILs is summarized in Table 3.2. The dissolution of cellulose in different ILs has also been the focus of screening studies, most notably those by Zavrel et al. (2009) and Vitz et al. (2009). Zavrel et al. (2009) conducted a high-throughput screening study of 21 different ILs. Vitz et al. (2009) observed that an increase in the water content of the IL resulted in a decrease in the cellulose solubility in the IL and that the

cellulose dissolved in 1-ethyl-3-methylimidazolium diethyl phosphate ([emim][Et$_2$PO$_4$]) could be tritylated with a degree of substitution of 1.17 (Vitz et al., 2009). Water, as well as ethanol and methanol have been determined to be "anti-solvents" for cellulose dissolved in ILs. These anti-solvents cause the rapid precipitation of cellulose upon sufficient addition to IL/cellulose solutions (Dadi et al., 2006).

Table 3.2: Examples of studies on the dissolution of cellulose in ionic liquids.

Conditions	Ionic Liquid	Source
25 wt%, microwave heating	[bmim]Cl	Swatloski et al., 2002
5-7 wt%	[bmim]Br	Swatloski et al., 2002
5-7 wt%	[bmim][SCN]	Swatloski et al., 2002
14.5 wt%	[amim]Cl	Zhang et al., 2005
5 wt%, 90°C, 12 hrs	[amim]Cl	Zavrel et al., 2009
5 wt%, 90°C, 12 hrs	[emim]Cl	Zavrel et al., 2009
5 wt%, 90°C, 12 hrs	[bmim]Cl	Zavrel et al., 2009
5 wt%, 90°C, 12 hrs	ECOENG	Zavrel et al., 2009
5 wt%, 90°C, 12 hrs	[emim][OAc]	Zavrel et al., 2009
5 wt%, 105°C, 12 hrs	[bmpy]Cl	Zavrel et al., 2009
12 wt%, 100°C	[emim][OAc]	Vitz et al., 2009
8 wt%, 100°C	[bmim][OAc]	Vitz et al., 2009
14 wt%, 100°C	[emim][Et$_2$PO$_4$]	Vitz et al., 2009

The processing of cellulose dissolved in ILs has also been frequently investigated. A brief survey of examples where cellulose was processed, either *in situ* or after being precipitated from dissolution in ILs is presented in Table 3.3. The acetylation of dissolved cellulose was demonstrated with degrees of substitution of 0.94-2.74 in [amim]Cl (Wu et al., 2004) and 2.5-3 in [bmim]Cl (Heinze et al., 2005). Heinze et al., 2005 also demonstrated that cellulose could be carboxymethylated within the same range of degree of substitution. Furthermore, yields >93% (by weight of the theoretical maximum) of cellulose acetate were obtained via functionalization of cellulose in [emim][OAc], with a degree of substitution between 0.55-1.86 (Köhler et al., 2007). The production of cellulose acetate in ILs is particularly interesting due to its industrial and commercial appeal as a fabric for clothing, use in sunglasses and for the production of playing cards. After cellulose dissolution in [bmim]Cl, electrospinning was used by Viswanathan

et al. (2006) and Sun et al. (2008) to produce cellulose/cellulose-heparin films and magnetic cellulose fibres, respectively.

Table 3.3: Examples of cellulose processing involving ionic liquids.

Process	Ionic Liquid	Source
Tritylation	[emim][Et$_2$PO$_4$]	Vitz et al., 2009
Acetylation	[amim]Cl	Wu et al., 2004
Acetylation	[bmim]Cl	Heinze et al., 2005
Carboxymethylation	[bmim]Cl	Heinze et al., 2005
Functionalization to cellulose acetate	[emim][OAc]	Köhler et al., 2007
Films of cellulose and cellulose heparin	[bmim]Cl	Viswanathan et al., 2006
Magnetic fibres	[bmim]Cl	Sun et al, 2008
Enzymatic hydrolysis	[bmim]Cl	Dadi et al, 2006
Enzymatic hydrolysis	Glycol-substituted ILs	Zhao et al., 2008
Enzymatic hydrolysis	[emim][OAc]	Zhao et al., 2009
Enzymatic hydrolysis	[bmim]Cl	Zhao et al., 2009
In situ hydrolysis	[bmim]Cl	Li and Zhao, 2007
In situ hydrolysis	[bmim]Cl	Li et al., 2008
In situ hydrolysis	[emim]Cl	Zhang et al., 2010

The conversion of cellulose to reducing sugars after treatment with ILs has also been of recent interest. Dadi et al. (2006) demonstrated that IL treatment of cellulose could enhance enzymatic hydrolysis kinetics; initial hydrolysis by *Trichoderma reesei* cellulase was at least 50 times higher for the treated as compared to untreated cellulose samples. Additionally, there was no difference in hydrolysis rate for IL pretreatments conducted at different temperatures and times and no difference in regenerated cellulose structure was found based on IL incubation time or choice of anti-solvent (water, ethanol, methanol) (Dadi et al., 2006). Zhao et al. (2008) synthesized new glycol-substituted ILs (with either an acetate or chloride anion) that demonstrated microcrystalline cellulose dissolution in ILs was feasible without enzyme, specifically lipase, denaturing. Furthermore, regenerated cellulose from dissolution in glycol-substituted ILs, [emim][OAc] and [bmim]Cl was hydrolyzed by *T. reesei*, with at least a 2-fold increase in hydrolysis rate and a 1.7-fold increase in reducing sugar concentration after 48 hours as compared to the untreated cellulose (Zhao et al., 2009). In addition, acid hydrolysis of cellulose treated with ILs has also been studied. H$_2$SO$_4$ added to cellulose dissolved in [bmim]Cl facilitated

56

in situ hydrolysis which resulted in glucose yield of 43% and a total reducing sugars (TRS) yield of 77% (of the theoretical maximum) (Li and Zhao, 2007; Li et al., 2008). Also, cellulose dissolved in [emim]Cl has also been converted to either reducing sugars (97% of the theoretical maximum) or hydroxymethylfurfural (HMF) (89% of the theoretical maximum) depending on catalyst addition (Zhang et al., 2010).

3.4.2.2 *Lignin*

In comparing studies investigating the use of ILs for dissolution and processing, there is far less literature on lignin compared to cellulose and lignocellulose, however, two key studies have focused on lignin dissolution in ILs Pu et al. (2007) studied the dissolution of a softwood lignin isolated from southern pine Kraft pulp in various ILs at 25°C to 120°C. Lee et al. (2008) investigated Indulin AT (lignin from the Kraft pulping process) solubility. A summary of lignin dissolution in each study is provided in Table 3.4. In addition, Lee et al. (2008) determined that [emim][OAc] could be recycled (after wood flour dissolution) without affecting the accumulation of dissolved lignin and lignin dissolution, resulting in lignin extraction of 0.68 - 0.72 wt% after 24 hours at 90°C for each cycle. Also, when 40% lignin was removed by [emim][OAc], hydrolysis of >90% of the theoretical maximum of cellulose in the maple wood flour was demonstrated by *Trichoderma viride* cellulase (Lee et al., 2008).

Table 3.4: Summary of key studies on the dissolution of lignin in ionic liquids.

Conditions	Ionic Liquid	Source
344 g/L at 50°C and 74.2 g/L at 25°C	[mmim][MeSO$_4$]	Pu et al., 2007
275 g/L at 70°C and <10 g/L at 50°C	[hmim][CF$_3$SO$_3$]	Pu et al., 2007
312 g/L at 50°C and 61.8 g/L at 25°C	[bmim][MeSO$_4$]	Pu et al., 2007
13.9 g/L at 75°C	[bmim]Cl	Pu et al., 2007
17.5 g/L at 75°C	[bmim]Br	Pu et al., 2007
14.5 g/L between 70°C-100°C	[bm$_2$im][BF$_4$]	Pu et al., 2007
>33 wt%, 90°C, 24 hrs	[mmim][MeSO$_4$]	Lee et al., 2008
>33 wt%, 90°C, 24 hrs	[bmim][CF$_3$SO$_3$]	Lee et al., 2008
>23 wt%, 90°C, 24 hrs	[emim][OAc]	Lee et al., 2008
>23 wt%, 90°C, 24 hrs	[amim]Cl	Lee et al., 2008
>10 wt%, 90°C, 24 hrs	[bmim]Cl	Lee et al., 2008
>9 wt%, 90°C, 24 hrs	[bzmim]Cl	Lee et al., 2008
~4 wt%, 90°C, 24 hrs	[bmim][BF$_4$]	Lee et al., 2008
~0.1 wt%, 90°C, 24 hrs	[bmim][PF$_6$]	Lee et al., 2008

3.4.2.3 *Lignocellulose*

A summary of the conditions for several lignocellulosic biomass dissolution in IL studies is presented in Table 3.5. Fort el al. (2007) investigated [bmim]Cl, diluted with 15 wt% deuterated dimethyl sulfoxide (DMSO-d_6) to reduce viscosity and allow for NMR investigation, as a solvent for oak, eucalyptus, poplar and pine at 100°C. Between 60 and 70 wt% of the lignocellulosic material for each species was dissolved within 24 hours. Interestingly, a cellulosic material to lignin extraction ratio of nearly 2:1 was observed throughout the study, which corresponded well to the chemical composition of the wood species. This demonstrated that both of the natural polymers were extracted in [bmim]Cl at approximately equal rates (Fort et al., 2007). Additionally, the dissolution of wood chips, Norway spruce (sawdust and thermomechanical pulp (TMP)) and Southern pine (powder and TMP) in two commonly used ILs was conducted by Kilpeläinen et al. (2007). The authors concluded that the dissolution rate of wood species in ILs was highly dependent on particle size, with smaller particles dissolving much more rapidly than larger ones in ILs. Additionally, an increase in the water content of the wood sample was found to significantly decrease the solubility of the wood in ILs. Finally, screening

studies for lignocellulosic biomass dissolution in ILs have been previously undertaken by Zavrel et al. (2009) and Lee et al. (2008). A high-throughput study of ILs for lignocellulose dissolution using cellulose (α-cellulose and Avicel (microcrystalline) cellulose) and both softwood (spruce and silver fir) and hardwood (common beech and chestnut) species was conducted by Zavrel et al. (2009). Dissolution experiments took place at 90°C for 12 hours with a 5 wt% biomass loading. It was determined that [amim]Cl could fully dissolve all species, [emim][OAc] could fully dissolve all species except for silver fir, while [emim]Cl, [bmim]Cl and ECOENG could only partially dissolve the lignocellulosic species but fully dissolve both types of cellulose (Zavrel et al., 2009). Lee et al. (2008) determined that maple wood flour could be dissolved at <0.5 wt% in [emim][OAc] and >2.9 wt% in [amim]Cl and [bmim]Cl at 80°C for 24 hours under a nitrogen atmosphere.

Table 3.5: Examples of studies on the dissolution of lignocellulosic biomass in ionic liquids.

Conditions	Ionic Liquid	Source
60-70 wt%, 15 wt% DMSO, 100°C, 24 hrs	[bmim]Cl	Fort et al., 2007
Partially-8 wt%, 110°C-130°C, 8-15 hrs	[bmim]Cl	Kilpeläinen et al., 2007
2-8 wt%, 80°C-130°C, 8-24 hrs	[amim]Cl	Kilpeläinen et al., 2007
5 wt%, 130°C, 8 hrs	[bzmim]Cl	Kilpeläinen et al., 2007
2-5 wt%, 130°C, 8 hrs	[bz-ome-mim]Cl	Kilpeläinen et al., 2007
2 wt%, 130°C, 8 hrs	[bzmim][Dca]	Kilpeläinen et al., 2007
5 wt%, 90°C, 12 hrs	[amim]Cl	Zavrel et al., 2009
Up to 5 wt%, 90°C, 12 hrs	[emim][OAc]	Zavrel et al., 2009
Partially, 90°C, 12 hrs	[emim]Cl	Zavrel et al., 2009
Partially, 90°C, 12 hrs	[bmim]Cl	Zavrel et al., 2009
Partially, 90°C, 12 hrs	ECOENG	Zavrel et al., 2009
<0.5 wt%, 80°C, 24 hrs	[emim][OAc]	Lee et al., 2008
>2.9 wt%, 80°C, 24 hrs	[amim]Cl	Lee et al., 2008
<2.9 wt%, 80°C, 24 hrs	[bmim]Cl	Lee et al., 2008

The processing of lignocellulosic biomass in ILs, beyond simple dissolution, has also come to the forefront. A brief summary of examples where lignocellulosic biomass was processed, either *in situ* or after being precipitated from dissolution in ILs is presented in Table 3.6. Sun et al. (2009) demonstrated the fractionation of both softwood (Southern yellow pine) and hardwood (Red oak) species in [emim][OAc]. The cellulose alone could be precipitated with a 1:1

acetone/water mixture, after which lignin was precipitated though the addition of pure acetone (Sun et al., 2009). Nearly 60% of the original hollocellulose (a combination of hemicellulose and cellulose) was recovered in the cellulosic rich fraction and nearly 1/3 of the original lignin was recovered in free form (Sun et al., 2009). Fractionation of model lignocellulosic biomass was demonstrated by Lateef et al. (2009), when cellulose fibres (between 0.02 and 1.5 mm diameter) and lignin (alkali, low sulfonate content) were dissolved in [bmim]Cl and 1-propyl-3-methylimidazolium bromide ([propylmim]Br). Upon the addition of water, cellulose floc precipitated out, after which ethanol was added to the IL/lignin mixture and lignin was precipitated in 69% and 49% yields (of the theoretical maximum) from [propylmim]Br and [bmim]Cl, respectively (Lateef et al., 2009).

Liu and Chen (2006) investigated the hydrolysis of wheat straw and steam exploded wheat straw (SEWS) by a cellulase solution over a 48 hour period both with and without [bmim]Cl treatment. The SEWS and wheat straw were fully and >70% (of the theoretical maximum) hydrolyzed after the [bmim]Cl treatment and only >40% and >65% (of the theoretical maximum) hydrolyzed with water treatment (Liu and Chen, 2006). *In situ* hydrolysis of lignocellulosic materials has also been demonstrated (Li et al., 2008). 7 wt% HCl was added to [bmim]Cl, at 100°C under atmospheric pressure, and after 60 minutes TRS yields for various biomass types were determined based on initial carbohydrate content (corn stalk - 66%, rice straw - 74%, pine wood - 81%, and bagasse - 68%). It was also observed that the hydrolysis and subsequent TRS degradation followed a consecutive first order reaction sequence, with the rate constant for TRS formation being an order of magnitude greater than TRS degradation (Li et al., 2008). Sievers et al. (2009) also demonstrated *in situ* reactions with lignocellulosic biomass and ILs, by adding 0.2 wt% trifluoroacetic acid (TFA) to nearly 5 wt% loblolly pine wood dissolved in [bmim]Cl for 2 hours at 120°C which resulted in 62% of the feedstock, by weight, being solubilized after 2 hours of reaction, corresponding to 97% (of the theoretical maximum) of the

carbohydrate fraction of the wood sample being dissolved to a combination of sugars, furfural and

HMF.

Table 3.6: Examples of lignocellulosic biomass processing involving ionic liquids.

Process	Ionic Liquid	Source
Fractionation	[emim][OAc]	Sun et al., 2009
Fractionation	[bmim]Cl	Lateef et al., 2009
Fractionation	[propylmim]Br	Lateef et al., 2009
Enzymatic hydrolysis	[bmim]Cl	Liu and Chen, 2006
In situ hydrolysis	[bmim]Cl	Li et al., 2008
In situ hydrolysis	[bmim]Cl	Sievers et al., 2009

3.5 Current Technological Barriers

There are two main difficulties associated with the processing of biomass in ILs. Firstly the high viscosity of most ILs makes their handling difficult and may inhibit their use as biomass solvents. This problem is intensified with increasing cellulose dissolution in the ILs. To overcome this issue ILs are typically diluted with an organic solvent that does not dissolve cellulose, often DMSO (Fort et al., 2007). However, large volumes of DMSO are required (typically ≥15 wt% to dissolve 5 wt% biomass), which can be expensive and combustible. The second technological barrier encountered in using ILs for the dissolution and processing of biomass is a lack of characterization tools and techniques (Joglekar et al., 2007). It is difficult to characterize new ILs and the quantitative determination of dissolved biomass content in an IL is not straightforward. Traditionally, the amount of biomass dissolved in an IL has been analyzed by visual inspection (Heinze et al., 2005; Kilpeläinen et al., 2007; Köhler et al., 2007; Pu et al., 2007). However, this is not quantitative. This technique cannot be applied to kinetic studies where biomass dissolution is at different stages of completion. Additionally, it is not sufficient to use visual inspection for rapid screening of whether or not an IL dissolves various types of biomass as it is not precise enough. This has led to the creation of elaborate rapid screening set-ups to determine if a given IL can dissolve cellulose or lignin. Characterization techniques that can be used to quantitatively describe how much of a particular biomass component is dissolved in an IL, as well as techniques

that can be used to rapidly and simply screen whether or not an IL can be used to dissolve biomass require further development.

3.6 References

Anderson, J.L., J. Ding, T. Welton, D.W. Armstrong, 2002. Characterizing ionic liquids on the basis of multiple solvation interactions, J.Am.Chem.Soc. 124, 14247-14254.

Andersson, S., H. Wikberg, E. Pesonen, S.L. Maunu, R. Serimaa, 2004. Studies of crystallinity of Scots pine and Norway spruce cellulose, Trees. 18, 346-353.

ASTM Committee E13 on Molecular Spectroscopy and Chromatography, 2005. Standard practices for infrared multivariate quantitative analysis, E 1655 - 05, 1-29.

Baeza, J., Freer, J., 2001. Chemical characterization of wood and its components, Wood and Cellulosic Chemistry. Marcel Dekker, New York, pp. 275-384.

Bonhote, P., A. Dias, N. Papageorgiou, K. Kalyanasundaram, M. Gratzel, 1996. Hydrophobic, highly conductive ambient-temperature molten salts, Inorg.Chem. 35, 1168-1178.

Brown Jr, R.M., I.M. Saxena, 2000. Cellulose biosynthesis: A model for understanding the assembly of biopolymers, Plant Physiol. Biochem. 38, 57-67.

Cao, Y., J. Wu, J. Zhang, H. Li, Y. Zhang, J. He, 2009. Room temperature ionic liquids (RTILs): A new and versatile platform for cellulose processing and derivatization, Chem. Eng. J. 147, 13-21.

Dadi, A.P., C.A. Schall, S. Varanasi, 2007. Mitigation of cellulose recalcitrance to enzymatic hydrolysis by ionic liquid pretreatment, Appl.Biochem.Biotechnol. 137, 407-421.

Dadi, A.P., S. Varanasi, C.A. Schall, 2006. Enhancement of cellulose saccharification kinetics using an ionic liquid pretreatment step, Biotechnol.Bioeng. 95, 904-910.

Deguchi, S., K. Tsujii, 2002. Flow cell for in situ optical microscopy in water at high temperatures and pressures up to supercritical state, Rev.Sci.Instrum. 73, 3938-3941.

Deguchi, S., K. Tsujii, K. Horikoshi, 2008. Crystalline-to-amorphous transformation of cellulose in hot and compressed water and its implications for hydrothermal conversion, Green Chem. 10, 191-196.

Deguchi, S., K. Tsujii, K. Horikoshi, 2006. Cooking cellulose in hot and compressed water, Chem.Commun. 2006, 3293-3295.

Dupont, J., P.A.Z. Suarez, 2006. Physico-chemical processes in imidazolium ionic liquids, Phys.Chem.Chem.Phys. 8, 2441-2452.

Endres, F., S.Z.E. Abedin, 2006. Air and water stable ionic liquids in physical chemistry, Phys.Chem.Chem.Phys. 8, 2101-2116.

Feng, L., Z. Chen, 2008. Research progress on dissolution and functional modification of cellulose in ionic liquids, J. Mol. Liq. 142, 1-5.

Fengel, D., Wegener, G., 1984. Wood: Chemistry, ultrastructure, reactions, de Gruyter, Berlin.

Fort, D.A., R.C. Remsing, R.P. Swatloski, P. Moyna, G. Moyna, R.D. Rogers, 2007. Can ionic liquids dissolve wood? Processing and analysis of lignocellulosic materials with 1-*n*-butyl-3-methylimidazolium chloride, Green Chem. 9, 63-69.

Ghose, T., 1987. Measurement of cellulase activities, Pure Appl.Chem. 59, 257-268.

Glasser, W.G., Sarkanen, S., 1989. Lignin: Properties and materials, American Chemical Society, Washington.

Goering, H.K., P.J. Van Soest, 1970. Forage fiber analyses (apparatus, reagents, procedures, and some applications), Agriculture Handbook. 379, 1-9.

Hames, B.R., S.R. Thomas, A.D. Sluiter, C.J. Roth, D.W. Templeton, 2003. Rapid biomass analysis, Appl.Biochem.Biotechnol. 105, 5-16.

Han, S., J. Li, S. Zhu, R. Chen, Y. Wu, X. Zhang, et al., 2009. Potential applications of ionic liquids in wood related industries, BioResources. 4, 825-834.

Hansmann, C., M. Schwanninger, B. Stefke, B. Hinterstoisser, W. Gindl, 2004. UV-microscopic analysis of acetylated spruce and birch cell walls, Holzforschung. 58, 483-488.

Hatfield, R., R.S. Fukushima, 2005. Can lignin be accurately measured? Crop Sci. 45, 832-839.

Heinze, T., K. Schwikal, S. Barthel, 2005. Ionic liquids as reaction medium in cellulose functionalization, Macromol.Biosci. 5, 520-525.

Hermanutz, F., F. Gähr, E. Uerdingen, F. Meister, B. Kosan, 2008. New Developments in Dissolving and Processing of Cellulose in Ionic Liquids, Macromol.Symp. 262, 23-27.

Hurtubise, F.G., H. Krassig, 1960. Classification of fine structural characteristics in cellulose by infared spectroscopy. Use of Potassium Bromide Pellet Technique, Anal.Chem. 32, 177-181.

Hyman, D., Sluiter,A., Crocker,D., Johnson,D., Sluiter,J., Black,S., Scarlata,C., 2008. Determination of acid soluble lignin concentration curve by UV-Vis spectroscopy, NREL/TP-510-42617, 1-13.

Joglekar, H., I. Rahman, B. Kulkarni, 2007. The path ahead for ionic liquids, Chem.Eng.Technol. 30, 819-828.

Johnson, D.B., W.E. Moore, L.C. Zank, 1961. The spectrophotometric determination of lignin in small wood samples, Tappi. 44, 793-798.

Kačuráková, M., P. Capek, V. Sasinková, N. Wellner, A. Ebringerová, 2000. FT-IR study of plant cell wall model compounds: pectic polysaccharides and hemicelluloses, Carbohydr.Polym. 43, 195-203.

Khanal, S.K., M. Montalbo, J.H. van Leeuwen, G. Srinivasan, D. Grewell, 2007. Ultrasound enhanced glucose release from corn in ethanol plants, Biotechnol.Bioeng. 98, 978-985.

Kilpeläinen, I., H. Xie, A. King, M. Granstrom, S. Heikkinen, D.S. Argyropoulos, 2007. Dissolution of wood in ionic liquids, J.Agric.Food Chem. 55, 9142-9148.

Köhler, S., T. Liebert, M. Schöbitz, J. Schaller, F. Meister, W. Günther, et al., 2007. Interactions of ionic liquids with polysaccharides 1. Unexpected acetylation of cellulose with 1-ethyl-3-methylimidazolium acetate, Macromol.Rapid Commun. 28, 2311-2317.

Kumar, R., G. Mago, V. Balan, C.E. Wyman, 2009. Physical and chemical characterizations of corn stover and poplar solids resulting from leading pretreatment technologies, Bioresour.Technol. 100, 3948-3962.

Lateef, H., S. Grimes, P. Kewcharoenwong, B. Feinberg, 2009. Separation and recovery of cellulose and lignin using ionic liquids: a process for recovery from paper-based waste, J.Chem.Technol.Biotechnol. 84, 1818-1827.

Lee, S.H., T.V. Doherty, R.J. Linhardt, J.S. Dordick, 2008. Ionic liquid-mediated selective extraction of lignin from wood leading to enhanced enzymatic cellulose hydrolysis, Biotechnol. Bioeng. 102, 1368-1376.

Lennholm, H., T. Larsson, T. Iversen, 1994. Determination of cellulose Iα and Iβ in lignocellulosic materials, Carbohydr.Res. 261, 119-131.

Li, C., Q. Wang, Z.K. Zhao, 2008. Acid in ionic liquid: An efficient system for hydrolysis of lignocellulose, Green Chem. 10, 177-182.

Li, C., Z.K. Zhao, 2007. Efficient acid-catalyzed hydrolysis of cellulose in ionic liquid, Adv.Synth.Catal. 349, 1847-1850.

Lipinsky, E.S., 1981. Chemicals from biomass: Petrochemical substitution options, Science. 212, 1465-1471.

Liu, L., H. Chen, 2006. Enzymatic hydrolysis of cellulose materials treated with ionic liquid [BMIM] Cl, Chinese Science Bulletin. 51, 2432-2436.

Lynd, L.R., P.J. Weimer, W.H. van Zyl, I.S. Pretorius, 2002. Microbial cellulose utilization: Fundamentals and biotechnology, Microbiol. Mol. Biol. Rev. 66, 506-577.

Lynd, L.R., C.E. Wyman, T.U. Gerngross, 1999. Biocommodity engineering, Biotechnol.Prog. 15, 777-793.

Mai, C., U. Kües, H. Militz, 2004. Biotechnology in the wood industry, Appl. Microbiol. Biotechnol. 63, 477-494.

Marson, G.A., O.A. El Seoud, 1999. Cellulose dissolution in lithium chloride/N,N-dimethylacetamide solvent system: Relevance of kinetics of decrystallization to cellulose

derivatization under homogeneous solution conditions, J.Polym.Sci.A Polym.Chem. 37, 3738-3744.

Miller, G.L., 1959. Use of dinitrosalicylic acid reagent for determination of reducing sugar, Anal.Chem. 31, 426-428.

Moore, A., N. Owen, 2001. Infrared spectroscopic studies of solid wood, Appl. Spectrosc. Rev. 36, 65-86.

Morohoshi, N., 1991. Chemical characterization of wood and its components, Wood and Cellulosic Chemistry. Dekker, New York, pp. 331-392.

Moulthrop, J.S., R.P. Swatloski, G. Moyna, R.D. Rogers, 2005. High-resolution 13C NMR studies of cellulose and cellulose oligomers in ionic liquid solutions, Chem.Commun. 2005, 1557-1559.

Nelson, M.L., R.T. O'Connor, 1964a. Relation of certain infrared bands to cellulose crystallinity and crystal lattice type. Part II. A new infrared ratio for estimation of crystallinity in celluloses I and II, J. Appl. Polym. Sci. 8, 1325-1341.

Nelson, M.L., R.T. O'Connor, 1964b. Relation of certain infrared bands to cellulose crystallinity and crystal latticed type. Part I. Spectra of lattice types I, II, III and of amorphous cellulose, J. Appl. Polym. Sci. 8, 1311-1324.

Oh, S.Y., D.I. Yoo, Y. Shin, H.C. Kim, H.Y. Kim, Y.S. Chung, et al., 2005. Crystalline structure analysis of cellulose treated with sodium hydroxide and carbon dioxide by means of X-ray diffraction and FTIR spectroscopy, Carbohydr.Res. 340, 2376-2391.

Okoturo, O.O., T.J. VanderNoot, 2004. Temperature dependence of viscosity for room temperature ionic liquids, J. Electroanal. Chem. 568, 167-181.

Pan, X., D. Xie, N. Gilkes, D.J. Gregg, J.N. Saddler, 2005. Strategies to enhance the enzymatic hydrolysis of pretreated softwood with high residual lignin content, Appl.Biochem.Biotechnol. 124, 1069-1079.

Pandey, K.K., 1999. A study of chemical structure of soft and hardwood and wood polymers by FTIR spectroscopy, J. Appl. Polym. Sci. 71, 1969-1975.

Phaiboonsilpa, N., Lu, X., Yamauchi, K., Saka, S., 2010. Chemical conversion of lignocellulosics as treated by two-step hot-compressed water, Zero-Carbon Energy Kyoto 2010. Springer, 166-170.

Pintar, A., J. Batista, J. Levec, 2002. In situ Fourier transform infrared spectroscopy as an efficient tool for determination of reaction kinetics, Analyst. 127, 1535-1540.

Pu, Y., N. Jiang, A.J. Ragauskas, 2007. Ionic liquid as a green solvent for lignin, J. Wood Chem. Tech. 27, 23-33.

Ragauskas, A.J., C.K. Williams, B.H. Davison, G. Britovsek, J. Cairney, C.A. Eckert, et al., 2006. The path forward for biofuels and biomaterials, Science. 311, 484-489.

Remsing, R.C., R.P. Swatloski, R.D. Rogers, G. Moyna, 2006. Mechanism of cellulose dissolution in the ionic liquid 1-n-butyl-3-methylimidazolium chloride: a 13C and 35/37Cl NMR relaxation study on model systems, Chem.Commun. 2006, 1271-1273.

Rinaldi, R., R. Palkovits, F. Schüth, 2008. Depolymerization of cellulose using solid catalysts in ionic liquids, Angew.Chem.Int.Ed. 47, 8047-8050.

Segal, L., J.J. Creely, A.E. Martin Jr., C.M. Conrad, 1959. An empirical method for estimating the degree of crystallinity of native cellulose using the X-ray diffractometer, Text.Res.J. 29, 786-794.

Sievers, C., M.B. Valenzuela-Olarte, T. Marzialetti, I. Musin, P.K. Agrawal, C.W. Jones, 2009. Ionic-liquid-phase hydrolysis of pine wood, Ind. Eng. Chem. Res. 48, 1277-1286.

Sjöström, E., 1981. Wood chemistry: Fundamentals and applications, Academic Press, Toronto.

Sluiter, A., Hames,B., Ruiz,R., Scarlata,C., Sluiter,J., Templeton,D., Crocker,D., 2008. Determination of structural carbohydrates and lignin in biomass, NREL/TP-510-42618, 1-14.

Somogyi, M., 1952. Notes on sugar determination, J.Biol.Chem. 195, 599-612.

Sun, N., M. Rahman, Y. Qin, M.L. Maxim, H. Rodríguez, R.D. Rogers, 2009. Complete dissolution and partial delignification of wood in the ionic liquid 1-ethyl-3-methylimidazolium acetate, Green Chem. 11, 646-655.

Sun, N., R.P. Swatloski, M.L. Maxim, M. Rahman, A.G. Harland, A. Haque, et al., 2008. Magnetite-embedded cellulose fibers prepared from ionic liquid, J. Mater. Chem. 18, 283-290.

Swatloski, R.P., S.K. Spear, J.D. Holbrey, R.D. Rogers, 2002. Dissolution of cellose with ionic liquids, J.Am.Chem.Soc. 124, 4974-4975.

Tan, S., MacFarlane, D., 2009. Ionic liquids in biomass processing, Springer, pp. 311-339.

Teeäär, R., R. Serimaa, T. Paakkarl, 1987. Crystallinity of cellulose, as determined by CP/MAS NMR and XRD methods, Polymer Bulletin. 17, 231-237.

Teramoto, Y., N. Tanaka, S. Lee, T. Endo, 2008. Pretreatment of eucalyptus wood chips for enzymatic saccharification using combined sulfuric acid-free ethanol cooking and ball milling, Biotechnol.Bioeng. 99, 75-85.

Tucker, M.P., Q.A. Nguyen, F.P. Eddy, K.L. Kadam, L.M. Gedvilas, J.D. Webb, 2001. Fourier transform infrared quantitative analysis of sugars and lignin in pretreated softwood solid residues, Appl.Biochem.Biotechnol. 91, 51-61.

Van Soest, P.J., R.W. McQueen, 1973. The chemistry and estimation of fibre, Proceedings of the Nutrition Society. 32, 123-130.

Veale, E.L., J. Irudayaraj, A. Demirci, 2007. An on-line approach to monitor ethanol fermentation using FTIR spectroscopy, Biotechnol.Prog. 23, 494-500.

Viswanathan, G., S. Murugesan, V. Pushparaj, O. Nalamasu, P.M. Ajayan, R.J. Linhardt, 2006. Preparation of biopolymer fibers by electrospinning from room temperature ionic liquids, Biomacromolecules. 7, 415-418.

Vitz, J., T. Erdmenger, C. Haensch, U.S. Schubert, 2009. Extended dissolution studies of cellulose in imidazolium based ionic liquids, Green Chem. 11, 417-424.

Wiselogel, A., S. Tyson, D. Johnson, 1996. Biomass feedstock resources and composition, Handbook on bioethanol: Production and utilization. Taylor and Francis, Washington, pp.105-118.

Wu, J., J. Zhang, H. Zhang, J. He, Q. Ren, M. Guo, 2004. Homogeneous acetylation of cellulose in a new ionic liquid, Biomacromolecules. 5, 266-268.

Wu, R., X. Wang, F. Li, H. Li, Y. Wang, 2009. Green composite films prepared from cellulose, starch and lignin in room-temperature ionic liquid, Bioresour.Technol. 100, 2569-2574.

Xie,H., Kilpeläinen,I., King,A., Leskinen,T., Järvi,P. and Argyropoulos,D. S. , 2010. Opportunities with wood dissolved in ionic liquids, ACS Symposium Series. 1033, 343-363.

Yang, Z., W. Pan, 2005. Ionic liquids: Green solvents for nonaqueous biocatalysis, Enzyme Microb.Technol. 37, 19-28.

Yemm, E.W., A.J. Willis, 1954. The estimation of carbohydrates in plant extracts by anthrone, Biochem.J. 57, 508-514.

Youngs, T.G.A., C. Hardacre, J.D. Holbrey, 2007. Glucose solvation by the ionic liquid 1,3-dimethylimidazolium chloride: A simulation study, J. Phys. Chem. B. 111, 13765-13774.

Zakzeski, J., P.C.A. Bruijnincx, A.L. Jongerius, B.M. Weckhuysen, 2010. The catalytic valorization of lignin for the production of renewable chemicals, Chem.Rev. 110, 3552-3599.

Zavrel, M., D. Bross, M. Funke, J. Buchs, A.C. Spiess, 2009. High-throughput screening for ionic liquids dissolving (ligno-)cellulose, Bioresour.Technol. 100, 2580-2587.

Zhang, Y., H. Du, X. Qian, E.Y.-. Chen, 2010. Ionic liquid−water mixtures: Enhanced Kw for efficient cellulosic biomass conversion, Energy Fuels. 4, 2410-2417.

Zhang, H., J. Wu, J. Zhang, J. He, 2005. 1-Allyl-3-methylimidazolium chloride room temperature ionic liquid: A new and powerful nonderivatizing solvent for cellulose, Macromolecules. 38, 8272-8277.

Zhang, Y.P., L.R. Lynd, 2004. Toward an aggregated understanding of enzymatic hydrolysis of cellulose: Noncomplexed cellulase systems, Biotechnol. Bioeng. 88, 797-824.

Zhao, H., G.A. Baker, Z. Song, O. Olubajo, T. Crittle, D. Peters, 2008. Designing enzyme-compatible ionic liquids that can dissolve carbohydrates, Green Chem. 10, 696-705.

Zhao, H., C.L. Jones, G.A. Baker, S. Xia, O. Olubajo, V.N. Person, 2009. Regenerating cellulose from ionic liquids for an accelerated enzymatic hydrolysis, J. Biotechnol. 139, 47-54.

Zhu, S., 2008. Use of ionic liquids for the efficient utilization of lignocellulosic materials, J.Chem.Technol.Biotechnol. 83, 777-779.

Zhu, S., Y. Wu, Q. Chen, Z. Yu, C. Wang, S. Jin, et al., 2006. Dissolution of cellulose with ionic liquids and its application: A mini-review, Green Chem. 8, 325-327.

Chapter 4

Quantitative Determination of Cellulose Dissolved in 1-Ethyl-3-Methylimidazolium Acetate Using Partial Least Squares Regression on FTIR Spectra

Michael FitzPatrick, Pascale Champagne, Michael F. Cunningham

4.1 Preface

As was noted in Chapters 2 and 3, the use of ionic liquids (ILs) as biomass solvents requires facile, rapid and reliable characterization techniques. Fourier transform infrared spectroscopy (FTIR) represents a simple and rapid technique to analyze solutions of cellulose and ILs. Additionally, the application of non-linear regression, specifically partial least squares (PLS) regression, to FTIR spectra provides an opportunity for quantitative analysis, with the use of appropriate calibration and validation standards.

In this chapter, cellulose was dissolved in 1-ethyl-3-methylimidazolium acetate ([emim][OAc]) to generate calibration and validation sets for FTIR analysis. The spectra were processed using a range of data preprocessing techniques, to reduce physical effects in the spectra, before PLS regression. The resulting FTIR models were evaluated on: 1) correctly predicting the cellulose content in the validation set and 2) the root mean squared error of prediction.

4.2 Abstract

Rapid and quantitative measurements of cellulose concentrations in ionic liquids (ILs) are difficult. In this study, FTIR operated in attenuated total reflectance (ATR) mode was investigated as a tool to measure cellulose concentration in 1-ethyl-3-methylimidazolium acetate ([emim][OAc]) and the spectra were subjected to Partial Least Squares (PLS) regression for the quantitative determination of cellulose content. Additionally, the spectra were subjected to 7 data preprocessing methods to reduce physical effects in the spectra. Peak normalization was found to be the technique that most improved the prediction of dissolved cellulose in [emim][OAc]. When peak normalization was used for data preprocessing, a model for the quantitative estimation of cellulose content between 0 wt% and 4 wt% with an error of 0.53 wt% was generated. The methods described here provide the basis for a rapid and facile technique for the determination of dissolved cellulose content in [emim][OAc].

4.3 Introduction

Ionic liquids are a class of organic salts that exist as liquids at low temperatures; often well below 100°C. They have low vapour pressures, good thermal stability, electroconductivity, tunable physico-chemical properties and unique solubility properties (FitzPatrick et al., 2010; Fort et al., 2007; Kiefer et al., 2008; Lee et al., 2008; Yang and Pan, 2005). Since Swatloski et al. (2002) first published their findings on the cellulose dissolution in 1-butyl-3-methylimidazolium chloride, there has been a great deal of interest in the use of ILs in a variety of studies involving biomass, including the dissolution of cellulose, lignin and complete biomass samples, as well as the *in situ* processing and modification of cellulose (Cao et al., 2009; Dadi et al., 2006; Fort et al., 2007; Heinze et al., 2005; Kilpeläinen et al., 2007; Lateef et al., 2009; Lee et al., 2008; Pu et al., 2007; Sun et al., 2009; Swatloski et al., 2002; Wu et al., 2004; Zhang et al., 2010; Zhao et al., 2009). However, the development of novel ILs and IL-biomass dissolution and processing systems is limited by a general lack of simple and reliable quantitative characterization tools and techniques (Joglekar et al., 2007).

There is a long history involving the use of infrared spectroscopy biomass samples analysis. It has been used to study the crystallinity and type of cellulose crystal lattice, as well as to distinguish different structural characteristics between cellulose sources (Hurtubise and Krassig, 1960; Nelson and O'Connor, 1964a; Nelson and O'Connor, 1964b). Infrared spectroscopy has been used to characterize phenolics (including lignin) in cell wall samples and to quantify lignin content (Hatfield and Fukushima, 2005). Fourier Transform Infrared (FTIR) spectroscopy has also been used in plant cell wall analysis, where the different polysaccharide structures and compositions are identified based on their unique spectral band positions (Kačuráková et al., 2000), as well as for the compositional analysis of potential biomass feedstocks, including corn stover and woody species (Hames et al., 2003; Moore and Owen, 2001). Lignin and reducing sugar content in hydrolysates from dilute acid pretreatment have been determined using FTIR analysis (Tucker et al., 2001). Furthermore, developments in the use of

real time FTIR for process monitoring have enabled *in situ* monitoring of liquid phase sucrose hydrolysis and the online monitoring of ethanol fermentation (Pintar et al., 2002; Veale et al., 2007). Recently, FTIR spectroscopy has been used to monitor the changes in cellulose crystallinity index and crystallite size after being subjected to NaOH and CO_2 treatments (Oh et al., 2005). FTIR spectroscopy, operated in ATR mode, has also been used to quantitatively determine α-D-glucose (from 0 mass % to 20 mass %) dissolved in [emim][OAc] (Kiefer et al., 2008).

Determination of the dissolved cellulose content in ILs, while simple in concept, is often experimentally difficult and/or time consuming (Sievers et al., 2009). Herein, the development of a quantitative FTIR model for predicting dissolved cellulose concentration in 1-ethyl-3-methylimidazolium acetate ([emim][OAc]), at 0 wt%-4 wt% loadings, through the application of Partial Least Squares (PLS) regression is reported. The model allows rapid predictions of dissolved cellulose content in ILs from FTIR spectra. Enhancement of the PLS regression model to improve the accuracy of the predicted cellulose wt% via data processing techniques was also investigated.

4.4 Materials and Methods

The ionic liquid, [emim][OAc], (≥90%, BASF) was used as received for all dissolution studies. Avicel PH-101 (Sigma-Aldrich), a model microcrystalline cellulose compound, was used as received. Ultra high purity nitrogen was supplied by Praxair.

4.4.1 IR Spectroscopy

FTIR spectra with a resolution of 4 cm^{-1} were obtained from a Nicolet 6700 spectrometer operating in ATR FTIR mode and equipped with a diamond crystal. Thirty-two scans were run per sample between 400 cm^{-1} and 4000 cm^{-1}. Each sample (calibration and validation) was analyzed in triplicate and the resulting spectra were averaged using OMNIC software. The resulting spectra were truncated to an extended fingerprint region (500 cm^{-1} to 1800 cm^{-1}) to

eliminate interference from the diamond crystal, nitrogen, and the signature of water in [emim][OAc], while maintaining the C=N peak observed at 1565 cm^{-1}. Representative FTIR spectra, for the full and the truncated fingerprint region, are shown in Figure 4.1 and 4.2, respectively.

4.4.2 Calibration Set

To develop the predictive FTIR model for cellulose content in [emim][OAc], a 25-sample calibration set was generated as per the ASTM Standard E 1655-05 (ASTM Committee E13, 2005). The calibration set contained samples that varied between 0-5 wt% cellulose per 1 mL of [emim][OAc] dissolved under a 20 psi nitrogen atmosphere.

4.4.3 Validation Set

To assess the predictive capability of the FTIR calibration model for cellulose content in [emim][OAc], a validation set of 10 samples ranging between 0-6 wt% cellulose dissolved under a 20 psi nitrogen atmosphere was employed. The cellulose concentrations used for all calibration and validation sample sets are shown in Table 4.1.

4.4.4 FTIR Model

Multivariate PLS regression was conducted on the ATR FTIR spectra to allow for quantitative analysis and validation of cellulose content dissolved in [emim][OAc]. Each spectrum was subjected to mean centering and scaling of the data to centre the data about the origin (Boysworth and Booksh, 2008). Additionally, the spectra were processed via different data preprocessing techniques to correct for physical effects and improve the predictive capabilities of the ATR FTIR model using The Unscrambler X by CAMO Software.
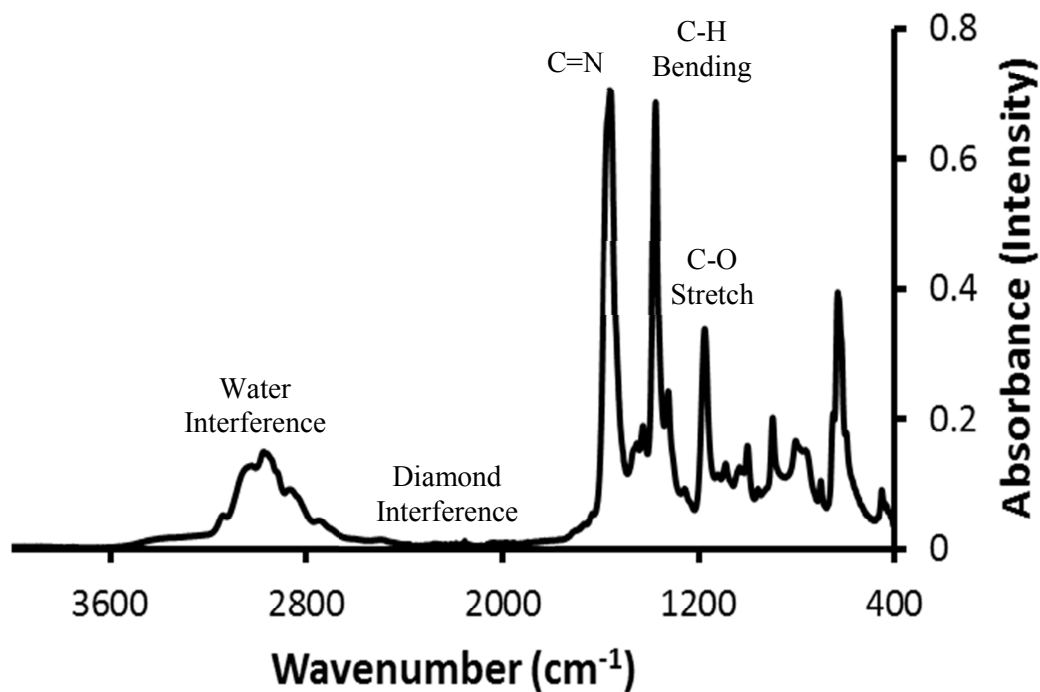
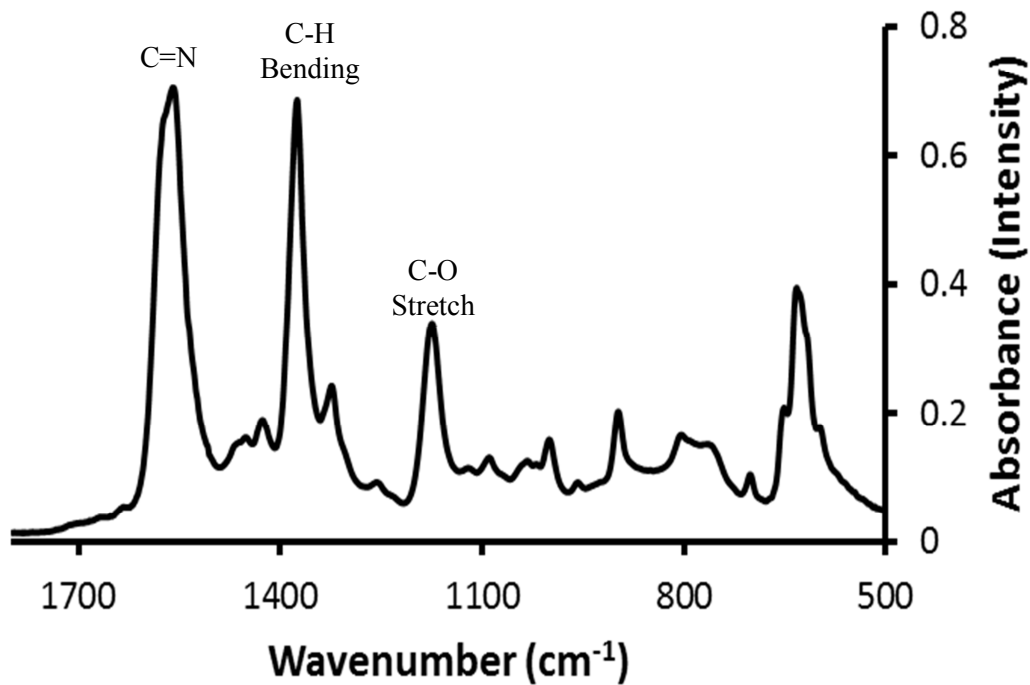**Figure 4.1: Representative ATR FTIR spectra (4 wt% cellulose in [emim][OAc]).**

**Figure 4.2: Representative truncated FTIR spectra (4 wt% cellulose in [emim][OAc])
demonstrating extended fingerprint region.**

Table 4.1: Cellulose concentrations for calibration and validation test sets. Samples beginning with C are calibration set samples and samples beginning with V are validation set samples.

Sample	Cellulose wt%	Sample	Cellulose wt%	Sample	Cellulose wt%
C1	4.00	C13	3.68	C25	2.96
C2	2.00	C14	1.99	V1	2.95
C3	3.97	C15	1.13	V2	3.98
C4	2.00	C16	2.96	V3	3.67
C5	0.98	C17	1.99	V4	6.02
C6	0.00	C18	0.00	V5	1.01
C7	1.00	C19	3.99	V6	1.00
C8	2.01	C20	1.98	V7	0.00
C9	0.00	C21	1.04	V8	2.95
C10	1.58	C22	3.02	V9	2.01
C11	2.49	C23	3.99	V10	2.04
C12	4.92	C24	0.00		

4.4.4.1 *Savitzky-Golay Differentiation: First and Second Derivative*

Savitzky-Golay differentiation computes derivatives based on a polynomial approximation of a portion of the curve to be regressed. This algorithm fits a polynomial to each successive curve segment, resulting in the replacement of the original curve values with values generating a smoothed curve (Gorry, 1990; Savitzky and Golay, 1964). For the generation of the curve segment to be smoothed, 13 right side and 13 left side points in addition to the starting point were chosen, resulting in a 27-point curve employed for each correction. These 27 points were chosen to ensure the curve exceeded the width of the largest spectral band (at 1565 cm^{-1}) at half of the maximum absorbance (full width half maximum). Additionally, for each correction a second order polynomial was selected to fit the data points.

The first derivative treatment typically results in the generation of a new spectrum that is composed of the slope of the spectral curve at each wavenumber. Generally, this treatment can be used to successfully reduce the effect of baseline offset and linear baseline shift in the spectra. The main drawback associated with this treatment is that it causes a shift in the characteristic peaks, making interpretation of the resulting spectra more difficult.

The second derivative treatment calculates the change in the slope of the curve at each data point and generates a new spectrum. Like the first derivative treatment, this technique is particularly effective in correcting baseline offset and linear baseline shift in spectra. Furthermore, the second derivative treatment does not shift, but rather preserves the location of characteristic peaks, unlike the first derivative treatment, potentially making it a more useful treatment than the first derivative.

4.4.4.2 *Multiplicative Scatter Correction (MSC)*

Multiplicative scatter correction (MSC) is a data transformation technique that is used to overcome additive and/or multiplicative effects seen in spectra (Dhanoa et al., 1994). Using this technique, two effects often seen in spectra, signal amplification and offset, are removed from the data yielding a clearer observation of the actual response. This data correction consists of calculating two correction coefficients, a (offset) and b (slope), from the average spectrum in the data set and using these two coefficients to correct a regression line for each individual spectrum, which is also computed as a function of the average value observed for each wavelength (Helland et al., 1995). As this technique uses the mean spectrum for the data set, its success depends on how well the calculated mean spectrum represents the true mean spectrum and, as such, is more representative when larger sample sets are employed.

4.4.4.3 *Standard Normal Variate (SNV)*

The SNV transform centers and scales each individual spectrum. The SNV correction results in the removal of multiplicative interferences of scatter and size effects from spectra. It only uses data contained within a given spectrum for standardization (of that spectrum) as opposed to the mean spectrum of the data set (Dhanoa et al., 1994). Practically, this correction is very similar to MSC, with the exception of the application of vertical scaling possible using MSC. This correction can be used in conjunction with detrending as a means to reduce multicollinearity, baseline shift and curvature in spectroscopic data.

4.4.4.4 *Linear Baseline Correction*

Baseline correction is a spectral treatment that adjusts a spectral offset by either adjusting the data to a minimum point common to all spectra or by making a linear correction based on pre-defined points (Brereton, 2003). In this study, a linear baseline correction was employed using the first and last truncated spectral points as the endpoints for the correction. These two points were automatically re-defined as 0 and the rest of the spectrum was linearly transformed according to this new baseline. The application of a linear baseline correction forces a sloped baseline into a horizontal baseline.

4.4.4.5 *Detrending*

Detrending is a correction that is applied to remove nonlinear trends in spectroscopic data by calculating a baseline function as a least squares fit of a polynomial to each individual spectrum (Barnes et al., 1989). Detrending corrections are applied to an individual spectrum, which is different from many other data treatments that operate at a specific wavelength across the entire spectral set. The order of the polynomial used in the detrending correction determines the baseline effects that are removed. In this study, a third order polynomial was used, allowing for the removal of baseline offset, slope and curvature. Additionally, this correction can be used in conjunction with SNV, where SNV can remove the multiplicative effect of baseline shift and detrending can remove baseline curvature (using a 2nd order or higher polynomial for detrending). Furthermore, the detrending correction does not change the shape of the data, which commonly occurs with derivative-based corrections.

4.4.4.6 *Normalization*

Normalization describes a series of transformations, computed on each sample individually, to convert all data to approximately the same scale. Specifically, peak normalization was used in this study. This transformation normalizes a sample using a selected data point, identical for both the calibration and validation sets. It is assumed that the spectral point selected

does not vary with concentration between different sample spectra. Therefore any change at this spectral point is attributed to an increase or decrease in sample path length, thus this technique corrects for any variation in path length. In this study, the first data point in each spectrum was used as the basis for the peak normalization correction.

4.5 Results and Discussion

When applying non-linear regression techniques to spectral data for quantitative analysis, as well as when applying data preprocessing techniques to reduce baseline effects, it is imperative that a reliable and consistent metric for model performance be selected. In this study, the root mean squared error (RMSE), after application of PLS on the calibration sample set, was used as the decision metric to determine the number of factors to be used in generating a predictive PLS model (Kjeldahl and Bro, 2010). Additionally, the number of correctly predicted validation set samples was determined, for each model, to assess performance. These two measures of model performance were selected for their "concrete" nature, as opposed to more relative indices of model performance such as R^2 (Kjeldahl and Bro, 2010). The percentage of explained variance, Hotelling T^2 statistic and the predicted cellulose wt% residuals vs. predicted cellulose wt% were also used, in addition to the RMSE of the actual cellulose wt% vs. predicted cellulose wt%, to determine how well the model described the calibration set.

In general, an increase in the explained variance represents an increase in the trend identified by the model. However, such a relative comparison is insufficient to compare the effect of data preprocessing techniques (Kjeldahl and Bro, 2010). The Hotelling T^2 statistic is used to identify sample outliers through the application of hypothesis testing. The predicted cellulose wt% residuals vs. predicted cellulose wt% provides a quick graphical representation of whether or not a trend in the residuals exists that is not explained by the model. Here, if the predicted cellulose wt% residuals vs. predicted cellulose wt% are randomly distributed, there is no apparent trend and the residuals represent noise, whereas if a relationship exists between the predicted

cellulose wt% residuals and the predicted cellulose wt%, there is trend in the residuals, suggesting that the model may be inadequate. Finally, the RMSE of the actual cellulose wt% vs. predicted cellulose wt% provides an indication of how close the predicted cellulose values were to the actual cellulose values. In this study, a lower RMSE represented a better model prediction of the actual cellulose wt% in the sample.

For internal model validation, cross-validation was employed using a segmented approach. Each model was subjected to a cross-validation consisting of 10 segments containing either 2 or 3 randomly selected samples, corresponding to roughly 10% of all the samples. This approach aimed to reduce the bias seen in leave-one-out cross-validation (Kjeldahl and Bro, 2010). Furthermore, cross-validation was used to ascertain the appropriate number of PLS regression factors through the selection of the number of factors for each model that minimized the RMSE (Ghasemi and Niazi, 2001). The resulting PLS models were compared for their prediction capability using the 10 samples in the independent validation set. The root mean squared error of prediction (RMSEP) and the number of samples, within a 95% confidence interval, predicted by the model were used as comparison metrics. The predicted vs. actual cellulose wt% for the validation standards of the PLS models using each of the data preprocessing techniques is shown in Figure 4.3.

PLS regression on the 500 cm^{-1} to 1800 cm^{-1} region of the original (untreated) FTIR calibration spectra set yielded a 3-factor model with an RMSE (for the internal validation) of 0.337. These three factors explained approximately 95% of the variance for both the calibration and validation sets. This model predicted the wt% of 5 of the 10 validation standards, as seen in Figure 4.3a. Finally, the RMSEP for this technique was 0.612 (Table 4.2). Since we did observe a linear trend in the residuals vs. predicted plot (Appendix B, Figure B.1), the original FTIR data was subjected to eight different data preprocessing treatments to address this noted trend and the results were compared with the untreated data model to assess preprocessing performance. A summary of the model prediction results, including the untreated case, is shown in Table 4.2.
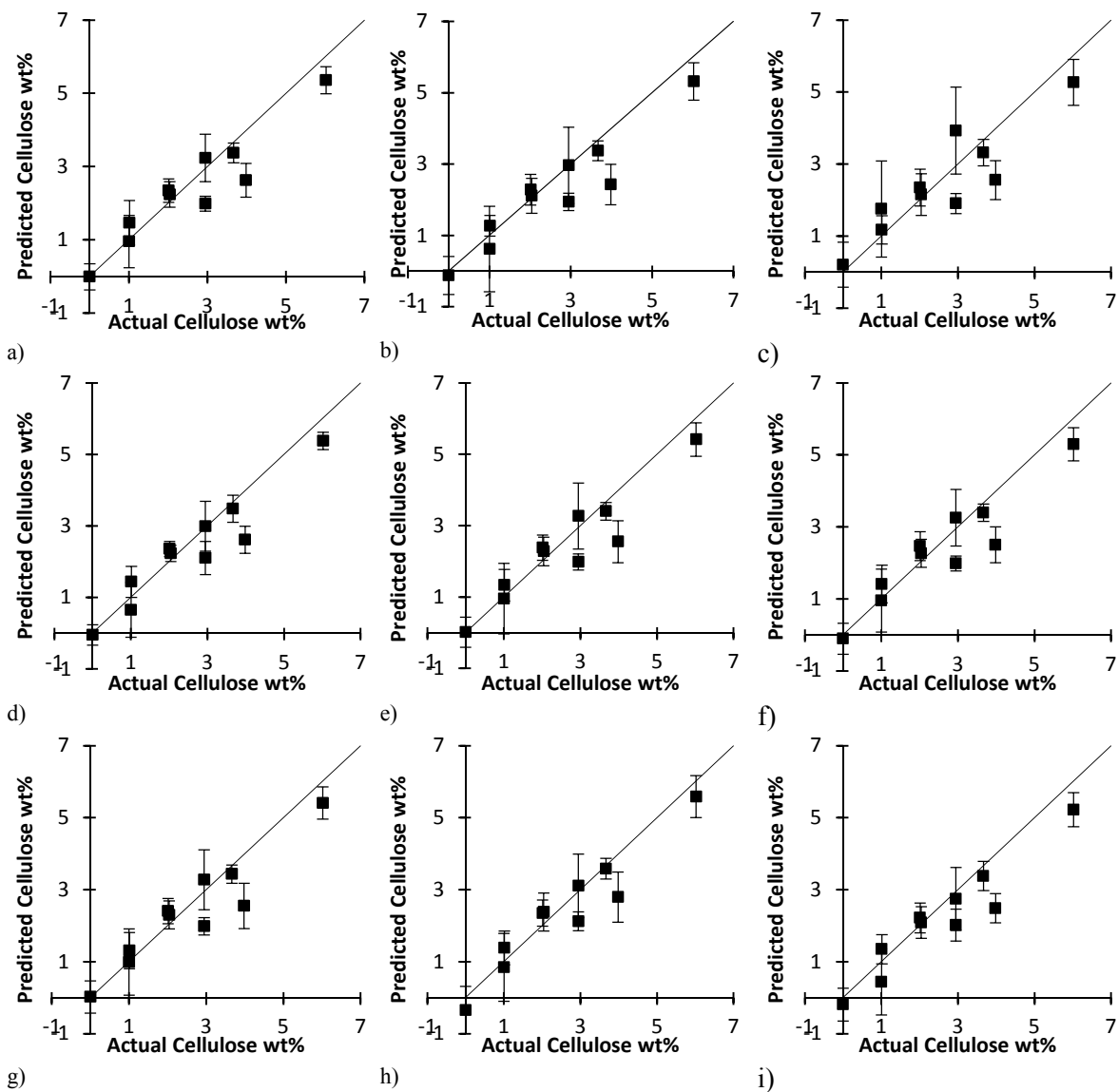
Figure 4.3: Predicted vs. actual cellulose wt% for the following data preprocessing FTIR models: a) untreated, b) Savitzky-Golay differentiation - 1st derivative, c) Savitzky-Golay differentiation - 2nd derivative, d) MSC, e) SNV, f) baseline correction, g) detrending, h) normalization, i) SNV-detrending. Error bars represent a 95% confidence interval.

Table 4.2: Summary of the number of factors in each model, the root mean squared error (RMSE), the number of validation set samples predicted within error and the root mean squared error of prediction (RMSEP) of different data preprocessing treatments on PLS FTIR models to predict cellulose wt%.

Technique	Number of Factors in PLS Model	RMSE (wt%)	Correct Number of Validation Predictions	RMSEP (wt%)
Untreated	3	0.337	5	0.612
Savitzky-Golay First Derivative	4	0.319	6	0.658
Savitzky-Golay Second Derivative	4	0.407	7	1.80
MSC	2	0.330	6	0.592
SNV	3	0.308	5	0.618
Baseline Correction - Linear	4	0.308	5	0.652
Detrending	3	0.332	6	0.619
Normalization	4	0.332	8	0.533
SNV-Detrending	2	0.353	7	0.662

4.5.1 Comparison of the Data Preprocessing Techniques

To qualitatively assess whether or not an appropriate number of factors were employed to develop a PLS model, qualitative evaluation metrics can be used. In this study, explained variance, Hotelling's T^2 statistic and the Y-residuals vs. predicted Y, were employed for this purpose and can be found in Appendix B (Figures B.1-B.9). Generally, a higher number of factors employed in PLS regression corresponds to an increase in the variance explained by the model, however, the use of too many factors in model development can lead to error being explained by the model and the model can, in such cases, over-fit the data. Chen et al. (2010) applied PLS on FTIR spectra to predict cellulose, hemicellulose and lignin content in both hard- and softwood samples. Although the authors were able to develop a model that could explain over 99% and 78% of the variance in the calibration and internal validation sets, respectively, and could predict cellulose content with an RMSEP of 0.96 wt%, their use of a 9-factor PLS model might suggest a model that over-fit the data (Chen et al., 2010). In this study ≤4 factors were used for the PLS regression model (Table 4.2). Also, the explained variance for the calibration and internal validation sets was well over 90% for each PLS regression model (Appendix B, Figures B.1a-

B.9a), which is considered an "excellent data explanation" (Chen et al., 2010). This demonstrates that a high percentage of the data was explained for both the calibration and internal validation sets by each model, while minimizing the potential error explained by the model.

Ghasemi and Niazi (2001) applied Savitzky-Golay first and second derivative treatments to electronic absorption spectra to determine the concentration of Co^{2+} and Ni^{2+} in binary solution mixtures. Similar to the [emim][OAc]/cellulose system, there is a high degree of overlap in the spectra of Co^{2+} and Ni^{2+}, and application of derivative treatments to the spectra led to a magnification of noise and an increase in the error of prediction (Ghasemi and Niazi, 2001). Thus, the poor performance in terms of predictive capability (Figures 4.3b and c) and high RMSEP (Table 4.2) of the two derivative methods used in this study was also attributed to magnification of noise in the spectra. This effect of derivative preprocessing on spectra also was also observed by Carlini et al. (2000). Furthermore, the original characteristic spectral peaks (Figure 4.2) were shifted after application of the first derivative correction to the calibration spectra. The changes in the characteristic spectra upon application of first and second derivative treatments were also noted by Ghasemi and Niazi (2001).

The use of MSC to correct for signal amplification and offset is a widely used data preprocessing technique (Carlini et al., 2000). Johansson et al. (2005) used MSC for data preprocessing in addition to PLS regression on Raman spectra for the quantitative assessment of active pharmaceutical ingredients in pharmaceutical immediate release tablets. They noted that MSC preprocessing prior to PLS regression resulted in a lower RMSE than both second derivative and SNV techniques, as well as assessment of the active pharmaceutical ingredient without data preprocessing and PLS regression. In this study, application of MSC preprocessing to the spectra also resulted in an improved (lower) RMSEP (Table 4.2), because this technique uses an average spectrum from the dataset to perform corrections (Carlini et al., 2000). However, since MSC depends on the accuracy of the mean spectrum of the data set, it is likely that with an

increase in the number of samples in the calibration set, MSC treatment may yield better results than those observed in this study.

The relatively poor performance (low number of correctly predicted samples and high RMSEP) of the linear baseline correction (Table 4.2) suggests that there was a nonlinear trend affecting the spectra. This was supported by the predictive enhancement afforded by the detrending preprocessing technique (when compared to the linear baseline correction) before PLS regression since detrending is designed to remove nonlinear trends from spectroscopic data. The detrending preprocessing treatment prior to PLS regression resulted in an RMSEP of 0.619 and the correct prediction of 6 of the 10 cellulose wt% validation standards (Figure 4.3g and Table 4.2). Garrido Frenich et al. (1996) applied both linear baseline and SNV-type centering preprocessing techniques, individually, to HPLC chromatograms to enhance the simultaneous determination of several pesticides via multivariate methods. It was shown that applying a linear baseline to the highly overlapped chromatogram peaks did not enhance the predictive capabilities of PLS, demonstrating that there was a stable baseline between samples. However the application of the SNV-type preprocessing technique enhanced the calibration of the PLS modeling, removing multiplicative interference effects from the chromatograms (Garrido Frenich et al., 1996). In this study, models generated from PLS regression on the overlapped calibration spectra (Figure 4.1) subjected to both SNV and detrending preprocessing treatments had a lower RMSEP than the linear baseline correction treatment (Table 4.2). Thus, the calibration spectra in this study likely had stable baselines between samples, but were affected by nonlinear trends in the physical spectral structure. However, both the SNV and detrending preprocessing techniques offered little improvement over the untreated data (Table 4.2).

When using infrared light for analysis, it is often assumed that the path length of the light is identical for all sample measurements, however slight differences between samples can readily cause a change in length and alter spectra (Kadam et al., 2010). In their experiments dissolving α-lactose monohydrate in water, Kadam et al. (2010) demonstrated that variability in light path

length could be eliminated by normalization of the spectra and a good correlation between the spectral data and the concentration could be achieved. In this study, peak normalization was applied to the first data point in each spectrum in the calibration set (4000cm^{-1}). Since this point contained no signature from either [emim][OAc] or cellulose, the goal of data preprocessing to minimize the physical (and not chemical) differences between sample spectra (Carlini et al., 2000) was achieved, while preserving the characteristic information contained within the original spectra. Here, the lowest RMSEP (0.533 wt%) and largest number of correct cellulose wt% validation predictions (8) was achieved by applying a normalization preprocessing treatment to the spectra (Table 4.2 and Figure 4.3h). This indicated the presence of a variable infrared light path length in the spectra that was subsequently minimized via the normalization preprocessing treatment.

Analysis of the Hotelling T^2 statistic indicated that for each of the PLS regression models, the 25 calibration set samples were within a hypothesis test set at a 95% level, implying that no samples within the calibration set were considered to be outliers (Appendix B, Figures B.1b-B.9b). Furthermore, there was good agreement between the predicted and actual cellulose wt% for both the calibration and validation data sets (Appendix B, Figures B.1c-B.9c). The Y-residuals vs. predicted Y (where Y is wt% cellulose) were plotted to determine if any trend could be noted in the residuals (Appendix B, Figures B.1d-B.9d), which would indicate the potential for model improvement. Only the models created using the two detrending techniques had no trend in the Y-residuals vs. predicted Y (Appendix B, Figures B.7d and B.9d) suggesting that, with the exception of MSC and normalization, the models generated using derivative, SNV and linear baseline data treatments may not be explaining sufficient trend. This is also reflected in the poor to moderate predictive capabilities of these models (Table 4.2). The relatively good predictive capabilities of the models using MSC and normalization preprocessing data treatments, coupled with the trend in the Y-residuals vs. Y predicted would imply that these preprocessing techniques are good candidates to provide model enhancement. This improvement, especially for the MSC

treatment, could be achieved through an increase in the size of the calibration set and potentially followed by a change in the number of PLS factors used to build the model.

4.6 Conclusions

In this study, the RMSEP and number of correct validation samples predicted were used to assess the precision and accuracy of each data preprocessing technique. The RMSEP provides an indication of the level of uncertainty associated with the predicted cellulose wt% from each model. The number of correctly predicted samples in the validation set provides an indication of the accuracy of the model as it assesses the model capability in repeatedly predicting an actual value (cellulose wt% in this study). As such, a good model would demonstrate a high accuracy (high number of validation samples predicted) and high precision (small RMSEP); a moderate model would demonstrate either high accuracy or high precision but not both; and a poor model would demonstrate neither high accuracy nor high precision.

Other model evaluation metrics, including the explained variance, Hotelling's T^2 statistic, and the Y-residuals vs. predicted Y, give a qualitative indication of how well the model explains the trend in the raw data. These were used to assess if the model over-fit the data or if there were trends unexplained by the model, which was indicative of whether or not an appropriate number of factors had been selected.

It was demonstrated that the application of a normalization data preprocessing treatment to PLS regression on truncated ATR FTIR spectra enabled the quantitative determination of cellulose loading in [emim][OAc] for samples between 0 wt% and 4 wt%, with an RMSEP of 0.533 wt%. Additionally, 8 of the 10 validation standards were correctly predicted using this method. The treatment of the spectral data via spectral peak normalization allowed for a nearly 13% decrease in the RMSEP compared to the untreated data case. It is believed that an increase in the number of samples used to build both the calibration and validation sets could further enhance these results. Additionally, optimization of the number of factors after PLS regression using the

most promising data preprocessing techniques for cellulose dissolved in ILs (normalization and MSC) for a larger calibration set is recommended to further improve the predictions achieved by the technique described in this study.

4.7 References

ASTM Committee E13 on Molecular Spectroscopy and Chromatography, 2005. Standard practices for infrared multivariate quantitative analysis, E 1655 - 05, 1-29.

Barnes, R.J., M.S. Dhanoa, S.J. Lister, 1989. Standard normal variate transformation and de-trending of near-infrared diffuse reflectance spectra, Appl.Spectrosc. 43, 772-777.

Boysworth, M.K., Booksh, K.S., 2008. Aspects of multivariate calibration applied to near-infrared spectroscopy, Handbook of near-infrared analysis. pp. 209-239.

Brereton, R.G., 2003. Chemometrics: Data analysis for the laboratory and chemical plant, John Wiley & Sons Canada Ltd, Etobicoke, ON, Canada.

Cao, Y., J. Wu, J. Zhang, H. Li, Y. Zhang, J. He, 2009. Room temperature ionic liquids (RTILs): A new and versatile platform for cellulose processing and derivatization, Chem. Eng. J. 147, 13-21.

Carlini, P., R. Massantini, F. Mencarelli, 2000. Vis-NIR measurement of soluble solids in cherry and apricot by PLS regression and wavelength selection, J.Agric.Food Chem. 48, 5236-5242.

Chen, H., C. Ferrari, M. Angiuli, J. Yao, C. Raspi, E. Bramanti, 2010. Qualitative and quantitative analysis of wood samples by Fourier transform infrared spectroscopy and multivariate analysis, Carbohydr.Polym. 82, 772-778.

Dadi, A.P., S. Varanasi, C.A. Schall, 2006. Enhancement of cellulose saccharification kinetics using an ionic liquid pretreatment step, Biotechnol.Bioeng. 95, 904-910.

Dhanoa, M.S., S.J. Lister, R. Sanderson, R.J. Barnes, 1994. The link between multiplicative scatter correction (MSC) and standard normal variate (SNV) transformations of NIR spectra, J. Near Infrared Spectrosc. 2, 43-47.

FitzPatrick, M., P. Champagne, M.F. Cunningham, R.A. Whitney, 2010. A biorefinery processing perspective: Treatment of lignocellulosic materials for the production of value-added products, Bioresour.Technol. 101, 8915-8922.

Fort, D.A., R.C. Remsing, R.P. Swatloski, P. Moyna, G. Moyna, R.D. Rogers, 2007. Can ionic liquids dissolve wood? Processing and analysis of lignocellulosic materials with 1-*n*-butyl-3-methylimidazolium chloride, Green Chem. 9, 63-69.

Garrido Frenich, A., M. Martínez Galera, J.L. Martínez Vidal, M.D. Gil García, 1996. Partial least-squares and principal component regression of multi-analyte high-performance liquid chromatography with diode-array detection, Journal of Chromatography A. 727, 27-38.

Ghasemi, J., A. Niazi, 2001. Simultaneous determination of cobalt and nickel. Comparison of prediction ability of PCR and PLS using original, first and second derivative spectra, Microchemical Journal. 68, 1-11.

Gorry, P.A., 1990. General least-squares smoothing and differentiation by the convolution (Savitzky-Golay) method, Anal.Chem. 62, 570-573.

Hames, B.R., S.R. Thomas, A.D. Sluiter, C.J. Roth, D.W. Templeton, 2003. Rapid biomass analysis, Appl.Biochem.Biotechnol. 105, 5-16.

Hatfield, R., R.S. Fukushima, 2005. Can lignin be accurately measured? Crop Sci. 45, 832-839.

Heinze, T., K. Schwikal, S. Barthel, 2005. Ionic liquids as reaction medium in cellulose functionalization, Macromol.Biosci. 5, 520-525.

Helland, I.S., T. Næs, T. Isaksson, 1995. Related versions of the multiplicative scatter correction method for preprocessing spectroscopic data, Chemometrics Intellig.Lab.Syst. 29, 233-241.

Hurtubise, F.G., H. Krassig, 1960. Classification of fine structural characteristics in cellulose by infared spectroscopy. Use of potassium bromide pellet technique, Anal.Chem. 32, 177-181.

Joglekar, H., I. Rahman, B. Kulkarni, 2007. The path ahead for ionic liquids, Chem.Eng.Technol. 30, 819-828.

Johansson, J., S. Pettersson, S. Folestad, 2005. Characterization of different laser irradiation methods for quantitative Raman tablet assessment, J.Pharm.Biomed.Anal. 39, 510-516.

Kačuráková, M., P. Capek, V. Sasinková, N. Wellner, A. Ebringerová, 2000. FT-IR study of plant cell wall model compounds: pectic polysaccharides and hemicelluloses, Carbohydr.Polym. 43, 195-203.

Kadam, S.S., d.W. van, P.J. Daudey, H.J.M. Kramer, 2010. A comparative study of ATR-FTIR and FT-NIR spectroscopy for in-situ concentration monitoring during batch cooling crystallization processes, Crystal Growth & Design. 10, 2629-2640.

Kiefer, J., K. Obert, A. Bösmann, T. Seeger, P. Wasserscheid, A. Leipertz, 2008. Quantitative analysis of alpha-D-glucose in an ionic liquid by using infrared spectroscopy, ChemPhysChem. 9, 1317-1322.

Kilpeläinen, I., H. Xie, A. King, M. Granstrom, S. Heikkinen, D.S. Argyropoulos, 2007. Dissolution of Wood in Ionic Liquids, J.Agric.Food Chem. 55, 9142-9148.

Kjeldahl, K., R. Bro, 2010. Some common misunderstandings in chemometrics, J. Chemometrics. 24, 558-564.

Lateef, H., S. Grimes, P. Kewcharoenwong, B. Feinberg, 2009. Separation and recovery of cellulose and lignin using ionic liquids: a process for recovery from paper-based waste, J.Chem.Technol.Biotechnol. 84, 1818-1827.

Lee, S.H., T.V. Doherty, R.J. Linhardt, J.S. Dordick, 2008. Ionic liquid-mediated selective extraction of lignin from wood leading to enhanced enzymatic cellulose hydrolysis, Biotechnol. Bioeng. 102, 1368-1376.

Moore, A., N. Owen, 2001. Infrared spectroscopic studies of solid wood, Appl. Spectrosc. Rev. 36, 65-86.

Nelson, M.L., R.T. O'Connor, 1964a. Relation of certain infrared bands to cellulose crystallinity and crystal lattice type. Part II. A new infrared ratio for estimation of crystallinity in celluloses I and II, J. Appl. Polym. Sci. 8, 1325-1341.

Nelson, M.L., R.T. O'Connor, 1964b. Relation of certain infrared bands to cellulose crystallinity and crystal latticed type. Part I. Spectra of lattice types I, II, III and of amorphous cellulose, J. Appl. Polym. Sci. 8, 1311-1324.

Oh, S.Y., D.I. Yoo, Y. Shin, H.C. Kim, H.Y. Kim, Y.S. Chung, et al., 2005. Crystalline structure analysis of cellulose treated with sodium hydroxide and carbon dioxide by means of X-ray diffraction and FTIR spectroscopy, Carbohydr.Res. 340, 2376-2391.

Pintar, A., J. Batista, J. Levec, 2002. In situ Fourier transform infrared spectroscopy as an efficient tool for determination of reaction kinetics, Analyst. 127, 1535-1540.

Pu, Y., N. Jiang, A.J. Ragauskas, 2007. Ionic liquid as a green solvent for lignin, J. Wood Chem. Tech. 27, 23-33.

Savitzky, A., M.J.E. Golay, 1964. Smoothing and differentiation of data by simplified least squares procedures, Anal.Chem. 36, 1627-1639.

Sievers, C., M.B. Valenzuela-Olarte, T. Marzialetti, I. Musin, P.K. Agrawal, C.W. Jones, 2009. Ionic-liquid-phase hydrolysis of pine wood, Ind. Eng. Chem. Res. 48, 1277-1286.

Sun, N., M. Rahman, Y. Qin, M.L. Maxim, H. Rodríguez, R.D. Rogers, 2009. Complete dissolution and partial delignification of wood in the ionic liquid 1-ethyl-3-methylimidazolium acetate, Green Chem. 11, 646-655.

Swatloski, R.P., S.K. Spear, J.D. Holbrey, R.D. Rogers, 2002. Dissolution of cellose with ionic liquids, J.Am.Chem.Soc. 124, 4974-4975.

Tucker, M.P., Q.A. Nguyen, F.P. Eddy, K.L. Kadam, L.M. Gedvilas, J.D. Webb, 2001. Fourier transform infrared quantitative analysis of sugars and lignin in pretreated softwood solid residues, Appl.Biochem.Biotechnol. 91, 51-61.

Veale, E.L., J. Irudayaraj, A. Demirci, 2007. An on-line approach to monitor ethanol fermentation using FTIR spectroscopy, Biotechnol.Prog. 23, 494-500.

Wu, J., J. Zhang, H. Zhang, J. He, Q. Ren, M. Guo, 2004. homogeneous acetylation of cellulose in a new ionic liquid, Biomacromolecules. 5, 266-268.

Yang, Z., W. Pan, 2005. Ionic liquids: Green solvents for nonaqueous biocatalysis, Enzyme Microb.Technol. 37, 19-28.

Zhang, Y., H. Du, X. Qian, E.Y.-. Chen, 2010. Ionic liquid−water mixtures: Enhanced Kw for efficient cellulosic biomass conversion, Energy Fuels. 4, 2410-2417.

Zhao, H., C.L. Jones, G.A. Baker, S. Xia, O. Olubajo, V.N. Person, 2009. Regenerating cellulose from ionic liquids for an accelerated enzymatic hydrolysis, J. Biotechnol. 139, 47-54.

Chapter 5

Application of Optical Microscopy as a Screening Technique for Cellulose and Lignin Solvent Systems

Michael FitzPatrick, Charlene Falkenburger, Pascale Champagne, Michael F. Cunningham

5.1 Preface

Chapter 4 demonstrated the use of FTIR, operated in ATR mode and coupled with PLS regression of the resulting spectra, for the quantitative analysis of dissolved cellulose content in [emim][OAc]. By using data preprocessing techniques, the predictive capabilities of PLS regression on the FT-IR spectra for cellulose content in [emim][OAc] was improved. The results obtained indicated that quantitative analysis of cellulose within 0.53 wt% in an IL was possible. However, there also exists a need for simpler, more rapid and inexpensive methods to screen potential solvents for biomass dissolution.

The current chapter examines the use of optical microscopy in the screening of solvents for cellulose and lignin dissolution. Cellulose dissolution was monitored using cross-polarized filters, while lignin dissolution was examined without cross-polarized filters. Two imidazolium based ILs, two phosphonium based ILs, and one non-IL solvents were investigated.

5.2 Abstract

Rapid and facile screening techniques to determine the effectiveness of solvents for cellulose or biomass dissolution can advance biomass processing research. In this chapter the use of a simple optical microscopy method to screen potential cellulose and lignin solvents is discussed. The described methodology was used to screen the dissolution of cellulose and lignin in two imidazolium-based ionic liquids (ILs), two phosphonium-based ILs, as well as an N,N-dimethylacetamide/lithium chloride (DMAc/LiCl) solution in less time than other techniques. The imidazolium-based ILs and the DMAc/LiCl were found to dissolve both cellulose and lignin. Also, it was observed that one of the phosphonium-based ILs dissolved lignin and not cellulose, demonstrating a potential for biomass fractionation applications.

5.3 Introduction

Lignocellulosic biomass is the most abundant renewable biological resource on the planet (Zhang, 2008). Lignocellulose mainly comprises cellulose (35-50 wt%), hemicellulose (20-35 wt%), and lignin (5-30 wt%), making cellulose the most plentiful biopolymer on earth and lignin, due to its complex aromatic structure, a potentially valuable source of aromatic compounds (van Haveren et al., 2008; Zavrel et al., 2009). The complex structure of lignocellulosic biomass, in which lignin forms a three-dimensional network that has cellulose and hemicellulose fibres embedded within it, coupled with the extensive intra- and intermolecular bonds present between cellulose fibres, resists chemical and microbial degradation (Mosier et al., 2005). Subsequently, this makes lignocellulosic biomass difficult to fractionate into its core polymeric components, which in turn increases cost of downstream processing to fuels, chemicals, and material products (Champagne, 2007; Zhbankov, 1992). To facilitate downstream processing, considerable work has been done on pretreatment technologies, which can open up the lignocellulosic matrix for further processing, such as enzymatic hydrolysis (FitzPatrick et al., 2010; Lynd et al., 2002).

Since 2002, ionic liquids (ILs) have been studied as solvents for a variety of biomass feedstocks. The use of ILs in dissolved biomass processing has been demonstrated, including: the synthesis of cellulose acetate (Heinze et al., 2005; Köhler et al., 2007); the *in situ* conversion of cellulose to reducing sugars or hydroxymethylfurfural (HMF) (Li et al., 2008; Zhang et al., 2010); the preferential extraction of lignin over cellulose, and fractionation of lignin and cellulose from lignocellulosic biomass (Lateef et al., 2009; Lee et al., 2008; Sun et al., 2009); and the *in situ* conversion of lignocellulosic biomass to a combination of sugars, furfural and HMF (Sievers et al., 2009). Most ILs are produced at small-scale and therefore sold at high cost (Joglekar et al., 2007). There is currently not sufficient demand for ILs to warrant commercial-scale production, as demand increases it is anticipated that cost will decrease dramatically. Thus, rapid screening

techniques to assess IL-biomass dissolution would be a valuable contribution to lignocellulosic biomass processing and characterization research.

The exact mechanism by which biomass dissolution in ILs occurs is believed to be two-fold. Firstly, anions which can deprotonate cellulose interrupt the internal hydrogen bonding present in, and act as non-derivatizing solvents for, cellulose and lignocellulosic biomass (Dadi et al., 2006; Kilpeläinen et al., 2007; Swatloski et al., 2002; Youngs et al., 2007; Zavrel et al., 2009). This is due to anion interaction with the proton in the cellulose hydroxyl group, disrupting the hydrogen bonding network (Dadi et al., 2006). Secondly, it has been suggested that cations can play a role in the dissolution of biomass in ILs (Dadi et al., 2006; Youngs et al., 2007; Zavrel et al., 2009). Zhang et al. (2005) suggested that cations also can interact with the oxygen in the cellulose hydroxyl group to disrupt the hydrogen bonding network. Additionally, the π-π electron interactions present in the cations of ILs may interact with the π-π bonds in lignin, further aiding in the dissolution process (Kilpeläinen et al., 2007).

Traditionally, visual inspection of a cellulose/IL and/or lignin/IL solution has been employed to rapidly assess the extent of dissolution (Heinze et al., 2005; Pu et al., 2007). However, the application of optical microscopy to evaluate biomass dissolution offers more sensitivity, especially to crystalline cellulose due to its birefringent nature. Zavrel et al. (2009) used optical microscopy to qualitatively monitor the dissolution of 1 wt% cellulose in 1-ethyl-3-methylimidazolium acetate without temperature control to demonstrate that optical methods could be used for online-monitoring of the dissolution process. BioLector technology (specialized scattered light measuring equipment) was employed by Zavrel et al. (2009) in high-throughput systems to assess the dissolution of cellulose and lignocellulose; however samples containing lignin affected the use of this equipment in the assessment of dissolution. A specialized high-temperature and high-pressure chamber was used with optical microscopy to qualitatively observe the dissolution of cellulose in water at temperatures $\leq 400°C$ and pressures ≤ 35 MPa (Deguchi and Tsujii, 2002; Deguchi et al., 2006; Deguchi et al., 2008). The authors determined that

crystalline cellulose underwent a transformation from crystalline to an amorphous state, followed by dissolution. Additionally, cross-polarized optical microscopy was used to qualitatively assess the dissolution of cellulose in: NaOH/thiourea/urea aqueous solutions (Jin et al., 2007), 1-ethyl-3-methylimidazolium acetate and 1-butyl-3-methylimidazolium acetate/lithium salt (Xu et al., 2010) via inspection of the optical clarity of the solution. A similar approach was also used to assess cellulose dissolution in different salts (potassium thiocyanate, sodium thiocyanate, potassium iodide and sodium iodide) dissolved in ethylene diamine (Frey et al., 2006; Xiao and Frey, 2007).

In this study, we monitored the dissolution of cellulose and lignin in four different ILs using optical microscopy and a temperature controlled stage. The methodology was designed as a rapid screening approach to assess the partial dissolution of the macromolecules rather than the simple qualitative observation of whether or not the cellulose or lignin was fully dissolved in the IL. Two imidazolium-based ILs (1-ethyl-3-methylimidazolium acetate and 1-butyl-3-methylimidazolium chloride) and two phosphonium-based ILs (trihexyl(tetradecyl)phosphonium bis(trifluoromethylsulfonyl)imide and tetrabutylphosphonium acetate) were screened as solvents for cellulose and lignin. Furthermore, to demonstrate the potential of this technique in assessing the dissolution of these macromolecules in solvents other than ILs, the dissolution of both lignin and cellulose were also investigated in N,N-dimethylacetamide/lithium chloride (DMAc/LiCl). The methodology outlined in this study offers a sensitive and facile method to rapidly monitor cellulose and lignin dissolution in potential solvents using small solvent volumes (≤ 0.45mL) with precise temperature control.

5.4 Materials and Methods

5.4.1 Model Biomass Compounds

Avicel PH-101 (Sigma-Aldrich), a microcrystalline cellulose compound, and Indulin AT, a Kraft lignin donated by MeadWestvaco, were employed as received, as biomass model

compounds. A summary of the dissolution conditions used in this rapid screening study can be found in Table 5.1.

Table 5.1: Rapid screening dissolution conditions summary.

Solvent	Melting Point (°C)	Boiling Point (°C)	Dissolution Temp. (°C)	Dissolution Time (mins)	Cellulose/Lignin Loading (wt%)
[emim][OAc]	<-20	N/A	75	60	4
[bmim]Cl	70	N/A	100	60	4
CYPHOS®109	N/A[†]	>270	75	60	4
CYPHOS®441	~65[*]	N/A	100	30	2
DMAc/LiCl	-19	163	150[‡]	60[‡]	1

[*]*IL was not transparent after melting*
[†]*Liquid at 25°C*
[‡]*Dissolution started at 150°C and allowed to cool to 25°C after 60 minutes (McCormick, 1981; McCormick et al., 1985)*

5.4.2 Ionic Liquids

The ionic liquids 1-ethyl-3-methylimidazolium acetate ([emim][OAc]) (≥90%, BASF), 1-butyl-3-methylimidazolium chloride ([bmim]Cl) (>95%, BASF), trihexyl(tetradecyl)phosphonium bis(trifluoromethylsulfonyl)imide (CYPHOS® 109) (>98%, Cytec) and tetrabutylphosphonium acetate (CYPHOS® 441) (>95%, Cytec) were used as received from the supplier, for all dissolution studies. These four ILs were selected to demonstrate the application of this rapid screening technique for a range of ILs, which were represented by two imidazolium-based and two phosphonium-based ILs. Furthermore, one of the imidazolium and phosphonium cations were paired with the acetate anion in the selected ILs. With the exception of CYPHOS® 441, for each of the IL dissolution experiments the cellulose or lignin was added to the crucible prior to the addition of 0.45 mL of IL. The ILs were pre-heated to the desired cellulose or lignin dissolution temperature (Table 5.1) under a nitrogen atmosphere (20 psi) to ensure they were in the liquid state. The ILs were observed to be transparent upon melting with the exception of CYPHOS® 441. 4 wt% cellulose or lignin loadings were used, as this loading of cellulose or lignin has been shown to be effectively dissolved in a variety of ILs (Lee et al., 2008; Zhu et al., 2006). For the cellulose dissolution experiments, cross-polarized optical lenses were

used (Leica, model numbers 505087 and 11555045), while for the lignin dissolution experiments optical microscopy without cross-polarization was employed. After IL addition to the microscope crucible, the crucible was placed on the temperature-controlled stage, pre-heated to the dissolution temperature (Table 5.1). Nitrogen (ultra high purity, Praxair) was used to minimize the effect of varying atmospheric humidity during the IL pre-heating step.

Due to its crystalline form, 0.2 g of CYPHOS® 441 was added to the crucible prior to cellulose or lignin addition and heated to 100°C for 10 minutes. 100°C was selected since the melting point of CYPHOS® 441 is 65°C. It was noted that this IL formed a gel after 30 minutes of heating, which limited the maximum dissolution time for CYPHOS® 441 rapid-screening experiments. Firestone et al. (2002) demonstrated that the addition of water causes certain ILs, such as 1-decyl-3-methylimidazolium bromide, to form gels upon the addition of as little as 5 wt% water. This phenomenon is not unique to 1-decyl-3-methylimidazolium bromide and may also occur in other ILs (Firestone et al., 2002). Thus, it was believed that CYPHOS® 441 formed a gel with atmospheric moisture. Additionally, due to the changes in viscosity associated with gel formation, only 2 wt% cellulose or lignin loading was used in dissolution studies with this IL. It was also noted that CYPHOS® 441 is birefringent (Figure 5.1), hence, optical microscopy without cross-polarized filters was employed to monitor both cellulose and lignin dissolution experiments.
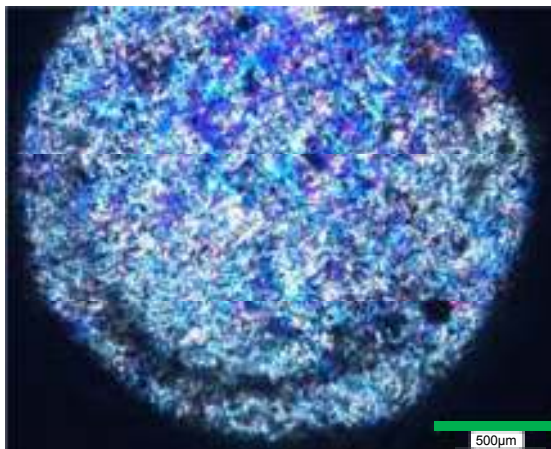
Figure 5.1: Micrograph displaying the birefringent nature of CYPHOS® 441.

5.4.3 DMAc/LiCl

N,N-dimethylacetamide (DMAc) (99%, Sigma) and lithium chloride (LiCl) (≥99%, Sigma-Aldrich) were used as received. A nitrogen atmosphere was also used in the DMAc/LiCl dissolution experiments. The dissolution technique outlined by McCormick (1981), for 1 wt% cellulose, was employed for all cellulose and lignin dissolution experiments in DMAc/LiCl (3 wt% LiCl). The methodology was adapted to allow dissolution monitoring via optical microscopy instead of visual inspection. Although the cellulose loading for the DMAc/LiCl trials was less than for the ILs, it was the same loading as employed in the study by McCormick (1981), and thus, results obtained herein could be compared to those observed by McCormick (1981).

The DMAc/LiCl solution was prepared by adding 3 mL of DMAc to 0.14 g of LiCl and mixing for 30 minutes by stir-bar at room temperature. After mixing, 0.45 mL of the solution was added to the 1 wt% biomass model compounds (Table 5.1) in the microscope crucible. The DMAc/LiCl solution in the crucible was then heated from 25°C to 150°C in 60 minutes. The temperature was held at 150°C for 20 minutes, before the crucible was allowed to cool to 25°C in 60 minutes (McCormick, 1981; McCormick et al., 1985).

5.4.4 Characterization Methods

5.4.4.1 *Optical Microscopy*

All microscope dissolution experiments were conducted in a Linkam THMS Quartz crucible (15 mm diameter) with temperature control of ± 0.1°C via a Linkam THMS 600 temperature controlled microscope stage. Cross-polarized light microscopy was employed to monitor the dissolution of cellulose in each solvent with the exception of CYPHOS® 441, as this solvent was observed to be birefringent. Optical micrographs were taken on a Leica DM LB2 microscope equipped with a Clemex L 1.3C (CL-13-212) camera. Prior to all studies, the polarizing lenses were adjusted to maximize their cross-polarization and ensure that maximum

extinction had been reached. Micrographs were observed using Clemex Vision PE 4.0 to monitor dissolution. All images were taken at 50x magnification.

5.5 Results and Discussion

Due to the birefringent nature of crystalline cellulose, cross-polarized microscopy can be employed to monitor its dissolution. A polarizing filter causes the light waves that pass through it to align with the filter. When a second filter is added in the path of the light, at 90 degrees to the first filter, no light passes. However, when light passes through a birefringent specimen it is split into two rays oriented at 90 degrees to each other and travelling at different velocities. As a result, when a birefringent material is placed between two polarized lenses, the light that passes through the birefringent regions can pass through the second filter (since the light is rotated) and thus only the birefringent material is illuminated.

When the sample is birefringent, as is the case with cellulose, the application of cross-polarized light microscopy can assist with monitoring dissolution as there is a greater contrast between the solvent and the solute. Figure 5.2 illustrates the difference between different optical microscopy techniques: (a) in optical microscopy the bright white/yellow represents both the IL and non-dissolved cellulose; (b) in cross-polarized opticalmicroscopy the dark areas represent either trapped gas or the IL, and the light area the non-dissolved cellulose; and (c) in cross-polarized optical microscopy with a λ compensator the bright blue phase represents the IL and the bright, multi-coloured area is the non-dissolved cellulose.
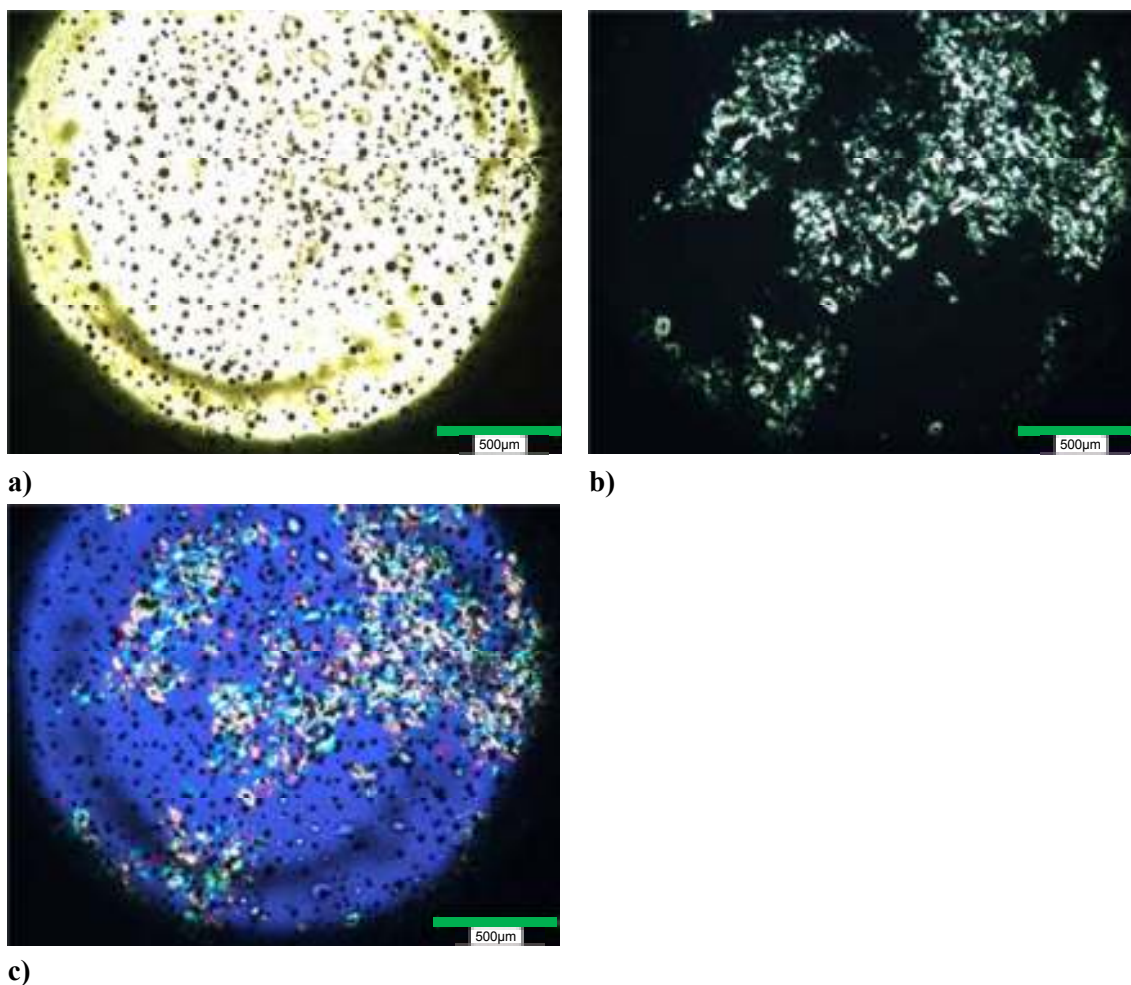
Figure 5.2: Cellulose dissolution in [emim][OAc] at 75°C, investigated with: a) light microscopy, b) cross-polarized light microscopy, c) cross-polarized light microscopy with a λ compensator.

A λ-compensator (Leica, model number 513569) was employed in the cross-polarized microscopy set-up enabling the visualization of the background solvent, which was black under cross-polarization alone (Figure 5.2b), but appeared blue with the addition of the compensator (Figure 5.2c). Additionally, it also increased the difference in polarization colour to facilitate the distinction between non-dissolved cellulose and gas bubbles, which appear as dark spots on the micrograph (Figure 5.2c). This provided more sensitive detection of cellulose dissolution in the cases where the solvent employed was not birefringent. Additionally, a dark ring is observed in

all microscopy images (Figures 5.1 – 5.3 and 5.6 – 5.10). This dark ring was an artifact from the temperature controlled microscope stage.

Optical microscopy, without cross-polarized lenses, was employed to monitor the dissolution of lignin in the five solvents, as well as the dissolution of cellulose in CYPHOS® 441. The microscopy set-up was the same as for the cross-polarized analysis without the use of the polarizing lenses and the λ-compensator. A reference image for all solvents used in this study prior to cellulose or lignin addition and following complete cellulose or lignin dissolution (where applicable) is provided in Figure 5.3.

The micrographs taken prior to and following complete cellulose dissolution (Figure 5.3a, b, e, f, m and n) were taken at the temperatures and cellulose loadings outlined in Table 5.1, but at extended dissolution times (6 hours for [emim][OAc] and [bmim]Cl and a cooling period of 90 minutes for DMAc/LiCl). These demonstrate that each solvent appears the same before and after cellulose dissolution under cross-polarized optical microscopy. Similarly, the micrographs taken prior to and following lignin dissolution (Figure 5.3c, d, g, h, k, l, o, and p) were taken at the temperatures and lignin loadings outlined in Table 5.1, but at extended dissolution times (6 hours for [emim][OAc] and [bmim]Cl and a heating period of 50 minutes in DMAc/LiCl). However, the micrographs taken following dissolution (Figure 5.3d, h, l, and p) were observed to be darker and redder than the micrographs taken prior to dissolution (Figure 5.3c, g, k, and o), a phenomenon also reported by Kilpeläinen et al. (2007) and Zavrel et al. (2009). The authors observed that the darkening and change in colour was indicative of lignin dissolution and also noted that the intensity of the dark red was dependent on the lignin loading in the solvent. Zavrel et al. (2009) noted that the IL colour change during the dissolution of lignin-containing samples hindered the use of the BioLector technology to measure scattered light to assess dissolution.
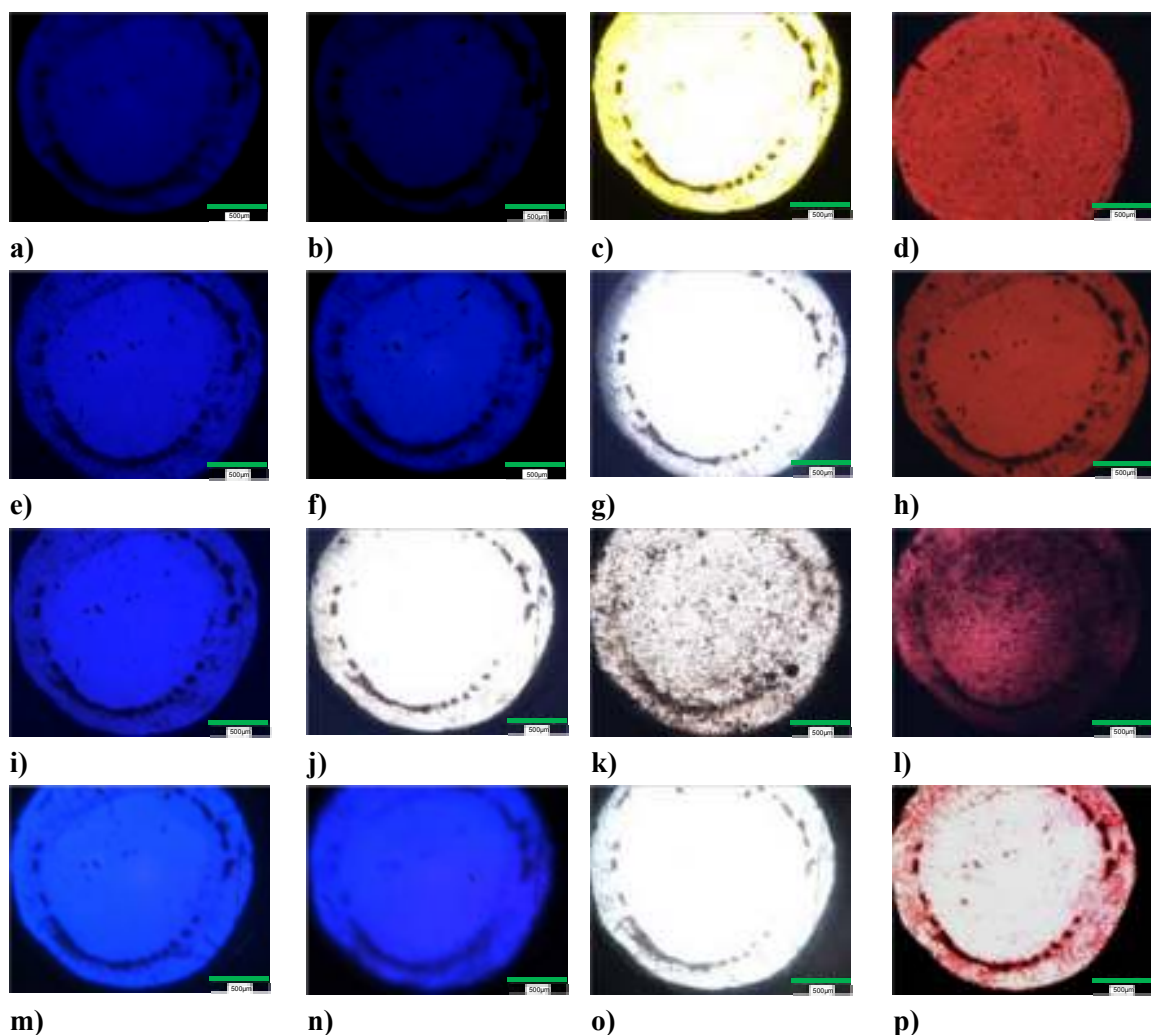
Figure 5.3: Reference images for solvents used in this study: a) [emim][OAc], alone, cross-polarized, b) [emim][OAc], cellulose fully dissolved, cross-polarized, c) [emim][OAc], alone, d) [emim][OAc], lignin fully dissolved, e) [bmim]Cl, alone, cross-polarized, f) [bmim]Cl, cellulose fully dissolved, cross-polarized, g) [bmim]Cl, alone, h) [bmim]Cl, lignin fully dissolved, i) CYPHOS® 109, alone, cross-polarized, j) CYPHOS® 109, alone, k) CYPHOS® 441, alone, l) CYPHOS® 441, lignin fully dissolved, m) DMAc/LiCl, alone, cross-polarized, n) DMAc/LiCl, cellulose fully dissolved, cross-polarized, o) DMAc/LiCl, alone, p) DMAc/LiCl, lignin fully dissolved.

As illustrated in Figures 5.4 and 5.5, visual inspection to assess cellulose or lignin dissolution in an IL solution or other solvent system is not always sufficient. If the solvent only partially dissolves a cellulose or lignin sample, this may not be detectable through visual inspection alone. For example, CYPHOS® 109 and 4 wt% cellulose were heated at 75°C for 1 hour under a nitrogen atmosphere and vigorous stirring.

a)   b)
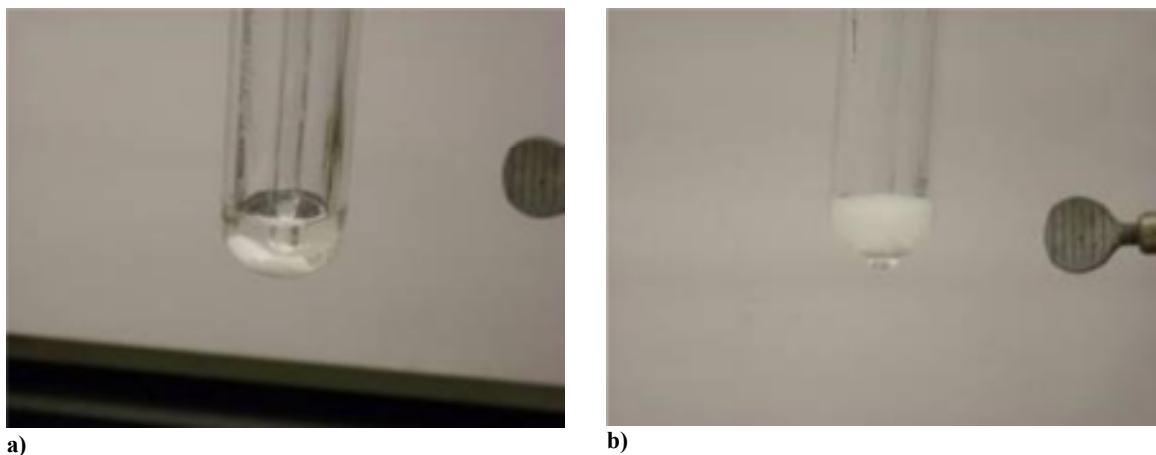
Figure 5.4: Cellulose dissolution in CYPHOS® 109 at 75°C a) initially, b) after one hour, assessed via visual inspection.

a)   b)
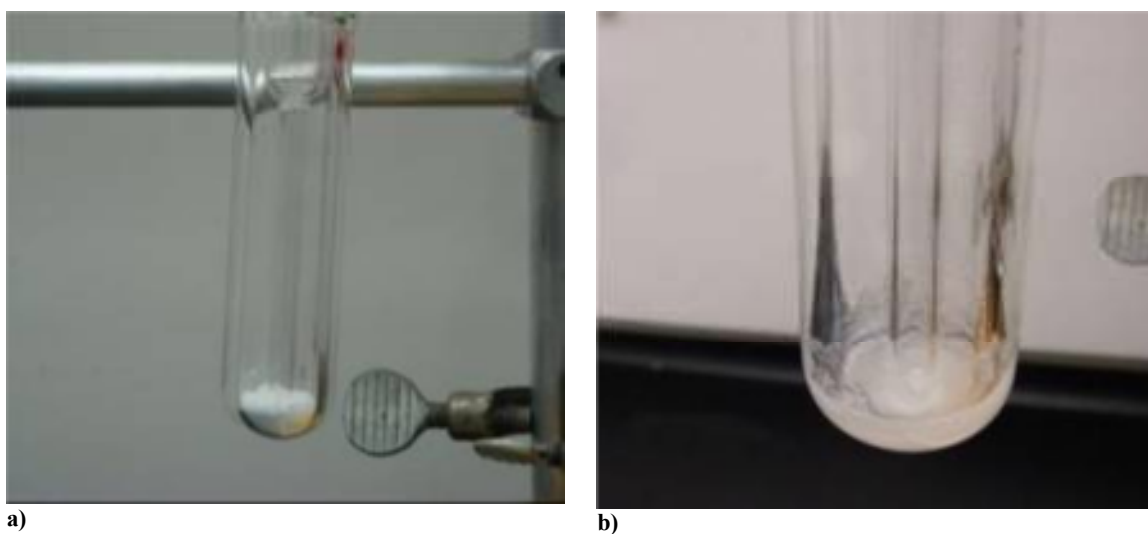
Figure 5.5: Cellulose dissolution in CYPHOS® 441 at 100°C: a) initially, b) after thirty minutes, assessed via visual inspection.

The samples, initially and after 1 hour of dissolution, are shown in Figure 5.4a and b. It is apparent from Figure 5.4b that the cellulose dispersed in the IL, but was not fully dissolved. However, the extent to which the cellulose is partially dissolved cannot be conclusively assessed from visual inspection of this suspension alone. In addition, if the IL is not optically transparent, as shown in Figure 5.5a, determination of cellulose dissolution in the IL by visual inspection is not possible. In Figure 5.5b, 4 wt% cellulose was added to CYPHOS® 441, heated to 100°C for

30 minutes under a nitrogen atmosphere and with vigorous stirring. As can be seen, partial cellulose dissolution could not be conclusively assessed by visual inspection.

5.5.1 Imidazolium-Based ILs

5.5.1.1 *[emim][OAc]*

[emim][OAc] was used to dissolve cellulose, as illustrated in Figure 5.6a and b. The blue area is the IL-phase as seen in Figure 5.3a for the [emim][OAc] alone and Figure 5.3b for the [emim][OAc] with fully dissolved cellulose. The multi-coloured areas in Figure 5.6a represent the non-dissolved cellulose. Within 1 hour at 75°C, the cellulose was found to be fully dissolved, as can be seen when comparing the dissolution experiment micrographs (Figure 5.6b) to the reference micrographs (Figure 5.3a and b). The remaining dark areas (Figure 5.6b) were believed to be gas bubbles initially trapped within the microcrystalline cellulose structure and released upon its dissolution. Zavrel et al. (2009) reported the dissolution of 4 wt% cellulose in [emim][OAc] at 80°C. The authors used BioLector technology to measure scattered light over an 8-hour period to monitor cellulose dissolution in their study. The complete dissolution of 4 wt% cellulose in [emim][OAc] was observed in 1 hour using the cross-polarized optical microscopy methodology outlined in this study.

The dissolution of lignin in [emim][OAc] is illustrated in Figure 5.6c and d. In Figure 5.6c, the brown area is lignin and the bright, off-white area the IL phase (Figure 5.3c), while in Figure 5.6d the red area is the IL-phase following lignin dissolution (Figure 5.3d) and the dark spots represent non-dissolved lignin. From the resulting microscopy images (Figure 5.6c and d), it can be seen that >90% of the lignin was dissolved within 1 hour. Lee et al. (2008) reported that [emim][OAc] at 90°C could dissolve more than 300 g of lignin per kilogram of IL (>23 wt%) in a 24-hour period. The authors added 0.5 g increments of lignin to 5 g IL until no further dissolution was observed, which was assessed by visual inspection. The results of our dissolution study

demonstrated that the partial lignin dissolution (>90% of the observed lignin) in [emim][OAc] could be rapidly assessed via optical microscopy.
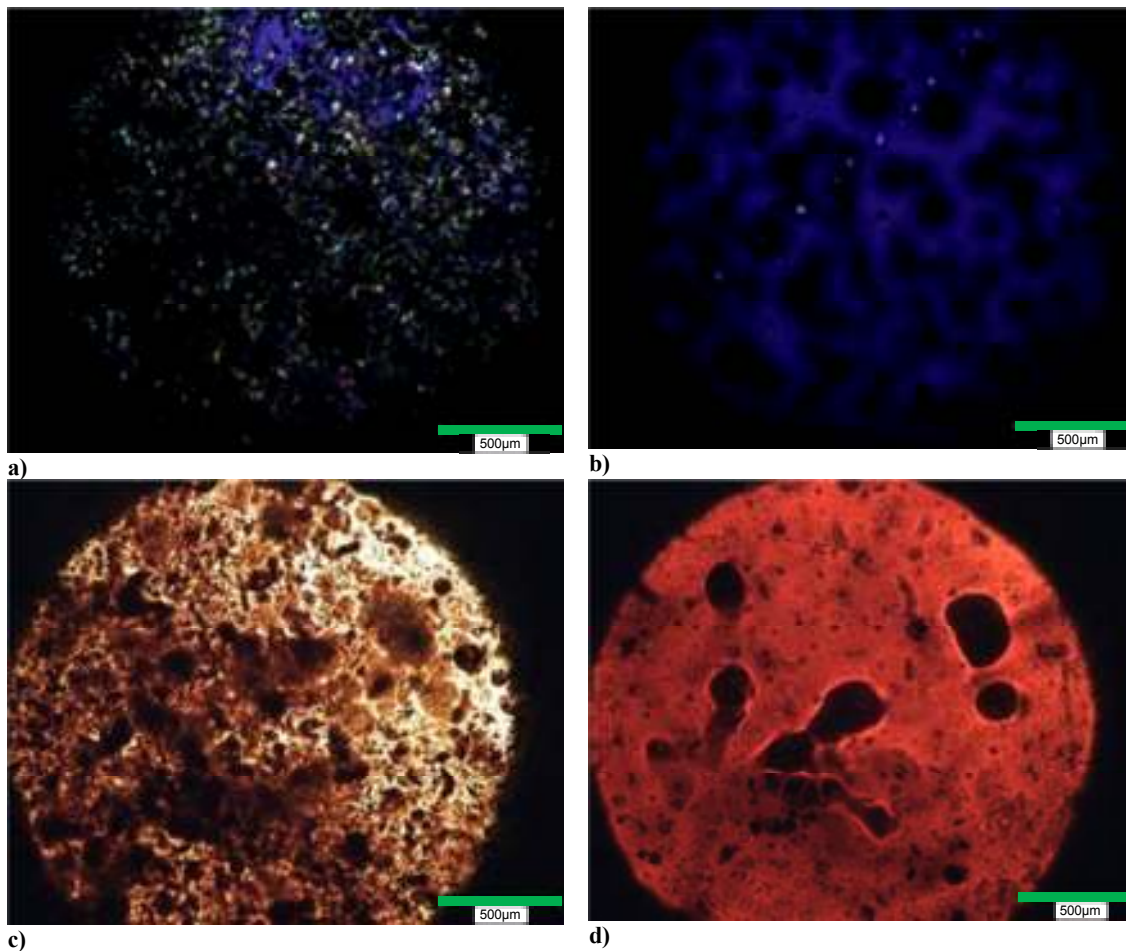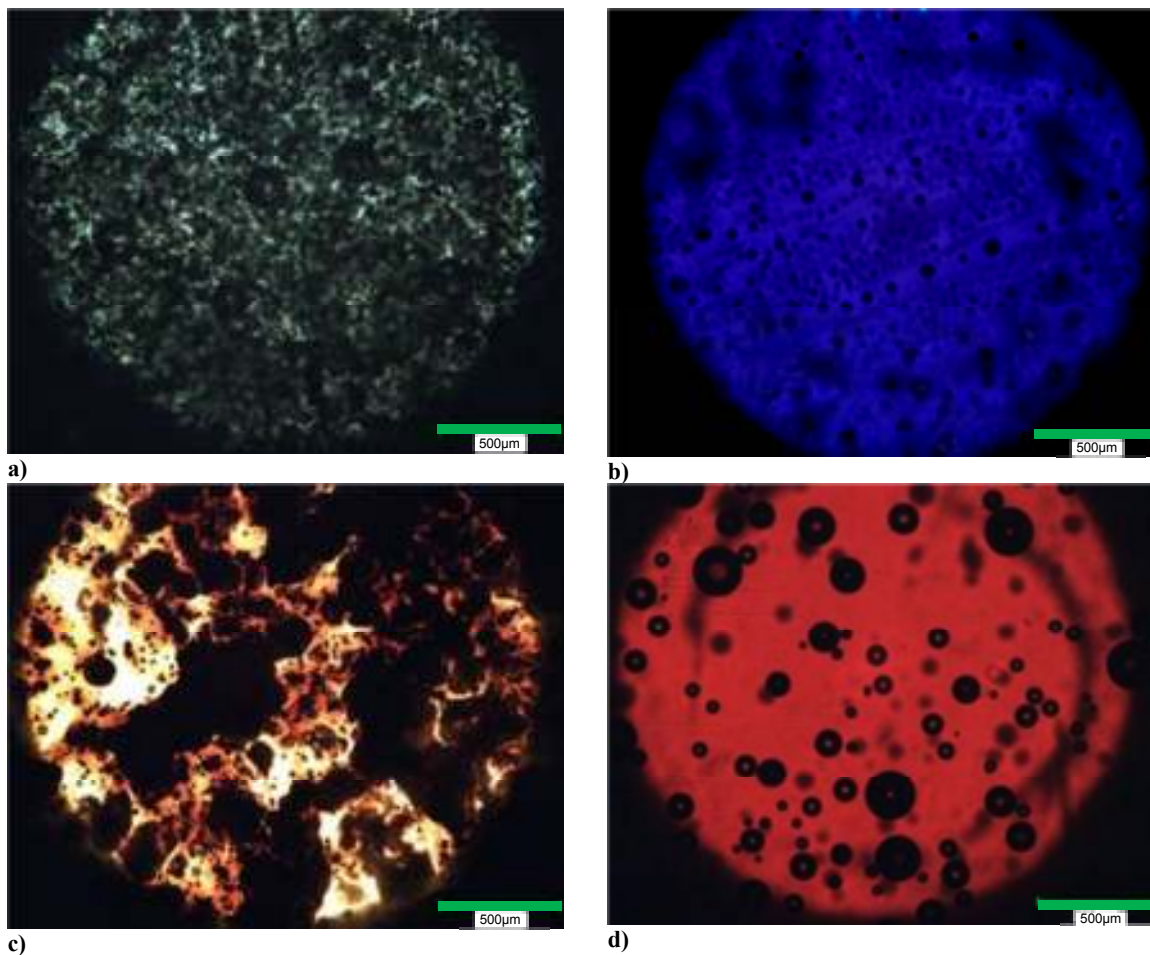

Figure 5.6: [Emim][OAc] dissolution experiments at 75°C: a) cellulose - initially, b) cellulose - after one hour, c) lignin - initially, d) lignin - after one hour.

5.5.1.2 *[bmim]Cl*

Results of cellulose dissolution in [bmim]Cl at 100°C assessed with cross-polarized microscopy are shown prior to and following dissolution in Figures 5.7a and b, respectively. In Figure 5.7a, the grey and bright, multi-coloured areas represent non-dissolved cellulose. In Figure 5.7b the blue area represents the IL (Figure 5.3e and f), the dark circles trapped gas and the

bright, multi-coloured area (at the top of the micrograph) non-dissolved cellulose (<3% of the original observed cellulose).
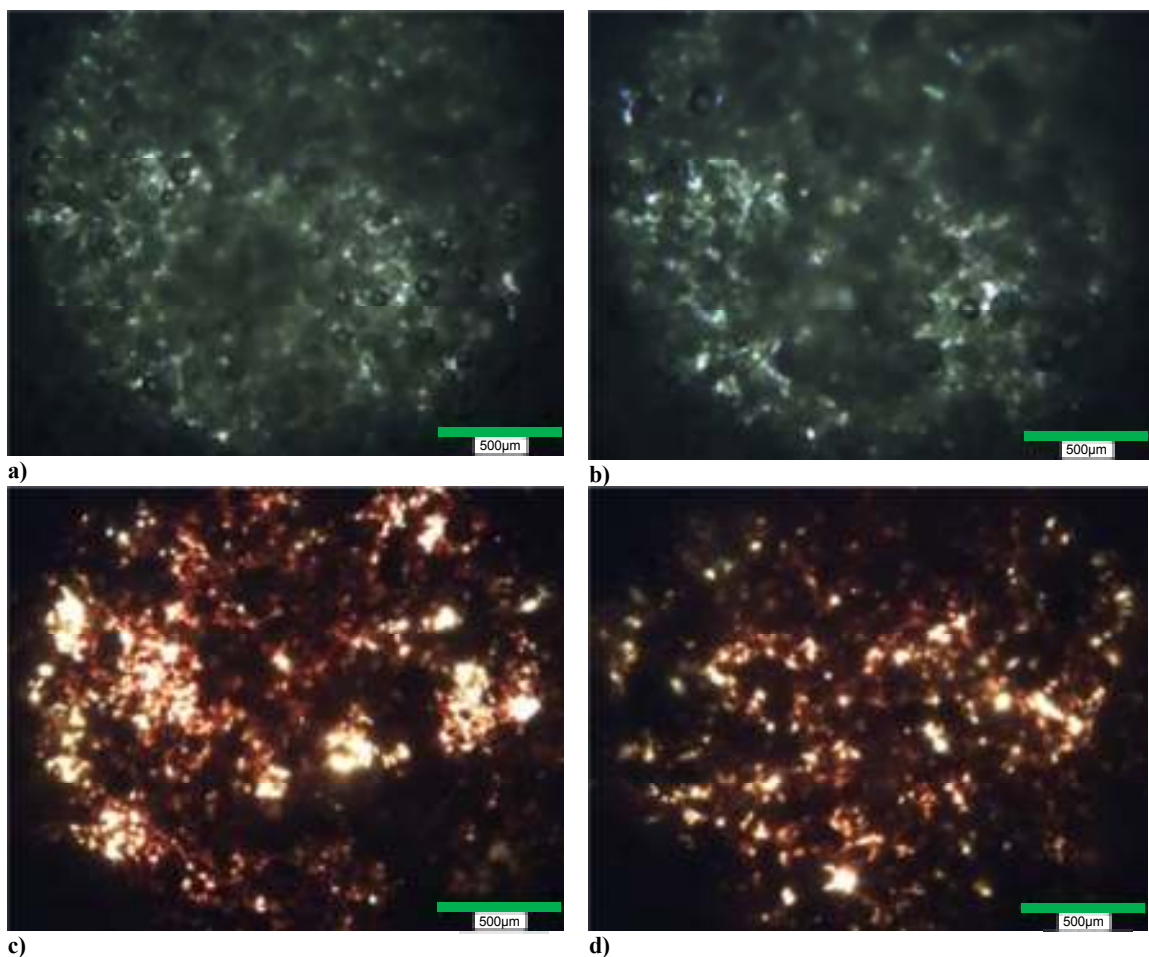

Figure 5.7: [bmim]Cl dissolution experiments at 100°C: a) cellulose - initially, b) cellulose - after one hour, c) lignin - initially, d) lignin - after one hour.

The use of [bmim]Cl for cellulose dissolution has been previously reported, where assessment of cellulose dissolution was conducted using visual inspection of the dissolution of 10 wt% cellulose at 83°C (Heinze et al., 2005) and 100°C (Swatloski et al., 2002). Additionally, Zavrel et al. (2009) used BioLector technology to measure scattered light to monitor the dissolution of 4 wt% cellulose at 80°C over an 8-hour period. Sievers et al. (2009) employed gravimmetry to assess 5 wt% cellulose dissolution and hydrolysis in [bmim]Cl at 120°C over a

14-hour period. As illustrated in Figure 5.7a and b, significant cellulose dissolution (>97% of the observed cellulose) was noted at 100°C after only 60 minutes using the cross-polarized optical microscopy methodology.

Lignin dissolution in [bmim]Cl was observed, for one hour at 100°C, via optical microscopy without the use of cross-polarization (Figure 5.7c and d). In Figure 5.7c the dark brown areas represent lignin and the bright white areas represent the IL-phase (Figure 5.3g). In Figure 5.7d, as with the [emim][OAc] (Figure 5.6d), the IL-phase turned red upon lignin dissolution (Figure 5.3h). As was observed for cellulose dissolution in [bmim]Cl (Figure 5.7b), the dark areas in Figure 5.7d were believed to be gas bubbles. Lignin dissolution in [bmim]Cl was reported by Pu et al. (2007). 13.9 g of lignin per 1 L of [bmim]Cl (1 wt%) was dissolved at 75°C for an unspecified amount of time and dissolution was assessed by visual inspection. In the present study, the results indicated that at 100°C, 4 wt% lignin was fully dissolved within 1 hour.

5.5.2 Phosphonium-Based ILs

5.5.2.1 *CYPHOS® 109*

The dissolution of cellulose in CYPHOS® 109 was monitored for 1 hour at 75°C using cross-polarized microscopy. As can be seen in Figure 5.8a and b, the initial and 1-hour dissolution micrographs, cellulose did not dissolve in CYPHOS® 109 under these conditions. The blue coloured areas in Figure 5.8a and b represent the IL (Figure 5.3i), visible amongst the non-dissolved cellulose, the grey and bright coloured areas in these two micrographs.

The dissolution of lignin in CYPHOS® 109 was also investigated for 1 hour at 75°C and monitored using optical microscopy, without cross-polarized lenses. The initial and 1-hour dissolution micrographs are illustrated in Figure 5.8c and d, where the bright white areas are the IL-phase (Figure 5.3j) and the non-dissolved lignin is represented by dark areas. These micrographs showed that lignin was also not dissolved in CYPHOS® 109 under these conditions.

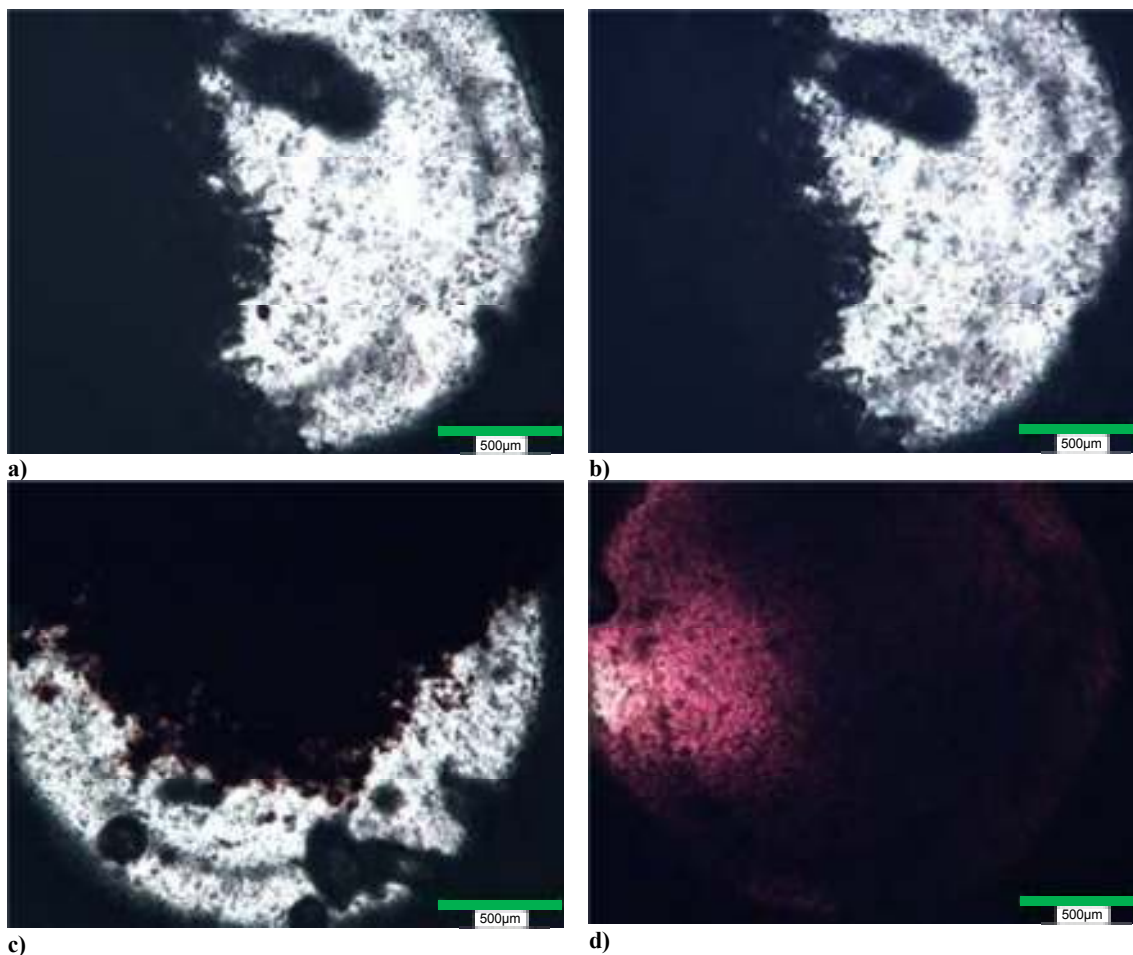**Figure 5.8: CYPHOS® 109 dissolution experiments at 75°C: a) cellulose - initially, b) cellulose - after one hour, c) lignin - initially, d) lignin - after one hour.**

5.5.2.2 *CYPHOS® 441*

Cross-polarized microscopy could not be employed to assess cellulose dissolution in CYPHOS® 441 due to the birefringence of this IL (Figure 5.1). Hence optical microscopy without cross-polarized lenses was used to monitor cellulose dissolution. Dissolution experiments were conducted at 100°C. In the initial and 30-minute micrographs, shown in Figure 5.9a and b, the white area represents the IL-phase (Figure 5.3k) and the dark area, on the left of the micrographs, represents the non-dissolved cellulose. Since both micrographs were identical, it can be concluded that no significant cellulose dissolution occurred in CYPHOS® 441.

Lignin dissolution experiments in CYPHOS® 441 were conducted at 100°C for 30 minutes, and monitored using optical microscopy without cross-polarization. The initial and 30-minute dissolution micrographs, shown in Figure 5.9c and d, indicate that lignin was dissolved in CYPHOS® 441, although the extent of the dissolution was difficult to assess from the micrographs. In the initial micrograph (Figure 5.9c) the dark brown area represents non-dissolved lignin and the white area (Figure 5.3k) represents the IL-phase, whereas in the 30-minute micrograph (Figure 5.9d) the dark red area represents the lignin dissolved in the IL (Figure 5.3l).

Figure 5.9: CYPHOS® 441 dissolution experiments at 100°C: a) cellulose - initially, b) cellulose - after thirty minutes, c) lignin - initially, d) lignin - after thirty minutes.

However, the entire image is not a uniform colour of red as was noted for lignin dissolution in [emim][OAc] (Figure 5.6d) and [bmim]Cl (Figure 5.7d). This was likely due to the high viscosity of the CYPHOS® 441, which formed a gel after 30 minutes of dissolution. The dissolution of lignin by CYPHOS® 441 is a significant finding as it represents the first phosphonium-based IL that could selectively dissolve lignin and not cellulose. These findings are different than those reported by Lee et al. (2008), where ILs that preferentially dissolved lignin but still dissolved cellulose were presented, and are important in efforts to efficiently fractionate lignocellulosic biomass.

5.5.3 DMAc/LiCl

To demonstrate the potential for optical microscopy to be applied more broadly in the screening of potential solvents for lignin and cellulose (and not being limited to only ILs), DMAc/LiCl, a well-established non-IL solvent system for cellulose (Dawsey and McCormick, 1990; McCormick et al., 1985; Potthast et al., 2002), was investigated (cellulose in Figures 5.10 a and b and lignin in Figures 5.10 c and d). First, DMAc/LiCl was used to dissolve cellulose. Cross-polarized optical microscopy was employed as the DMAc/LiCl solution was not birefringent. Cellulose dissolution was noted after cooling from 150°C to 25°C over a 1-hour period in DMAc/LiCl. The resulting initial and after cooling cross-polarized micrographs, shown in Figure 5.10a and b, illustrate that the observed cellulose (the grey and bright coloured areas) was >95% dissolved. The bright blue colour represents the DMAc/LiCl (Figure 5.3m and n). The observation of cellulose dissolution, under these conditions, is consistent with the findings of McCormick et al. (1985), who used visual inspection to monitor the dissolution of 1-3 wt% cellulose in DMAc/LiCl.
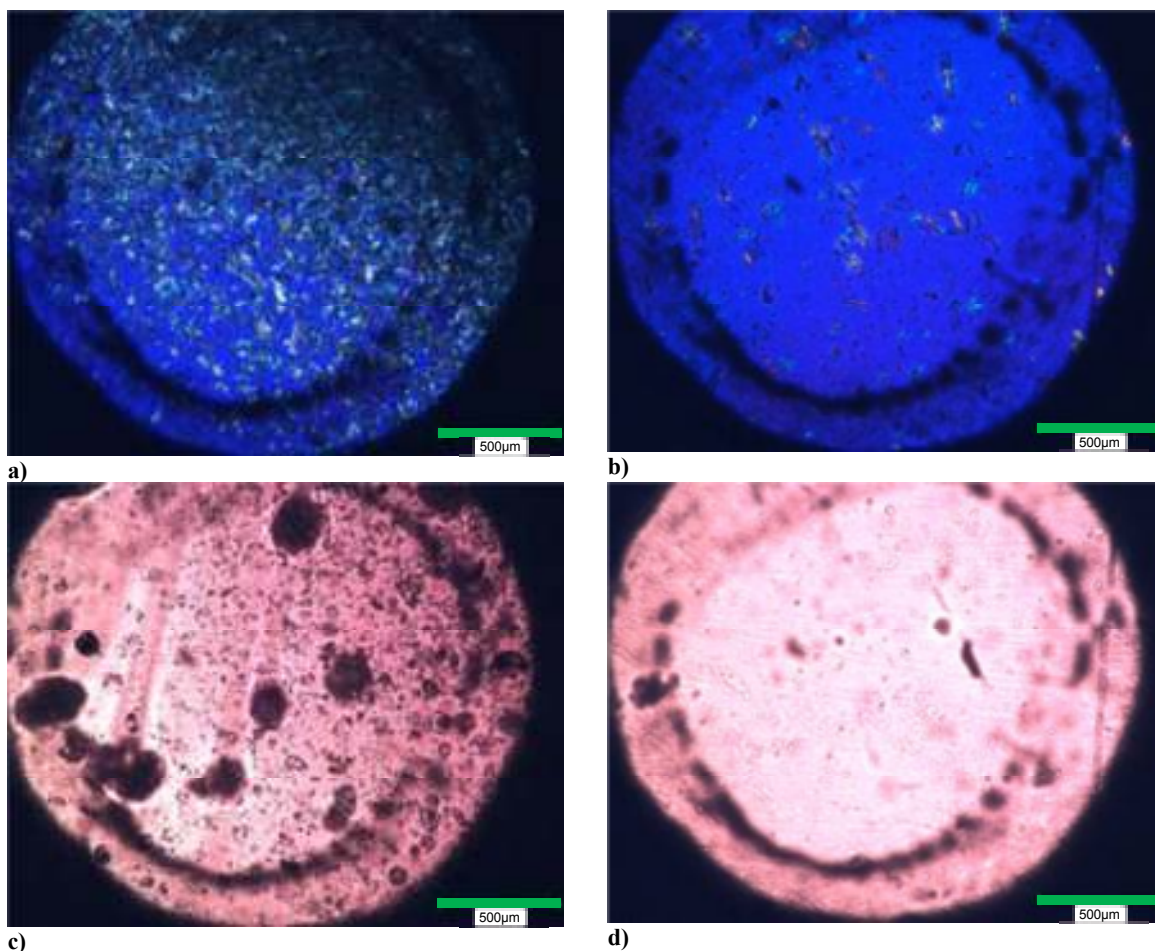
Figure 5.10: DMAc/LiCl dissolution experiments under a N_2 atmosphere: a) cellulose - initially, b) cellulose - after cooling, c) lignin - initially, d) lignin - after forty-five minutes of heating.

Lignin dissolution in DMAc/LiCl was also investigated. The lignin, when subjected to the same dissolution conditions as the cellulose, showed signs of dissolution in the DMAc/LiCl immediately. This can be seen in Figure 5.10c, the initial micrograph, where the pink area represents the DMAc/LiCl phase after lignin dissolution (Figure 5.3o and p) and the dark, circular areas represent the non-dissolved lignin. After heating for 45 minutes (Figure 5.10d), when the system reached approximately 120°C, from an initial 25°C, the lignin was fully dissolved and the DMAc/LiCl turned pink (Figure 5.3p). The use of DMAc/LiCl has been reported for the dissolution of lignin in size exclusion chromatography where the DMAc/LiCl is the mobile phase

(Sjöholm et al., 1999). This present work represents the first study where DMAc/LiCl is employed as a solvent for lignin and the dissolution evaluated via optical microscopy.

5.6 Conclusions

It was demonstrated that optical microscopy, both with and without the use of cross-polarized lenses and small quantities of solvent and solute, can be used to rapidly screen and monitor cellulose or lignin dissolution in a range of IL and non-IL solvents. The methodology presented in this study to assess cellulose and lignin dissolution in ILs was more sensitive than optical microscopy without temperature control and traditional visual inspection. Furthermore, the assessment of lignin dissolution in ILs was not hindered by the observed colour change.

The techniques described here were more rapid (1 hour) than gravimmetry (14 hours), and scattered light measurement methods used in previous studies. Also, the methodology used was more facile than BioLector technology and a specialized high pressure and temperature chamber used in optical microscopy monitoring of cellulose dissolution in water. Furthermore, the results of the DMAc/LiCl screening experiments demonstrated that the optical microscopy technique outlined in this study could be employed to screen for potential cellulose and lignin solvents other than ILs.

In order for this methodology to be applied in real industrial settings, the technique will need to be demonstrated on actual lignocellulosic biomass samples. It is recommended that the dissolution of cellulose (Avicel PH-101) and lignin (Indulin AT) be investigated together to determine if differentiation between the dissolution of the two macromolecules is possible with this methodology. After the investigation of the dissolution of Avicel and Indulin AT, real lignocellulosic feedstocks with potential for use in biorefining should be investigated in order to demonstrate that this methodology can be applied to beyond model biomass compounds. Furthermore, due to the ease of use of this technique, there is potential to automate the methodology, which could enhance its usefulness in an industrial setting.

5.7 References

Champagne, P., 2007. Feasibility of producing bio-ethanol from waste residues: A Canadian perspective Feasibility of producing bio-ethanol from waste residues in Canada, Res.Con.&Rec. 50, 211-230.

Dadi, A.P., Varanasi, S., Schall, C.A., 2006. Enhancement of cellulose saccharification kinetics using an ionic liquid pretreatment step. Biotechnol. Bioeng. 95, 904-910.

Dawsey, T.R., C.L. McCormick, 1990. The lithium chloride/dimethylacetamide solvent for cellulose: A literature review, Polym.Rev. 30, 405-440.

Deguchi, S., K. Tsujii, 2002. Flow cell for in situ optical microscopy in water at high temperatures and pressures up to supercritical state, Rev.Sci.Instrum. 73, 3938-3941.

Deguchi, S., K. Tsujii, K. Horikoshi, 2008. Crystalline-to-amorphous transformation of cellulose in hot and compressed water and its implications for hydrothermal conversion, Green Chem. 10, 191-196.

Deguchi, S., K. Tsujii, K. Horikoshi, 2006. Cooking cellulose in hot and compressed water, Chem.Commun. 2006, 3293-3295.

Firestone, M.A., J.A. Dzielawa, P. Zapol, L.A. Curtiss, S. Seifert, M.L. Dietz, 2002. Lyotropic liquid-crystalline gel formation in a room-temperature ionic liquid, Langmuir. 18, 7258-7260.

FitzPatrick, M., P. Champagne, M.F. Cunningham, R.A. Whitney, 2010. A biorefinery processing perspective: Treatment of lignocellulosic materials for the production of value-added products, Bioresour.Technol. 101, 8915-8922.

Frey, M.W., L. Li, M. Xiao, T. Gould, 2006. Dissolution of cellulose in ethylene diamine/salt solvent systems, Cellulose. 13, 147-155.

Heinze, T., K. Schwikal, S. Barthel, 2005. Ionic liquids as reaction medium in cellulose functionalization, Macromol.Biosci. 5, 520-525.

Jin, H., C. Zha, L. Gu, 2007. Direct dissolution of cellulose in NaOH/thiourea/urea aqueous solution, Carbohydr.Res. 342, 851-858.

Joglekar, H., I. Rahman, B. Kulkarni, 2007. The path ahead for ionic liquids, Chem.Eng.Technol. 30, 819-828.

Kilpeläinen, I., H. Xie, A. King, M. Granstrom, S. Heikkinen, D.S. Argyropoulos, 2007. Dissolution of wood in ionic liquids, J.Agric.Food Chem. 55, 9142-9148.

Köhler, S., T. Liebert, M. Schöbitz, J. Schaller, F. Meister, W. Günther, et al., 2007. Interactions of ionic liquids with polysaccharides 1. Unexpected acetylation of cellulose with 1-ethyl-3-methylimidazolium acetate, Macromol.Rapid Commun. 28, 2311-2317.

Lateef, H., S. Grimes, P. Kewcharoenwong, B. Feinberg, 2009. Separation and recovery of cellulose and lignin using ionic liquids: a process for recovery from paper-based waste, J.Chem.Technol.Biotechnol. 84, 1818-1827.

Lee, S.H., T.V. Doherty, R.J. Linhardt, J.S. Dordick, 2008. Ionic liquid-mediated selective extraction of lignin from wood leading to enhanced enzymatic cellulose hydrolysis, Biotechnol. Bioeng. 102, 1368-1376.

Li, C., Q. Wang, Z.K. Zhao, 2008. Acid in ionic liquid: An efficient system for hydrolysis of lignocellulose, Green Chem. 10, 177-182.

Lynd, L.R., P.J. Weimer, W.H. van Zyl, I.S. Pretorius, 2002. Microbial cellulose utilization: Fundamentals and biotechnology, Microbiol. Mol. Biol. Rev. 66, 506-577.

McCormick,C. L., 1981. Novel Cellulose Solutions, 4,278,790.

McCormick, C.L., P.A. Callais, B.H. Hutchinson, 1985. Solution studies of cellulose in lithium chloride and N,N-dimethylacetamide, Macromolecules. 18, 2394-2401.

Mosier, N., C. Wyman, B. Dale, R. Elander, Y.Y. Lee, M. Holtzapple, et al., 2005. Features of promising technologies for pretreatment of lignocellulosic biomass, Bioresour.Technol. 96, 673-686.

Potthast, A., T. Rosenau, R. Buchner, T. Röder, G. Ebner, H. Bruglachner, et al., 2002. The cellulose solvent system N,N-dimethylacetamide/lithium chloride revisited: the effect of water on physicochemical properties and chemical stability, Cellulose. 9, 41-53.

Pu, Y., N. Jiang, A.J. Ragauskas, 2007. Ionic liquid as a green solvent forl, J. Wood Chem. Tech. 27, 23-33.

Sievers, C., M.B. Valenzuela-Olarte, T. Marzialetti, I. Musin, P.K. Agrawal, C.W. Jones, 2009. Ionic-liquid-phase hydrolysis of pine wood, Ind. Eng. Chem. Res. 48, 1277-1286.

Sjöholm, E., K. Gustafsson, A. Colmsjö, 1999. Size exclusion chromatography of lignins using lithium chloride/n,n-dimethylacetamide as mobile phase. I. Dissolved and residual birch Kraft lignins, J.Liq.Chromatogr.Rel.Technol. 22, 1663.

Sun, N., M. Rahman, Y. Qin, M.L. Maxim, H. Rodríguez, R.D. Rogers, 2009. Complete dissolution and partial delignification of wood in the ionic liquid 1-ethyl-3-methylimidazolium acetate, Green Chem. 11, 646-655.

Swatloski, R.P., S.K. Spear, J.D. Holbrey, R.D. Rogers, 2002. Dissolution of cellose with ionic liquids, J.Am.Chem.Soc. 124, 4974-4975.

van Haveren, J., E. Scott, J. Sanders, 2008. Bulk chemicals from biomass, Biofuels, Bioprod. Bioref. 2, 41-57.

Xiao, M., M.W. Frey, 2007. The role of salt on cellulose dissolution in ethylene diamine/salt solvent systems, Cellulose. 14, 225-234.

Xu, A., J. Wang, H. Wang, 2010. Effects of anionic structure and lithium salts addition on the dissolution of cellulose in 1-butyl-3-methylimidazolium-based ionic liquid solvent systems, Green Chem. 12, 268-275.

Youngs, T.G.A., C. Hardacre, J.D. Holbrey, 2007. Glucose solvation by the ionic liquid 1,3-dimethylimidazolium chloride: A simulation study, J. Phys. Chem. B. 111, 13765-13774.

Zavrel, M., D. Bross, M. Funke, J. Buchs, A.C. Spiess, 2009. High-throughput screening for ionic liquids dissolving (ligno-)cellulose, Bioresour.Technol. 100, 2580-2587.

Zhang, H., J. Wu, J. Zhang, J. He, 2005. 1-Allyl-3-methylimidazolium chloride room temperature ionic liquid: A new and powerful nonderivatizing solvent for cellulose, Macromolecules. 38, 8272-8277.

Zhang, Y., H. Du, X. Qian, E.Y.-. Chen, 2010. Ionic liquid−water mixtures: Enhanced Kw for efficient cellulosic biomass conversion, Energy Fuels. 4, 2410-2417.

Zhang, Y.-.P., 2008. Reviving the carbohydrate economy via multi-product lignocellulose biorefineries, J.Ind.Microbiol.Biotechnol. 35, 367-375.

Zhbankov, R.G., 1992. Hydrogen bonds and structure of carbohydrates, J.Mol.Struct. 270, 523-539.

Zhu, S., Y. Wu, Q. Chen, Z. Yu, C. Wang, S. Jin, et al., 2006. Dissolution of cellulose with ionic liquids and its application: a mini-review, Green Chem. 8, 325-327.

Chapter 6

The Effect of Subcritical Carbon Dioxide on the Dissolution of Cellulose in the Ionic Liquid 1-Ethyl-3-Methylimidazolium Acetate

Michael FitzPatrick, Pascale Champagne, Michael F. Cunningham

6.1 Preface

As was shown in Chapters 4 and 5, the application of PLS to FTIR spectra and optical microscopy can be used to quantitatively determine cellulose content in an IL solution (Chapter 4) and screen solvents for their potential to dissolve biomass (Chapter 5). In this chapter, a simple and low-cost method to reduce the viscosity of IL/cellulose solutions will be addressed.

In this chapter, the application of a subcritical CO_2 environment to [emim][OAc] during the dissolution of cellulose was investigated. CO_2 is soluble in [emim][OAc] and it affects the viscosity but not the polarity of the IL (Jessop and Subramaniam, 2007; Shiflett and Yokozeki, 2009). The goal of the work in this chapter was to determine the effect of 50 psi CO_2 on the dissolution of cellulose in [emim][OAc] at both 50°C and 75°C as compared to a 20 psi N_2 control environment. Additionally, the crystallinity of the cellulose dissolve in IL, after regeneration, was measured to determine if 50 psi CO_2 caused any changes in crystallinity.

6.2 Abstract

The ionic liquid (IL) 1-ethyl-3-methylimidazolium acetate ([emim][OAc]) readily dissolves high concentrations of cellulose. However, the high viscosity of [emim][OAc] (162 cP at 20°C) could limit its use as a solvent for cellulose. Dissolved CO_2 has been shown to decrease the viscosity of ILs. In this study, a 50 psi CO_2 environment was applied for the dissolution of cellulose in [emim][OAc] and compared against a 20 psi N_2 control environment at 50°C and 75°C to determine if the cellulose dissolution could be enhanced. Dissolution profiles of 4 wt% cellulose dissolved in [emim][OAc] were obtained over a 24 hour period. A nearly 2-fold increase in the amount of dissolved cellulose was observed with the application of a 50 psi CO_2 environment, compared to the 20 psi N_2 control standards at 50°C after 24 hours.

6.3 Introduction

The use of ionic liquids (ILs) to disrupt the complex hydrogen bonding network in biomass for promoting the dissolution of lignocellulosic feedstocks has gained popularity within the last 5 years (Dadi et al., 2007; Fort et al., 2007; Kadokawa et al., 2008a; Zavrel et al., 2009). 1-Ethyl-3-methylimidazolium acetate ([emim][OAc]) (Figure 6.1) has been of particular interest. For example, it has been demonstrated that 5 wt% and 12 wt% cellulose can be fully dissolved in [emim][OAc] at 90°C and 100°C, respectively (Vitz et al., 2009; Zavrel et al., 2009).
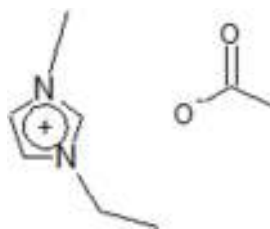
Figure 6.1: Structure of [emim][OAc].

The production of cellulose acetate is industrially important due to its widespread commercial appeal in products such as fabric for clothing, sunglasses and for the production of playing cards. Cellulose can be reacted with 2-furoyl chloride in [emim][OAc] to yield cellulose acetate with a degree of substitution reaching 1.86 and yields of up to 98.5% (Köhler et al., 2007). However the high viscosity of [emim][OAc] (162 cP at 20°C), although lower than many other cellulose dissolving ILs, makes its handling and use in cellulose processing difficult (Bonhote et al., 1996). This problem is exacerbated by cellulose dissolution since the viscosity increases with dissolved cellulose content (Gericke et al., 2009; Hermanutz et al., 2008; Song et al., 2010). In addition to cellulose dissolution, other applications such as catalysis in the IL phase (Dupont et al., 2002; Sheldon, 2001; Welton, 1999) could also benefit from a decrease in IL viscosity.

In addition to their use as biomass solvents, ILs have been investigated for CO_2 capture and sequestration (Bates et al., 2002). Additionally, supercritical CO_2 has been used to separate

IL/organic mixtures (Blanchard et al., 2001; Scurto et al., 2002), leading to investigations aimed at determining the phase behaviour of CO_2 in ILs (Blanchard et al., 2001; Shiflett and Yokozeki, 2005). Shiflett and Yokozeki (2009) reported that CO2 strongly (chemically) absorbs in the ionic liquid [emim][Ac] yielding a highly unusual (nonideal) phase behavior, and at low CO2 concentrations [100x1 < 15 mole fraction] at 25-75°C, the binary mixtures exhibited hardly any vapor pressures, reflecting a strong attractive (or complex formation) interaction between the CO2 and [emim][OAc]. They also showed that the complex is reversible in a separate absorption-desorption experiment at 25°C. The phase behavior belongs to an extremely rare case where the CO2 solubility is highly asymmetric with respect to CO2 concentration. The behavior and properties of gas-expanded liquids have been presented in a comprehensive review by Jessop and Subramaniam (2007). CO_2 is particularly soluble in [emim][OAc]; at 50 psi the CO_2 dissolved in [emim][OAc] ranges from nearly 23 mol% to 30 mol% and decreases with increasing temperatures (from 25°C to 75°C) (Shiflett and Yokozeki, 2009). Aki et al. (2004) showed that, in general, a moderate amount of CO_2 dissolved in ILs (less than 10 mol% at 60°C under an approximately 50 psi CO_2 environment) resulted in only a slight corresponding volume expansion (<10% at up to 30 mol% CO_2). Other IL properties, such as viscosity, change significantly with CO_2 dissolution. Liu et al. (2003) observed that the viscosity of [bmim][PF_6] decreased from approximately 60 cP with no dissolved CO_2 to approximately 36 cP upon the dissolution of 30 mol% CO_2 at 50°C. IL properties important to cellulose dissolution, such as polarity and accepting and donating of hydrogen-bonds, quantified by the Kamlett-Taft parameters ß and α, were left unchanged with CO_2 dissolution in ILs (Fredlake et al., 2004; Jessop and Subramaniam, 2007).

Rinaldi (2011) reporting the use of large volumes of different molecular solvents to dilute ILs for the purpose of cellulose dissolution. Similar to CO_2 dissolution in ILs, the dilution of ILs with molecular solvents does not reduce the cellulose dissolution properties of ILs (Rinaldi, 2011). Fourteen different molecular solvents were explored for IL dilution to a molecular fraction

of 0.08-0.59 of the solution to improve cellulose dissolution. The authors reported the instantaneous dissolution of 10 wt% cellulose by 0.18 molecular fraction [emim][OAc] in solution with, 3,-dimethyl-2-imidazolidinone (Rinaldi, 2011).

We report the use of benign CO_2 to assist in the dissolution of cellulose in [emim][OAc]. The dissolution profiles of 4 wt% cellulose under 50 psi CO_2, compared to a 20 psi N_2 control environment, were obtained at 50°C and 75°C. In addition, the crystallinity of the regenerated cellulose was measured to determine if the application of 50 psi CO_2 resulted in changes in crystallinity with cellulose dissolution in the IL. Catalytic amounts of acid (Li et al., 2008) and water (Zhang et al., 2010) have been reported to hydrolyze cellulose to glucose. Thus, after cellulose regeneration a dinitrosalicylic acid (DNS) assay was performed on the [emim][OAc] to determine if cellulose hydrolysis to glucose had occurred during the dissolution process.

6.4 Materials and Methods

6.4.1 Materials

The ionic liquid 1-ethyl-3-methylimidazolium acetate ([emim][OAc]) (≥90%, BASF) was used as received for all dissolution studies. Karl Fisher titration showed that the IL had a water content of approximately 4200 ppm or 0.42 wt%. Avicel PH-101 (Sigma-Aldrich), a model microcrystalline cellulose compound, was used as received. Ultra high purity nitrogen and medical grade carbon dioxide were obtained from Praxair. All dissolution experiments were conducted in 15 mL Ace Glass Pressure Tubes with Plunger Valve and a modified Thermowell (Ace Glass, USA). For the gravimetric studies, Fisherbrand P8 filter paper (Fisher Scientific) was used. For the dinitrosalicylic acid (DNS) assay for reducing sugar content, dinitrosalicylic acid (98%, Aldrich), phenol - loose crystals (>99%, Fisher), anhydrous sodium sulphite (>99%, Fisher), sodium hydroxide (>97%, Fisher), and potassium sodium tartrate tetrahydrate (reagent grade, MP Biomedicals), were used as received.

6.4.2 Cellulose Dissolution Experiments

Dissolution experiments were conducted in 15 mL Ace Glass pressure tubes immersed in a heated oil bath at 50°C and 75°C (±2°C). Prior to cellulose addition, 6 mL of [emim][OAc] was allowed to equilibrate with the gas (either 50 psi CO_2 or 20 psi N_2) for 3 hours to ensure equilibrium was reached (Shiflett and Yokozeki, 2009), leaving approximately 8 mL of headspace in the pressure tube after the addition of [emim][OAc]. 50 psi CO_2 was selected based on safety considerations with the apparatus used. At 50 psi CO_2 23 and 27 mol% CO_2 can be dissolved in [emim][OAc] at 75°C and 50°C, respectively (Shiflett and Yokozeki, 2009). All dissolution experiments involved cellulose loadings of 4 wt%. Cellulose was manually added to the pressure tubes after the 3 hour equilibration period. Mixing was provided using a stir bar. As ILs, in general, preferentially dissolve CO_2 over N_2 (Lodge, 2008), 20 psi N_2 was used as a control environment to minimize the effect of varying atmospheric humidity on the dissolution of cellulose in [emim][OAc]. Dissolutions were conducted in triplicate, for 0.5, 3, 12, or 24 hours after cellulose addition. At the completion of each dissolution experiment, the 6 mL [emim][OAc]/cellulose solution was filtered through glass wool (~1 cm^3) inside a 10 mL syringe to separate the non-dissolved cellulose.

6.4.3 Cellulose Recovery

The cellulose dissolution experiment filtrate was regenerated in distilled water after the [emim][OAc]/cellulose samples were cooled to room temperature in a desiccator. 1 mL of [emim][OAc]/cellulose was regenerated in 10 mL of distilled water and mixed using a stir bar for 2 hours. The regenerated cellulose was then allowed to settle for 20 hours at room temperature.

6.4.4 Analysis

6.4.4.1 *Gravimetric*

For each dissolution experiment, 3 separate 1 mL cellulose regenerations were conducted and then added together for gravimetric analysis. Each 10:1 (mL) water:[emim][OAc]/cellulose solution was filtered through a pre-weighed Fisherbrand P8 filter paper and washed with an additional 90 mL of distilled water. The cellulose regeneration filtrate was reserved for the DNS assay. The regenerated cellulose and filter paper were then dried in a vacuum oven at 75°C, between -67 and -85 kPa (-20 to -25 in Hg) for 18 hours. They were allowed to cool in a desiccator for 1 hour at room temperature prior to weighing.

6.4.4.2 *Thermogravimetric*

Thermogravimetric analysis was conducted using a TGA Q500 (TA Instruments). Samples were heated from 20°C to 600°C at a rate of 10°C/min. Samples ranged between 5-10 mg in weight.

6.4.4.3 *Dinitrosalicylic Acid (DNS) Assay*

The modified DNS assay (specific details of this methodology are provided in Appendix D), with the inclusion of phenol for colour intensification and potassium sodium tartrate for colour stabilization, described by Miller (1959), was followed. 3 mL of 1% dinitrosalicylic acid, 0.2% phenol, 0.5% sodium sulfite and 1% sodium hydroxide were added to 3 mL 33% cellulose regeneration filtrate in water and boiled for 7 minutes. After boiling, 1 mL of 40% potassium sodium tartrate was added before cooling to room temperature. UV absorbance of the mixture was measured at 540 nm.

6.4.4.4 *X-Ray Diffraction*

X-Ray Diffraction (XRD) analysis was conducted using a Philips X'Pert Pro MPD diffractometer fitted with an X'Celerator high speed strip detector. Sample count time was 20

seconds at 0.02° 2θ increments, scanned from 6° to 60° (2θ), while the sample rotated at 2 seconds/revolution.

6.5 Results and Discussion

6.5.1 Cellulose Dissolution

The high viscosity of ILs, generally ranging from tens to hundreds of cP, makes their use difficult and can hinder their effectiveness as biomass solvents due to inherent mass transfer limitations and slow dissolution kinetics associated with higher viscosity liquids (Bonhote et al., 1996; Gericke et al., 2009). In addition, viscosity increases when cellulose is dissolved in ILs (Gericke et al., 2009; Hermanutz et al., 2008; Song et al., 2010). To address this issue, subcritical CO_2 was employed to reduce the viscosity of [emim][OAc]. Initial experiments conducted at 75°C showed that 50 psi CO_2 improved the amount of cellulose dissolved in [emim][OAc] in a given time period; complete dissolution (±3.6%) after 24 hours as compared to 91.9 ±1.3% dissolution after 24 hours under the 20 psi N_2 control environment (Figure 6.2). Further studies conducted at 50°C, revealed no enhancement in cellulose dissolution with the CO_2 compared to the N_2 environment after 3 hours (13.8 ±5.4% and 20.7 ±7.9%, respectively) and 12 hours (35.5 ±8.9% and 36.3 ±11.9%, respectively) as seen in Figure 6.3. After 24 hours, however, a significant difference between the two environments was observed; where under the N_2 environment 38.4 ±5.9% cellulose was dissolved, while 66.7 ±4.3% cellulose was dissolved under the CO_2 environment. A summary of the 4 wt% cellulose dissolution experiments in [emim][OAc] under both 20 psi N_2 and 50 psi CO_2 environments is shown in Appendix C, Table C.1 and Table C.2. Each % cellulose dissolved value represents an average of 3 dissolution experiments with a 95% confidence interval calculated from the triplicate sets (complete data provided in Appendix C, Table C.1 and Table C.2). In addition to the gravimetric study of the dissolution of cellulose in [emim][OAc], a DNS assay was conducted to determine if any of the dissolve cellulose was hydrolyzed to glucose. It was determined that glucose generation was

negligible under each of these environments the data for the DNS assay is provided in Appendix D, Table D.1. Thus, the regenerated cellulose accounted for all of the cellulose dissolved in the [emim][OAc].

The difference between the 50°C and 75°C dissolution profiles is attributed to the difference in the magnitude of viscosity reduction of [emim][OAc] resulting from changes in temperature and amount of dissolved CO_2. Rodriguez and Brennecke (2006) observed that for several 1-ethyl-3-methylimidazolium containing ILs, the viscosity decreased by 53%-63% and 72%-82% at 50°C and 75°C, respectively, as compared to the viscosity at room temperature. Gericke et al. (2009) demonstrated that the viscosity of 4 wt% cellulose in [emim][OAc] was approximately 40 Pa·s. They also observed that the relative viscosity (defined as the ratio of the solution viscosity to the viscosity of the solvent alone) of 4 wt% cellulose in [emim][OAc] decreased by approximately 40% at 60°C and 55% at 80°C, compared to the relative viscosity (~50) at 20°C. It has also been shown that 23 mol% and 27 mol% CO_2, corresponding to the amount of CO_2 dissolved in [emim][OAc] at 75°C and 50°C, reduces the viscosity of [bmim][PF_6] by 33% and 35% at 50°C and 14% and 18% at 60°C (Liu et al., 2003; Shiflett and Yokozeki, 2009). Hence, temperature appears to contribute more significantly to reductions in viscosity than CO_2 in [emim][OAc]. At 75°C the results suggested that the viscosity of [emim][OAc] was more significantly reduced by temperature compared to 50 psi CO_2 and, that the 50 psi CO_2 environment only resulted in a slight increase in cellulose dissolution. At 50°C the results also indicated that the viscosity of [emim][OAc] was dominated by the effect of temperature and was higher than the corresponding effects observed at 75°C. The kinetics of cellulose dissolution (Figure 6.2 and Figure 6.3) were comparatively slower at 50°C than at 75°C, implying a larger viscosity reduction as a result of temperature than due to the presence of 27 mol% vs. 23 mol% CO_2 (Gericke et al., 2009; Liu et al., 2003; Shiflett and Yokozeki, 2009). However, the benefit of CO_2 on cellulose dissolution in [emim][OAc] was more evident under conditions where slower dissolution kinetics due to higher viscosity from lower temperature and

cellulose addition (Gericke et al., 2009) were offset by the increase in mol % CO_2 dissolved in the IL (Shiflett and Yokozeki, 2009). This was observed after 24 hours at 50°C, where there was nearly a 2-fold increase over the N_2 control standards (Appendix E, **Error! Reference source not ound.**).
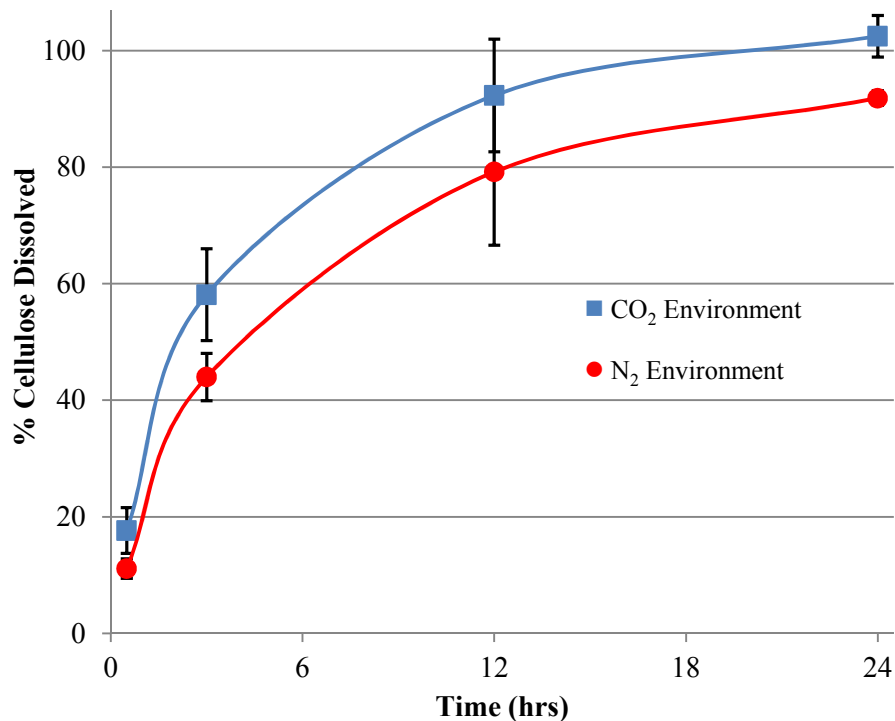
Figure 6.2: Dissolution profile of 4 wt% cellulose in [emim][OAc] at 75°C under both 50 psi CO_2 and 20 psi N_2 environments. Error bars are 95% confidence intervals.
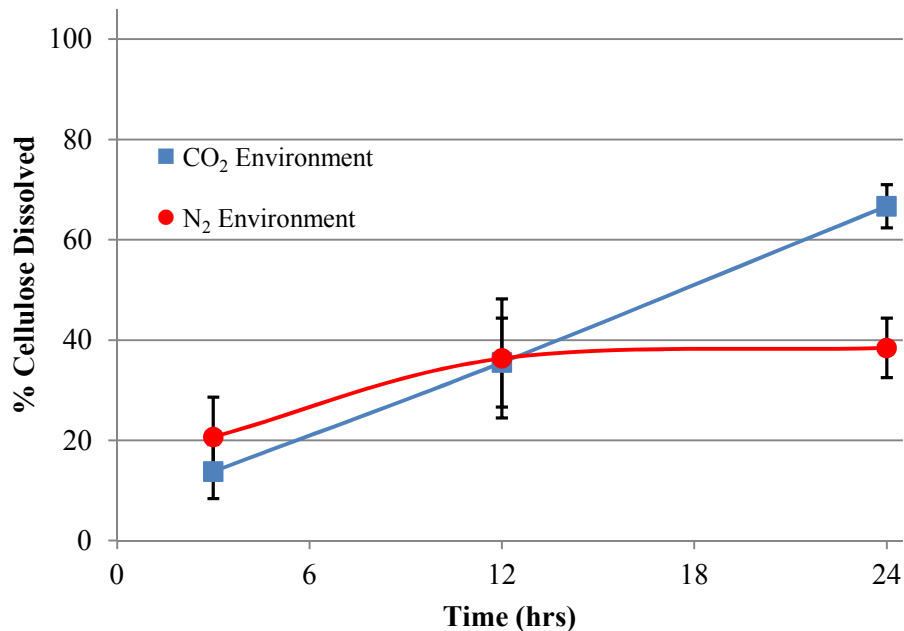
Figure 6.3: Dissolution profile of 4 wt% cellulose in [emim][OAc] at 50°C under both 50 psi CO_2 and 20 psi N_2 environments. Error bars are 95% confidence intervals.

6.5.2 Regenerated Cellulose

After regeneration the recovered cellulose was analyzed to determine if dissolution and regeneration, in [emim][OAc] and distilled water, respectively, had noticeably affected the crystallinity of the cellulose. TGA profiles for the as received cellulose and the 3- and 24-hour dissolutions under either N_2 or CO_2 environments at 50°C (Figure 6.4) and 75°C (Figure 6.5) were obtained. Each profile exhibited a slight drop in weight near 100°C, which was attributed to the loss of water (Fort et al., 2007). For the as received cellulose, the temperature at the onset of decomposition, T_{dec}, and the temperature at the maximum rate of decomposition, T_{max}, occurred at 318.8°C and 337.3°C, respectively. For the regenerated cellulose samples, T_{dec} and T_{max} within 11°C and 5°C of the as received cellulose were noted, respectively (Table 6.1).

Table 6.1: Summary of T_{dec}, T_{max}, and char yield from TGA profiles of as received and regenerated cellulose after dissolution at 50°C or 75°C.

Sample	Dissolution Temperature (°C)	T_{dec} (°C)	T_{max} (°C)	Char Yield (above 600°C)
3hrs - CO_2	50	322.4	337.9	12.1
3hrs - N_2	50	321.8	336.1	6.7
24hrs - CO_2	50	315.0	335.7	21.8
24hrs - N_2	50	320.2	338.6	21.5
3hrs - CO_2	75	318.6	335.8	18.2
3hrs - N_2	75	318.4	339.0	18.5
24hrs - CO_2	75	313.6	334.3	20.9
24hrs - N_2	75	308.4	333.1	38.0
As Received	N/A	318.8	337.3	1.4
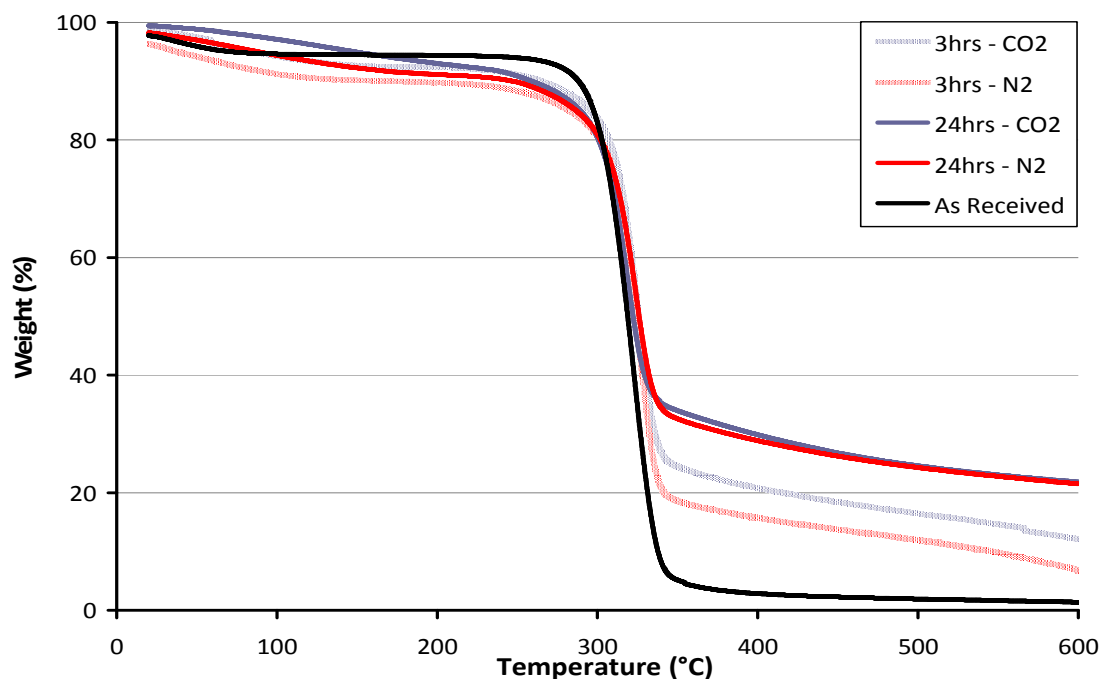
Figure 6.4:TGA profile of regenerated cellulose subject to dissolution at 50°C under both 50 psi CO_2 and 20 psi N_2 environments. Samples were heated from 20°C to 600°C at a rate of 10°C/min.
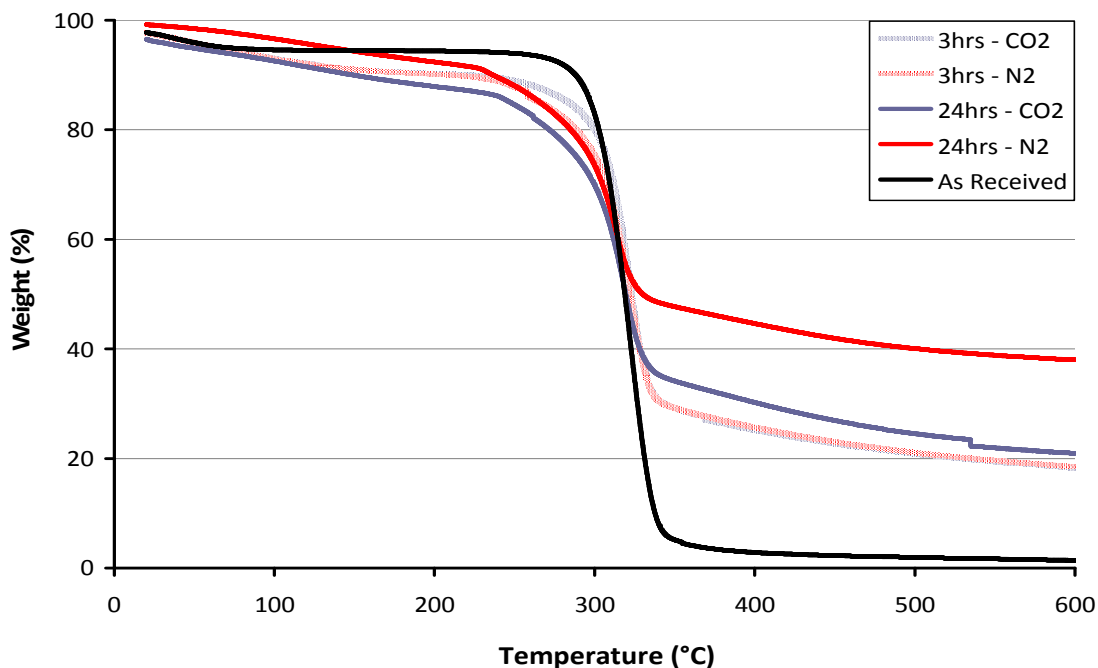
Figure 6.5: TGA profile of regenerated cellulose subject to dissolution at 75°C under both CO_2 and N_2 environments. Samples were heated from 20°C to 600°C at a rate of 10°C/min.

A decrease of more than 50°C for both the T_{dec} and T_{max} for the regenerated cellulose, compared to the original cellulose, has been reported and qualitatively described as representing a decrease in the crystallinity of the cellulose (Fort et al., 2007; Kadokawa et al., 2008; Swatloski et al., 2002). In addition, high char yield (upwards of 40%) was observed in the regenerated cellulose in this study. Char yields of upwards of 40% (residual mass) were also reported by Swatloski et al. (2002) and Zhang et al. (2007) and attributed to the incomplete pyrolysis of the nonvolatile carbonaceous material, characteristic of regenerated cellulose (Swatloski et al., 2002; Zhang et al., 2007). Qualitatively, the TGA profiles (Figure 6.4 and Figure 6.5) suggested that no quantifiable differences in crystallinity were observed between the as received and the regenerated cellulose.

In addition to TGA, XRD analyses were performed on selected regenerated cellulose samples. The XRD spectra of the as received cellulose, 3-hour dissolution and 24-hour dissolution samples, under both N_2 and CO_2 environments at both 50°C (Figure 6.6) and 75°C

(Figure 6.7) were obtained. The as received cellulose was cellulose I, indicated by the crystalline region peak at $2\theta = 22.5°$ and the amorphous region peak at $2\theta = 18°$ (Oh et al., 2005). The shifting of the crystalline region peak at $2\theta = 22.5°$ to $2\theta = 19.8°$ and the amorphous region peak from $2\theta = 18°$ to $2\theta = 16°$ (Figure 6.6 and Figure 6.7) indicated that, for all samples, the regenerated cellulose was cellulose II (Oh et al., 2005; Zhang et al., 2007). This was expected as cellulose I is native cellulose and the change to cellulose II, the crystalline form that is more thermodynamically stable, has been reported for regenerated cellulose from a number of cellulose solvents (Kolpak and Blackwell, 1975; Kolpak and Blackwell, 1976; Oh et al., 2005; Zhang et al., 2007).
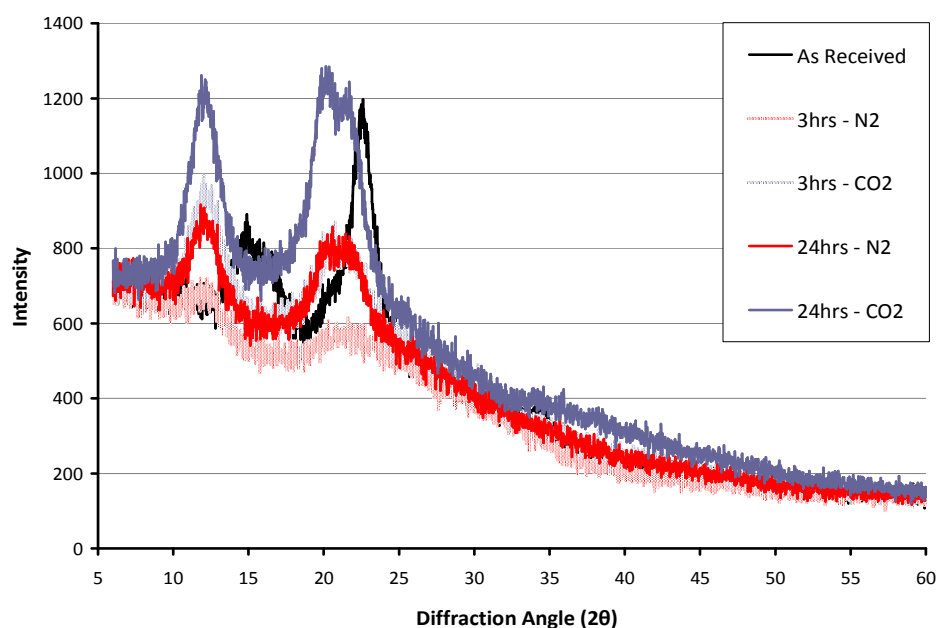
Figure 6.6: XRD profile of as received cellulose and cellulose regenerated after dissolution at 50°C under both CO_2 and N_2 environments. Sample count time was 20 seconds at 0.02° 2θ increments, scanned from 6° to 60° (2θ) while the sample rotated at 2 seconds/revolution.
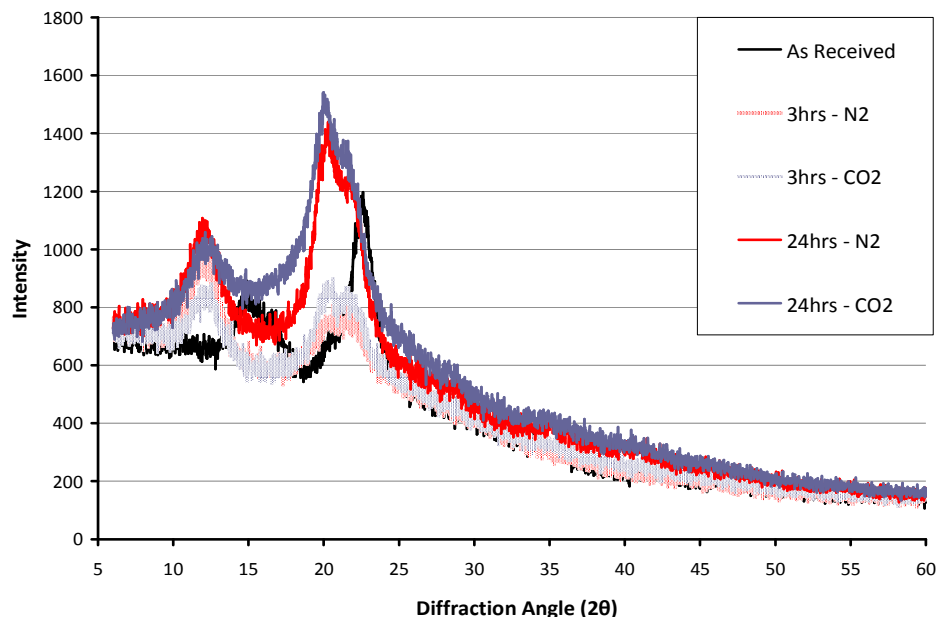
Figure 6.7: XRD profile of as received cellulose and cellulose regenerated after dissolution at 75°C under both CO_2 and N_2 environments. Sample count time was 20 seconds at 0.02° 2θ increments, scanned from 6° to 60° (2θ) while the sample rotated at 2 seconds/revolution.

The crystallinity index (CrI), a relative measure of the degree of crystallinity of a cellulose sample, was calculated for each sample, using their respective XRD spectra and the following relationship:

$$CrI = \left(\frac{I_{Cr} - I_{Am}}{I_{Cr}}\right) \times 100$$

where I_{Cr} is the maximum intensity of the crystalline region (using the 002 reflection measured at 2θ=22.5° for cellulose I or the 101 reflection measured at 2θ=19.8° for cellulose II) and I_{Am} is the maximum intensity of the amorphous region (where 2θ=18° for cellulose I and 2θ=16° for cellulose II) (Oh et al., 2005; Segal et al., 1959). The resulting CrI for selected cellulose samples is shown in Table 6.2. The CrI indicated that the crystallinity of the regenerated cellulose increased with increasing dissolution time and temperature. It was also found to increase, in general, under the CO_2 environment, compared to the N_2 environment for samples under similar experimental conditions (temperature and time). Since CrI is a measure of the relative amounts of crystalline and amorphous cellulose in a sample (Segal et al., 1959), and the amount of the 4 wt%

134

cellulose dissolved in [emim][OAc] increased with time, the increase in CrI with increasing dissolution time indicates that crystalline cellulose dissolves slower than amorphous cellulose. This is the same dissolution behaviour that is typically observed with the hydrolysis of cellulose to glucose, where amorphous cellulose is hydrolyzed much faster than crystalline cellulose (Mosier et al., 2005). Upon regeneration, the CrI of the fully dissolved cellulose (under 50 psi CO_2 for 24 hours at 75°C) decreased; a phenomenon frequently observed in cellulose dissolution in ILs (Dadi et al., 2007; Murakami et al., 2007; Zhang et al., 2005).

Table 6.2: Crystallinity summary of as received cellulose and cellulose regenerated after dissolution at either 50°C or 75°C under both CO_2 and N_2 environments.

Sample	Cellulose I or II	CrI
As Received	Cellulose I	47.3
50°C: 3hrs - N_2	Cellulose II	4.4
50°C: 3hrs - CO_2	Cellulose II	16.9
50°C: 24hrs - N_2	Cellulose II	24.1
50°C: 24hrs - CO_2	Cellulose II	38.5
75°C: 3hrs - N_2	Cellulose II	16.8
75°C: 3hrs - CO_2	Cellulose II	27.0
75°C: 24hrs - N_2	Cellulose II	44.6
75°C: 24hrs - CO_2	Cellulose II	38.4

6.6 Conclusions

Dissolution profiles of 4 wt% cellulose dissolved in [emim][OAc] were obtained over a 24 hour period. It was demonstrated that the application of 50 psi of CO_2 to [emim][OAc] increased the amount of dissolved cellulose at both 50°C (after a 24 hour dissolution period) and 75°C, compared to 20 psi N_2. The effect of the CO_2 environment was most evident at 50°C, where 66.7 ±4.3% cellulose was dissolved under 50 psi CO_2 compared to 38.4 ±5.9% cellulose dissolved under 20 psi N_2 after 24 hours. This was due to the increased amount of CO_2 dissolved in [emim][OAc] at the lower temperature. At 75°C the reduction in viscosity resulting from the higher temperature may be a dominant effect observed affecting the amount of

cellulose dissolved. The increased CrI for regenerated cellulose indicated that the amorphous cellulose dissolved in the IL faster than the crystalline cellulose.

As the enhancement in cellulose dissolution was more apparent at 75°C as opposed to 50°C, it is possible that a further increase in temperature may further enhance cellulose dissolution in the N_2 environment. Future work should involve dissolution studies at room temperature (25°C) and at elevated temperatures (100°C to 120°C). In addition, CO_2 pressures up to 150 psi should be explored to establish an optimum between pressure, temperature, energy conservation and operational safety for cellulose dissolution. Additionally, *in situ* rheometry studies should be undertaken to determine real-time viscosity change of the [emim][OAc]/cellulose mixture, with and without gas expansion for a range of temperatures and pressures.

6.7 References

Aki, S.N.V.K., B.R. Mellein, E.M. Saurer, J.F. Brennecke, 2004. High-pressure phase behavior of carbon dioxide with imidazolium-based ionic liquids, J. Phys. Chem. B. 108, 20355-20365.

Bates, E.D., R.D. Mayton, I. Ntai, J.H. Davis, 2002. CO2 capture by a task-specific ionic liquid, J.Am.Chem.Soc. 124, 926-927.

Blanchard, L.A., Z. Gu, J.F. Brennecke, 2001. High-pressure phase behavior of ionic liquid/CO2 systems, J. Phys. Chem. B. 105, 2437-2444.

Bonhote, P., A. Dias, N. Papageorgiou, K. Kalyanasundaram, M. Gratzel, 1996. Hydrophobic, highly conductive ambient-temperature molten salts, Inorg.Chem. 35, 1168-1178.

Dadi, A.P., C.A. Schall, S. Varanasi, 2007. Mitigation of cellulose recalcitrance to enzymatic hydrolysis by ionic liquid pretreatment, Appl.Biochem.Biotechnol. 137, 407-421.

Dupont, J., R.F.d. Souza, P.A.Z. Suarez, 2002. Ionic liquid (molten salt) phase organometallic catalysis, Chem.Rev. 102, 3667-3692.

Fort, D.A., R.C. Remsing, R.P. Swatloski, P. Moyna, G. Moyna, R.D. Rogers, 2007. Can ionic liquids dissolve wood? Processing and analysis of lignocellulosic materials with 1-*n*-butyl-3-methylimidazolium chloride, Green Chem. 9, 63-69.

Fredlake, C.P., M.J. Muldoon, S.N.V.K. Aki, T. Welton, J.F. Brennecke, 2004. Solvent strength of ionic liquid/CO2 mixtures, Phys.Chem.Chem.Phys. 6, 3280-3285.

Gericke, M., K. Schlufter, T. Liebert, T. Heinze, T. Budtova, 2009. Rheological properties of cellulose/ionic liquid solutions: From dilute to concentrated states, Biomacromolecules. 10, 1188-1194.

Hermanutz, F., F. Gähr, E. Uerdingen, F. Meister, B. Kosan, 2008. New developments in dissolving and processing of cellulose in ionic liquids, Macromol.Symp. 262, 23-27.

Jessop, P.G., B. Subramaniam, 2007. Gas-expanded liquids, Chem.Rev. 107, 2666-2694.

Kadokawa, J., M. Murakami, Y. Kaneko, 2008a. A facile method for preparation of composites composed of cellulose and a polystyrene-type polymeric ionic liquid using a polymerizable ionic liquid, Composites Sci.Technol. 68, 493-498.

Kadokawa, J., M. Murakami, Y. Kaneko, 2008b. A facile preparation of gel materials from a solution of cellulose in ionic liquid, Carbohydr.Res. 343, 769-772.

Köhler, S., T. Liebert, M. Schöbitz, J. Schaller, F. Meister, W. Günther, et al., 2007. Interactions of ionic liquids with polysaccharides 1. Unexpected acetylation of cellulose with 1-ethyl-3-methylimidazolium acetate, Macromol.Rapid Commun. 28, 2311-2317.

Kolpak, F.J., J. Blackwell, 1976. Determination of the structure of cellulose II, Macromolecules. 9, 273-278.

Kolpak, F.J., J. Blackwell, 1975. The structure of regenerated cellulose, Macromolecules. 8, 563-564.

Li, C., Wang, Q., Zhao, Z.K., 2008. Acid in ionic liquid: An efficient system for hydrolysis of lignocellulose. Green Chem. 10, 177-182.

Liu, Z., W. Wu, B. Han, Z. Dong, G. Zhao, J. Wang, et al., 2003. Study on the phase behaviors, viscosities, and thermodynamic properties of CO2/[C4mim][PF6]/methanol system at elevated pressures, Chem.Eur.J. 9, 3897-3903.

Lodge, T.P., 2008. Materials science: A unique platform for materials design, Science. 321, 50-51.

Miller, G.L., 1959. Use of dinitrosalicylic acid reagent for determination of reducing sugar, Anal.Chem. 31, 426-428.

Mosier, N., C. Wyman, B. Dale, R. Elander, Y.Y. Lee, M. Holtzapple, et al., 2005. Features of promising technologies for pretreatment of lignocellulosic biomass, Bioresour.Technol. 96, 673-686.

Murakami, M., Y. Kaneko, J. Kadokawa, 2007. Preparation of cellulose-polymerized ionic liquid composite by in-situ polymerization of polymerizable ionic liquid in cellulose-dissolving solution, Carbohydr.Polym. 69, 378-381.

Oh, S.Y., D.I. Yoo, Y. Shin, H.C. Kim, H.Y. Kim, Y.S. Chung, et al., 2005. Crystalline structure analysis of cellulose treated with sodium hydroxide and carbon dioxide by means of X-ray diffraction and FTIR spectroscopy, Carbohydr.Res. 340, 2376-2391.

Rinaldi, R., 2010. Instantaneous dissolution of cellulose in organic electrolyte solutions, Chem.Commun. 47, 511-513.

Rodríguez, H., J.F. Brennecke, 2006. Temperature and composition dependence of the density and viscosity of binary mixtures of water + ionic liquid, J. Chem. Eng. Data. 51, 2145-2155.

Scurto, A.M., S.N.V.K. Aki, J.F. Brennecke, 2002. CO2 as a separation switch for ionic liquid/organic mixtures, J.Am.Chem.Soc. 124, 10276-10277.

Segal, L., J.J. Creely, A.E. Martin Jr., C.M. Conrad, 1959. An empirical method for estimating the degree of crystallinity of native cellulose using the X-ray diffractometer, Text.Res.J. 29, 786-794.

Sheldon, R., 2001. Catalytic reactions in ionic liquids, Chem.Commun. 2001, 2399-2407.

Shiflett, M.B., A. Yokozeki, 2009. Phase behavior of carbon dioxide in ionic liquids: [emim][Acetate], [emim][Trifluoroacetate], and [emim][Acetate] + [emim][Trifluoroacetate] mixtures, J.Chem.Eng.Data. 54, 108-114.

Shiflett, M.B., A. Yokozeki, 2005. Solubilities and diffusivities of carbon dioxide in ionic liquids: [bmim][PF6] and [bmim][BF4], Ind. Eng. Chem. Res. 44, 4453-4464.

Song, H., J. Zhang, Y. Niu, Z. Wang, 2010. Phase transition and rheological behaviors of concentrated cellulose/ionic liquid solutions, J. Phys. Chem. B. 114, 6006-6013.

Swatloski, R.P., S.K. Spear, J.D. Holbrey, R.D. Rogers, 2002. Dissolution of cellose with ionic liquids, J.Am.Chem.Soc. 124, 4974-4975.

Vitz, J., T. Erdmenger, C. Haensch, U.S. Schubert, 2009. Extended dissolution studies of cellulose in imidazolium based ionic liquids, Green Chem. 11, 417-424.

Welton, T., 1999. Room-Temperature Ionic Liquids. Solvents for synthesis and catalysis, Chem.Rev. 99, 2071-2084.

Zavrel, M., D. Bross, M. Funke, J. Buchs, A.C. Spiess, 2009. High-throughput screening for ionic liquids dissolving (ligno-)cellulose, Bioresour.Technol. 100, 2580-2587.

Zhang, Y., Du, H., Qian, X., Chen, E.Y.-X., 2010. Ionic Liquid−Water Mixtures: Enhanced Kw for Efficient Cellulosic Biomass Conversion. Energy Fuels 4, 2410-2417.

Zhang, H., Z. . Wang, Z. . Zhang, J. Wu, J. Zhang, J. . He, 2007. Regenerated-cellulose/multiwalled- carbon-nanotube composite fibers with enhanced mechanical properties prepared with the ionic liquid 1-allyl-3-methylimidazolium chloride, Adv Mater. 19, 698-704.

Zhang, H., J. Wu, J. Zhang, J. He, 2005. 1-Allyl-3-methylimidazolium chloride room temperature ionic liquid: A new and powerful nonderivatizing solvent for cellulose, Macromolecules. 38, 8272-8277.

Chapter 7

Conclusions and Recommendations for Future Work

7.1 Conclusions

In the last decade, ILs have been investigated as solvents for lignocellulosic biomass species. Additionally, the *in situ* functionalization of cellulose and production of value-added chemicals from lignin have been accomplished in ILs. However, there are two main difficulties associated with the processing of biomass in ILs and the research presented in this thesis focused on developing solutions to these obstacles.

The first goal of this work was to develop methods to quantitatively monitor and screen the dissolution of biomass, specifically cellulose and lignin that were simple, rapid and inexpensive. To achieve this goal, truncated ATR FTIR spectra from cellulose dissolved in [emim][OAc] were subjected to partial least squares regression to model cellulose content. Up to 4 wt% cellulose loading in [emim][OAc] was quantitatively determined within 0.533 wt%, when a spectral normalization data preprocessing technique was applied. This represented a nearly 13% decrease in the RMSEP as compared to the untreated spectra and there was an increase in the number of predicted validation standards from 5 to 8 out of 10.

The RMSEP of 0.533 wt% is more significant at lower cellulose weight loadings, thus it is desirable to be at as high cellulose loading as possible for quantitative measure using this technique. This corresponds well to industrial requirements, since the range of dissolved cellulose will have to be expanded over 10 wt% to be in a more realistic industrial range of conditions. FTIR for compositional analysis of corn stover determined cellulose composition within 1.4 wt%, though 100 samples were used for the calibration set. If the range of dissolved cellulose was expanded to 10 wt% for the methodology in this thesis, then the wt% error, relative to the cellulose concentration assessed, would be the same as was reported for corn stover. It should also be noted that the [emim][OAc] used in this FTIR study had a purity ≥90%, which was less

pure than ILs used in other cellulose dissolution studies. As such, the purity of the IL is not as critical to this quantitative analytical technique.

Optical microscopy was used to monitor cellulose and lignin dissolution in 4 ILs; 2 imidazolium-based ([emim][OAc] and [bmim]Cl) and 2 phosphonium-based (CYPHOS[®]109 and CYPHOS[®]441). The facile methodology presented in this work was more sensitive than traditional techniques such as visual inspection and optical microscopy without temperature control. The techniques were more rapid than gravimmetry (14 hours) and the BioLector technology (up to 8 hours). It was demonstrated, via the DMAc/LiCl screening experiments, that the outlined methodology could be employed to qualitatively screen for potential cellulose and lignin solvents beyond ILs. However, as with any microscopy technique, there will be concerns over the accuracy of each micrograph and how representative they are. Though the entire sample is not being analyzed with the quick screening technique, the small view of the dissolution of cellulose or lignin provided by this methodology will suffice since it was intended to qualitatively screen for biomass dissolution, and not to be used quantitatively.

The high viscosity of IL/cellulose solutions can slow down the dissolution of cellulose. Investigating a low-cost and environmentally benign method to reduce the viscosity of IL/cellulose was the second goal of this work. At both 50°C and 75°C, an increase in the amount of dissolved cellulose was observed when a 50 psi CO_2, compared to 20 psi N_2, was applied to [emim][OAc]. The increase in dissolved cellulose due to CO_2 was most pronounced at 50°C due to the increased amount of CO_2 dissolved in [emim][OAc]. At 75°C, the reduction in viscosity as a result of the higher temperature may be a dominant effect observed affecting cellulose dissolution. The effect of the 50 psi CO_2 environment was most evident at 50°C after 24 hours, where 66.7 ±4.3% cellulose was dissolved, compared to 38.4 ±5.9% cellulose dissolved under 20 psi N_2.

The aforementioned findings can be applied in the development of value-added products from biomass to aid in both design (in terms of CO_2 addition to decrease the viscosity of

IL/cellulose solutions) and operation (in terms of FTIR *in situ* dissolution monitoring in ILs and optical microscopy screening for potential IL biomass solvents). The FTIR dissolution monitoring technique could be adapted for use in determining lignocellulosic biomass composition or to monitor hydrolysis of cellulose and hemicellulose to their reducing sugars. The microscopy technique can be applied to broadly study potential biomass solvents, not just ILs, as demonstrated in Chapter 5. This technique was shown to be especially useful for non-transparent solvents, where visual inspection of the solution is ineffectual. The CO_2 dissolution in ILs, resulting in a decrease in their viscosity while maintaining many other properties, also has potential applications in biorefining and IL-phase catalysis.

7.2 Recommendations for Future Work

PLS regression on FTIR spectra for determination of cellulose dissolved in [emim][OAc], in Chapter 4, quantitatively determined the cellulose content within 0.533 wt%. However, it is recommended that the number of samples used to build both the calibration and validation sets be increased to improve the predictive capabilities of the model. Though 100 samples were used in developing a calibration set for compositional analysis of corn stover, it is recommended that the calibration set for this study only be expanded to 50 samples. It is believed that 50 samples should be sufficient since corn stover is more complex than the model cellulose compound. Also, optimization of the number of factors, after increasing the size of the calibration set, for PLS regression is also recommended to further enhance the predictive capabilities of the technique described in Chapter 4.

It terms of further expanding the utility of the techniques developed, different solvents, actual lignocellulosic biomass feedstocks and industrial application all need to be considered. For the FTIR technique developed in Chapter 4, the procedure is translatable, though the developed models are not. The ease of developing an FTIR model with PLS regression makes its use for a specific solvent/cellulose system fairly routine. Since the development of the calibration set is the

most time consuming step in the development of a PLS regressed FTIR model, frequent changes of solvent would negate the time savings associated with FTIR analysis. Therefore, it is recommended that this methodology only be used in industrial applications once the solvent for the process has been decided upon. The range of cellulose wt% should be increased well above 4 wt% and dissolved lignin should be investigated to increase the utility of the models and methodology and reflect the requirements of industrial application. Furthermore, it is recommended that FTIR be used to predict cellulose content in analysis of lignocellulosic biomass composition and to monitor cellulose hydrolysis, enhancing biorefining technologies, however the use of actual lignocellulosic feedstocks cannot be implemented until prediction of dissolved lignin is benchmarked using this methodology.

As noted in Chapter 5, the optical microscopy screening method could be broadly used to determine if a solvent can dissolve cellulose or lignin independently on a variety of solvents. However, in order for this methodology to be applied in real industrial settings, the technique will need to be demonstrated on actual lignocellulosic biomass samples. First it is recommended that the dissolution of the two model biomass compounds (Avicel PH-101) and Indulin AT) be investigated together to determine if differentiation between the dissolution of the two is possible with this methodology. Secondly, lignocellulosic feedstocks with potential for use in biorefining should be investigated in order to demonstrate that this methodology can be applied beyond model biomass compounds.

Due to the ease of use of this technique, there exists potential for the automation of the screening method, which could enhance its usefulness in an industrial setting. However, the air bubbles observed in some of the micrographs in Chapter 5 will make automation more difficult. The gas bubbles were believed to originate when the cellulose or lignin was added to the microscope crucible. The gas was initially trapped within the fibrous cellulose or lignin structure and released upon dissolution. When the cellulose or lignin was not entirely dissolved, these gas bubbles were subtracted from the baseline image to approximate % observed cellulose dissolved.

Thus, it is recommended that prior to screening the solvents be degassed and/or a vacuum be applied to the temperature controlled stage during dissolution. These two modifications to the existing methodology could potentially remove the observed air bubbles.

During the screening study, it was shown that CYPHOS® 441 dissolved lignin and not cellulose. As such, this IL could be applied in lignocellulosic biomass fractionation methodologies. It is recommended that further studies be undertaken to determine the extent of lignin dissolution in CYPHOS® 441. Furthermore, dissolution of mixtures of cellulose and lignin together to determine potential for lignocellulosic biomass fractionation should be investigated. The regeneration of lignin from the IL/lignin solution, separate from cellulose, needs to be investigated to ensure that fractionation of biomass is achievable with this IL.

In Chapter 6 the effect CO_2 on the dissolution of cellulose in an IL was investigated. Future studies to further investigate the effect of temperature on the observed improvement of cellulose dissolution in an IL under a CO_2 environment are recommended. It is recommended that additional cellulose dissolution studies be conducted at room temperature (20°C) and at elevated temperatures (100°C to 120°C) to further examine how temperature may affect cellulose dissolution in an IL between CO_2 and N_2 environments. Further, CO_2 pressures up to 150 psi should be explored to determine if an optimum between pressure, temperature, energy conservation and operational safety can be achieved.

In situ rheometry studies should be undertaken to determine the real-time viscosity change of the [emim][OAc]. These studies should be both with and without CO_2 and for a range of temperatures and pressures. Additionally any changes in viscosity should be compared to cellulose dissolution (at the same temperature, gas pressure, and time) to enhance the understanding of the effect of a CO_2 environment on cellulose dissolution. Once the rheometry studies are conducted and an increased range of temperatures and CO_2 pressures are explored for their effect on the dissolution for cellulose in [emim][OAc], lignin dissolution should be investigated. Due to the complex aromatic structure of lignin, there exists a greater potential for
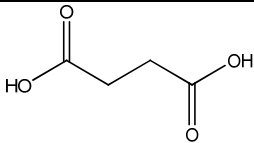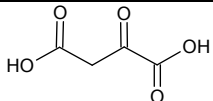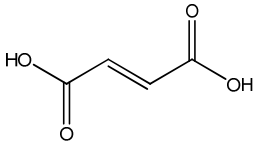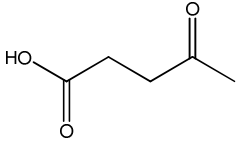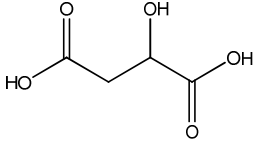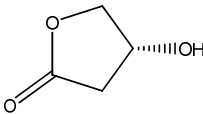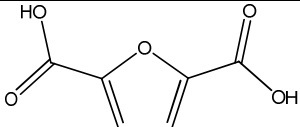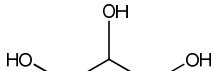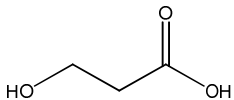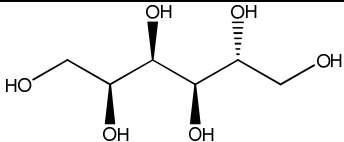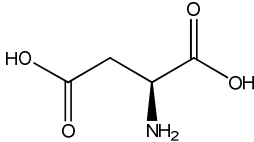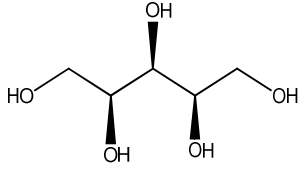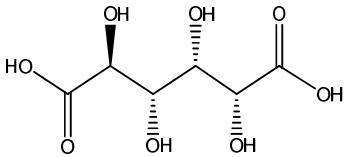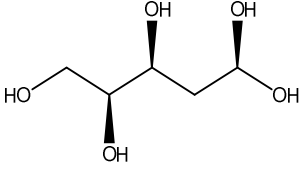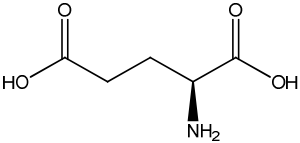
interaction with CO_2 than for cellulose. Furthermore, [emim][OAc] has been shown to dissolve lignin in greater concentrations than cellulose, potentially making the effect of CO_2 of greater importance to lignin, over cellulose, dissolution in the IL. Once the effect of CO_2 has been investigated on the dissolution on cellulose and lignin, actual lignocellulosic biomass should then be investigated to determine if this technique can potentially be applied to potential biorefinery feedstocks. However, as there are nearly limitless combinations of anions and cations to develop ILs, with a variety of complex chemical structures, CO_2 may interact differently with different ILs. As such, the methodology used to assess the effect of CO_2 on cellulose dissolution in [emim][OAc] is translatable to different solvents, but the increase in cellulose dissolution may not be observed in other solvents Additionally, a life cycle assessment of the dissolution process at different temperatures and CO_2 pressures should be conducted to fully understand any economic and /or environmental benefits of using CO_2 to enhance cellulose, and even lignocellulosic biomass feedstocks, dissolution in ILs to assess industrial applicability.

Overall, before use in industrial applications, especially for biorefining applications, the cost associated with the use of ILs will need to be reduced. This still is the major obstacle that needs to be overcome by research in this area. The necessary reduction in costs could be accomplished in many ways, such as: by decreasing the cost of IL production to far below the $1000/kg that many current production techniques cost; by recycling ILs after cellulose, and even complete lignocellulosic biomass, dissolution and regeneration; and by increasing the amount of biomass dissolved in each dissolution run. Further hindering research in the biorefining area is the high costs and time requirements associated with traditional wet chemical analysis techniques. The FTIR quantitative analysis technique has the potential to reduce the cost of analysis by an order of magnitude, which will help in the industrial adoption of not just ILs in biorefining, but the overall implementation of biorefineries. The optical microscopy screening method may offer a simple and inexpensive way to screen potential biomass solvents, aiding in research to develop novel, low-cost ILs and IL-biomass dissolution approaches. Finally, CO_2 study may offer a

potential to increase the amount of cellulose dissolved in a dissolution run and/or decrease the energy requirements, through lowered viscosity and dissolution temperature requirements, of cellulose dissolution, potentially improving the economics of the use of ILs in a biorefinery context. The developments in this thesis can be used to further research efforts towards lowering the cost of using ILs, and other potential solvents, in a biorefinery context.

Appendix A - Qualitative ATR FTIR Analysis

Table A.1: The structure of the DOE's top twelve building block chemicals.

Building Block Chemicals	Structure	Building Block Chemicals	Structure
1,4 diacids (succinic, fumaric and malic)	1,4 succinic acid fumaric acid malic acid	itaconic acid	
		levulinic acid	
		3-hydroxybutyrolactone	
2,5 furan dicarboxylic acid		glycerol	
3 hydroxy propionic acid		sorbitol	
aspartic acid		xylitol/arabinitol	xylitol arabinitol
glucaric acid			
glutamic acid			

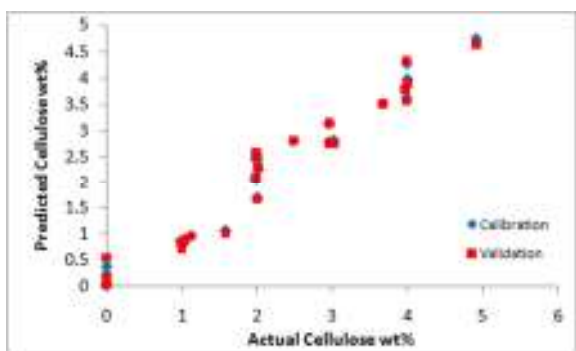# Appendix B - Qualitative ATR FTIR Analysis

a)

b)

c)

d)
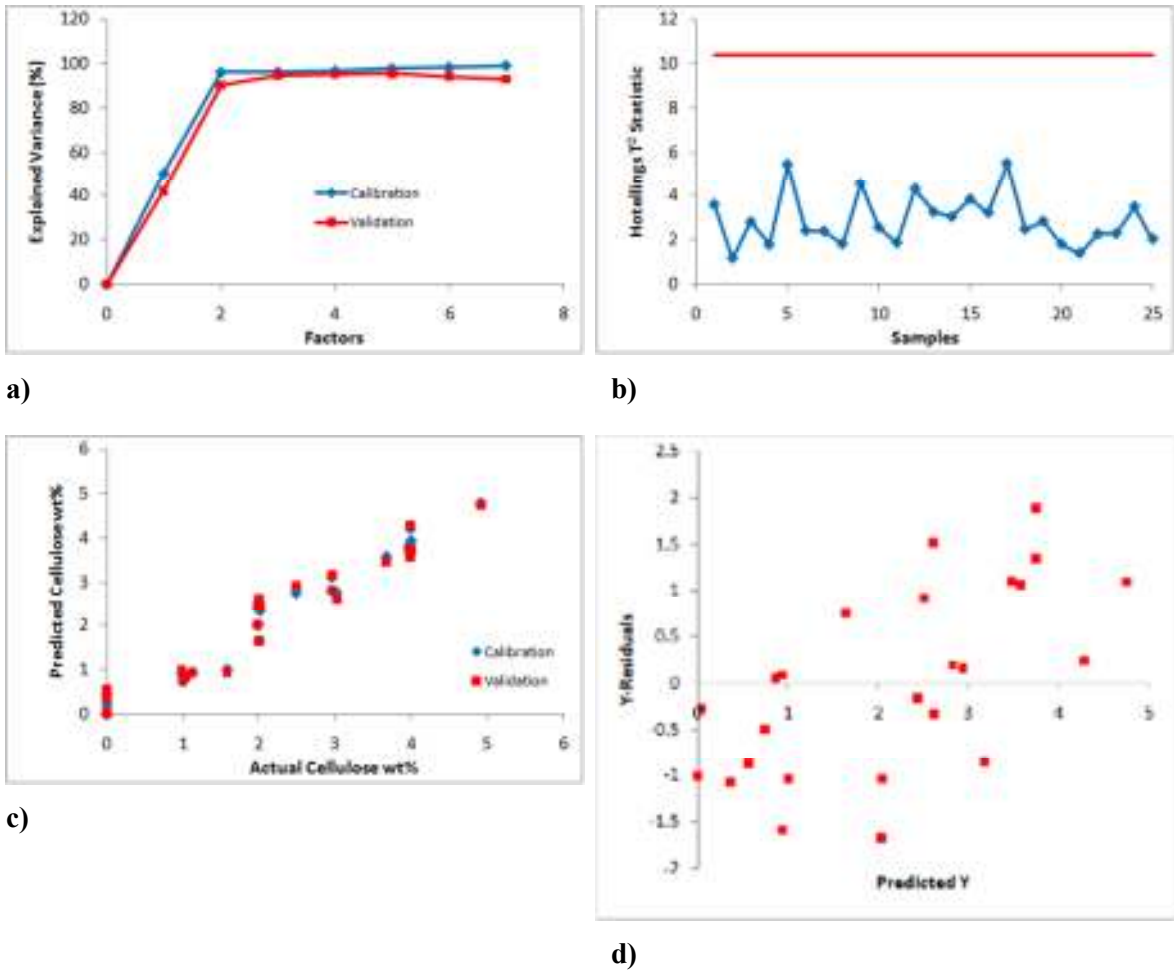
Figure B.1: Diagnostics for the untreated PLS model: a) explained variance (%), b) Hotelling T^2 statistic, c) predicted vs. actual cellulose wt%, d) Y-residuals vs. predicted Y.
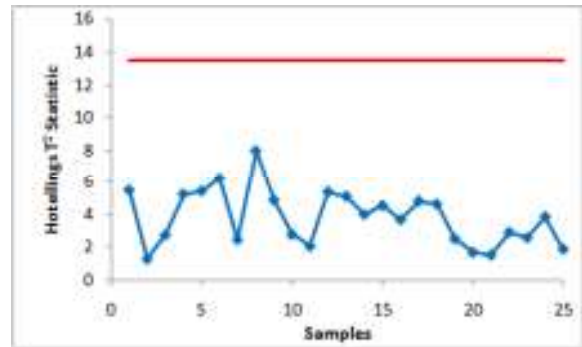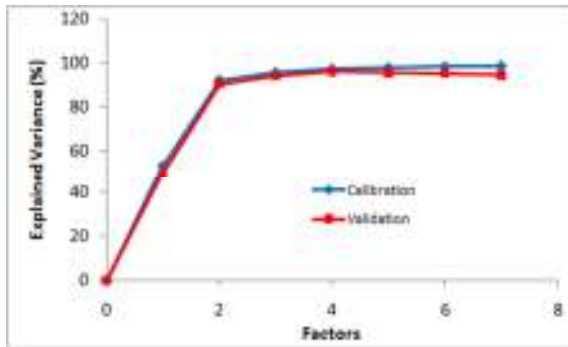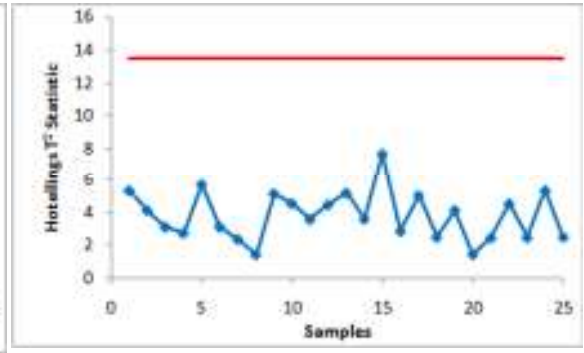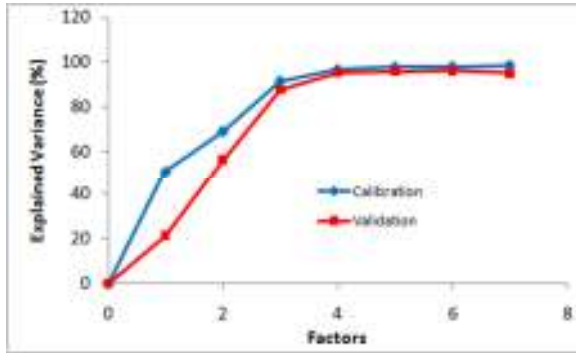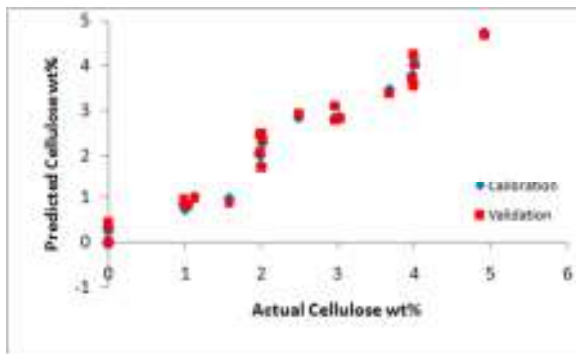
a)

b)
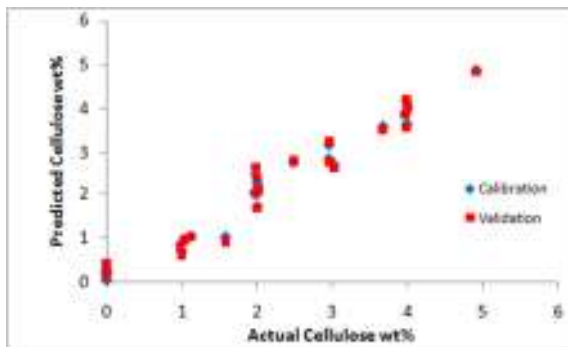
c)
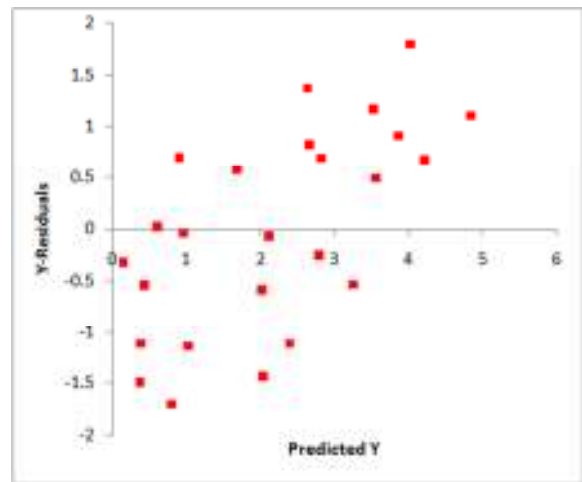
d)

Figure B.2: Diagnostics for the Savitzky-Golay differentiation - 1st derivative PLS model: a) explained variance (%), b) Hotelling T^2 statistic, c) predicted vs. actual cellulose wt%, d) Y-residuals vs. predicted Y.
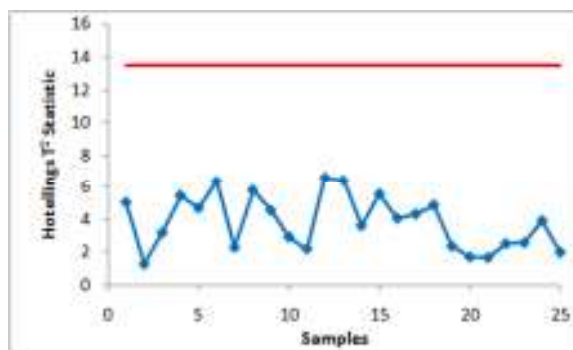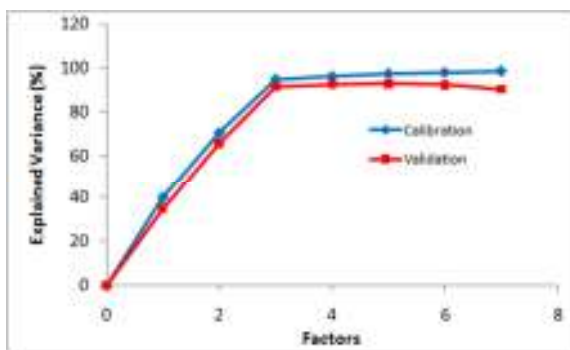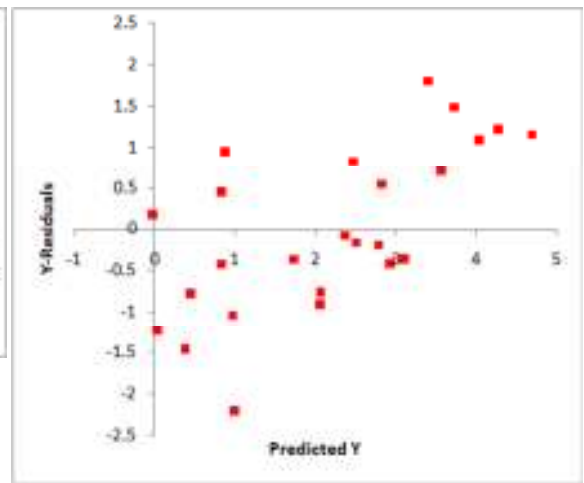
a)

b)
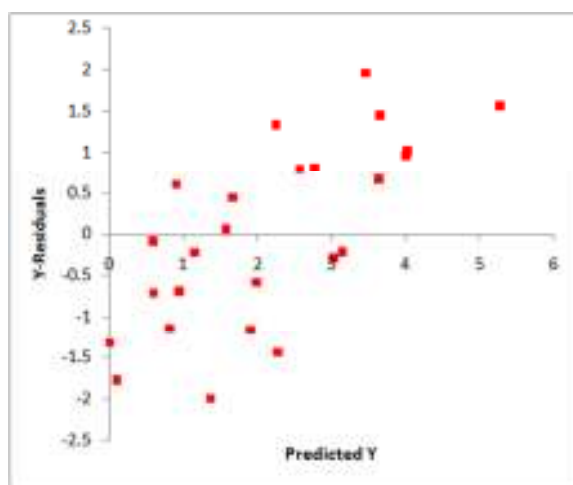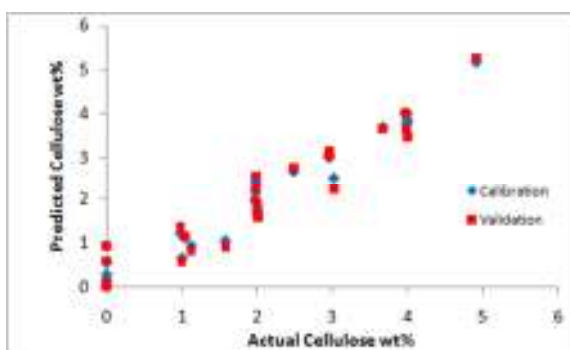
c)

d)

Figure B.3: Diagnostics for the Savitzky-Golay differentiation - 2nd derivative PLS model: a) explained variance (%), b) Hotelling T^2 statistic, c) predicted vs. actual cellulose wt%, d) Y-residuals vs. predicted Y.

a)

b)

c)

d)
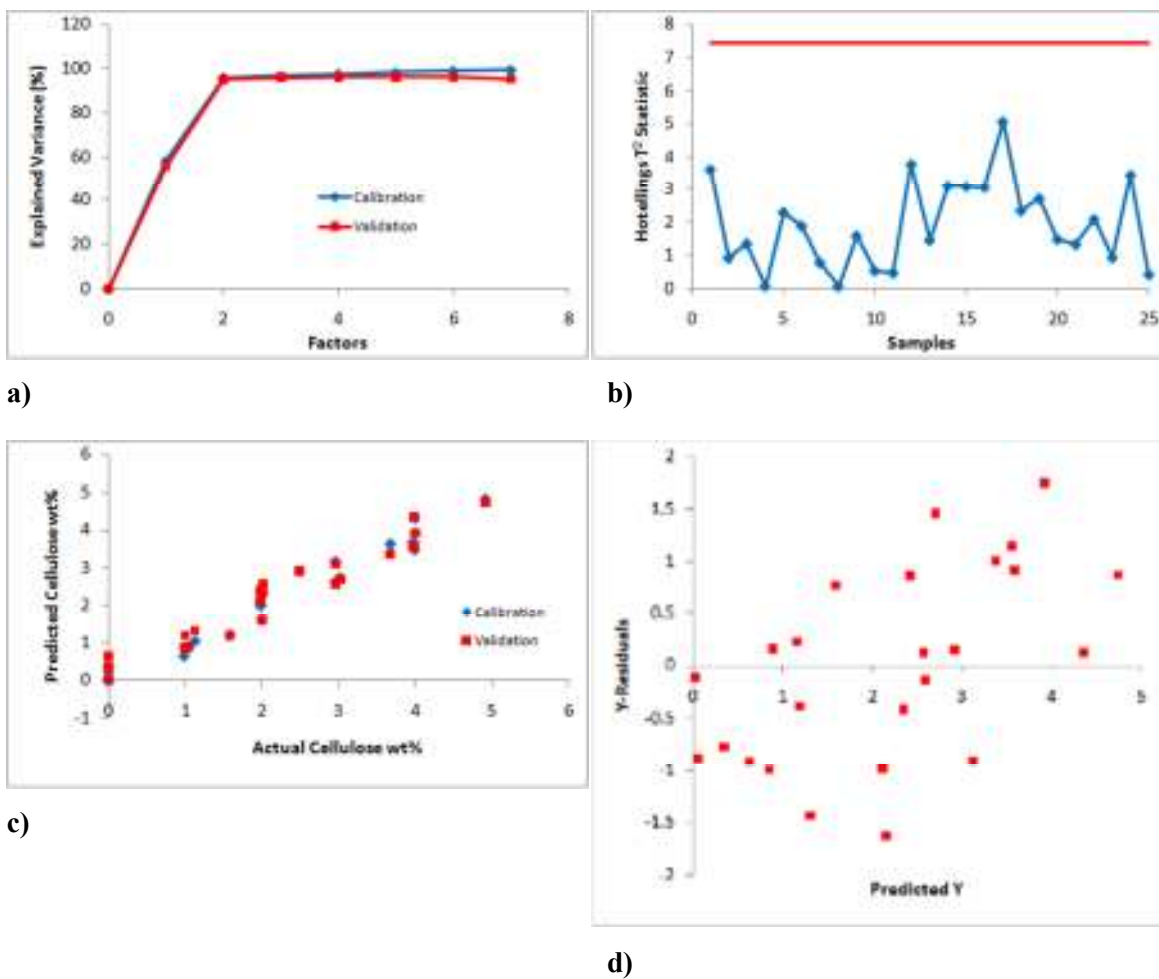
Figure B.4: Diagnostics for the MSC PLS model: a) explained variance (%), b) Hotelling T^2 statistic, c) predicted vs. actual cellulose wt%, d) Y-residuals vs. predicted Y.
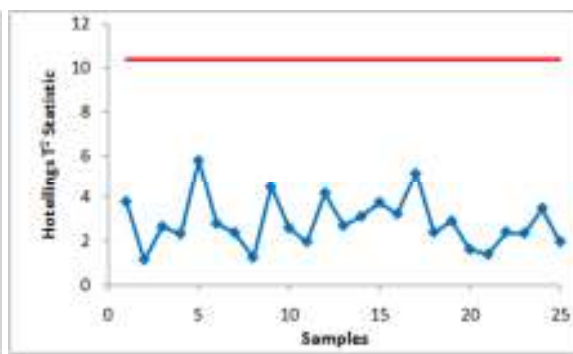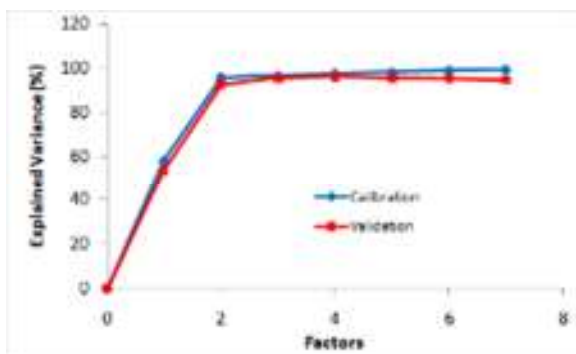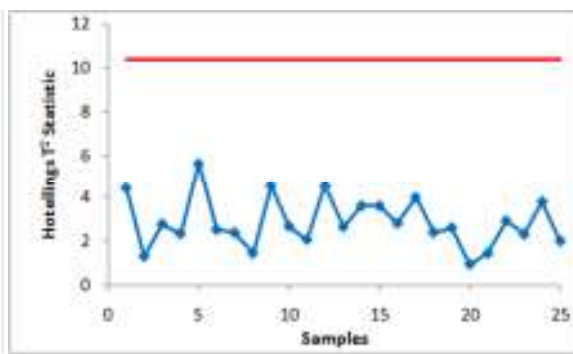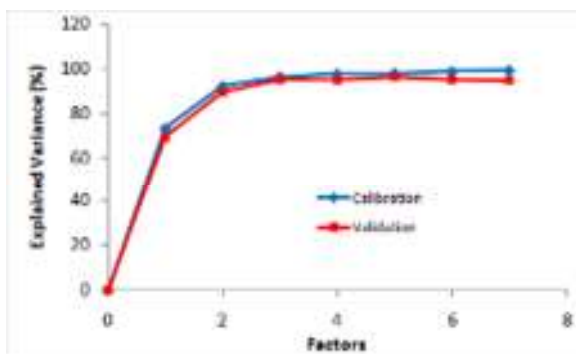
a)

b)
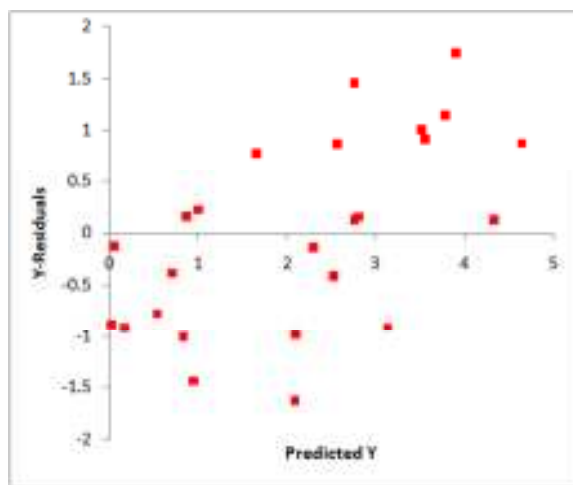
c)

d)

Figure B.5: Diagnostics for the SNV PLS model: a) explained variance (%), b) Hotelling T^2 statistic, c) predicted vs. actual cellulose wt%, d) Y-residuals vs. predicted Y.
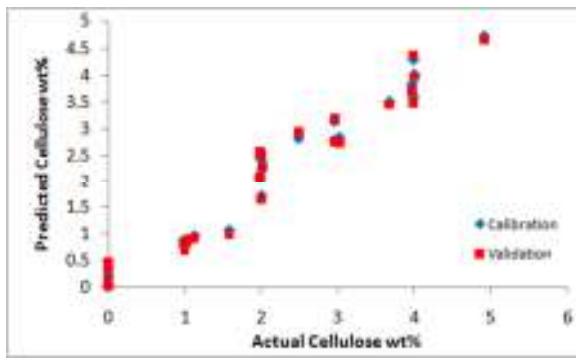
a)

b)

c)

d)

Figure B.6: Diagnostics for the baseline correction PLS model: a) explained variance (%), b) Hotelling T^2 statistic, c) predicted vs. actual cellulose wt%, d) Y-residuals vs. predicted Y.
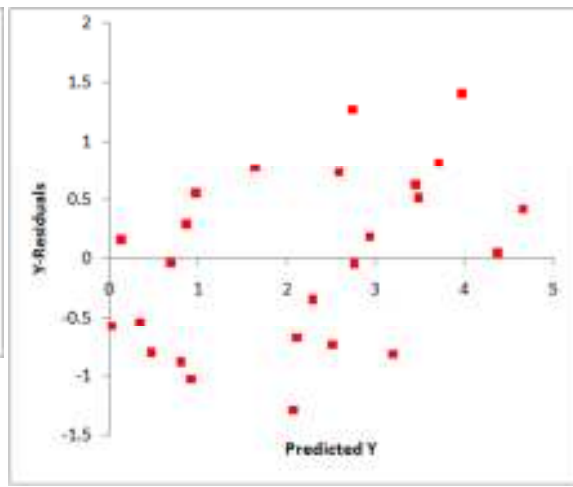
Figure B.7: Diagnostics for the detrending PLS model: a) explained variance (%), b) Hotelling T^2 statistic, c) predicted vs. actual cellulose wt%, d) Y-residuals vs. predicted Y.
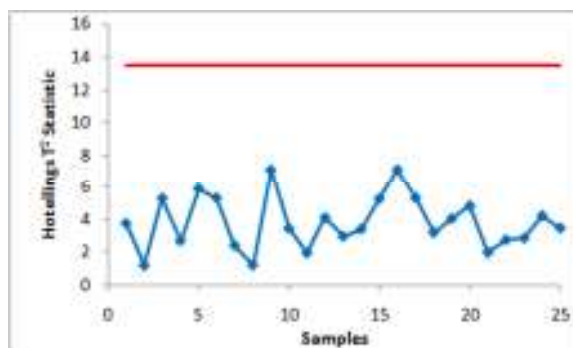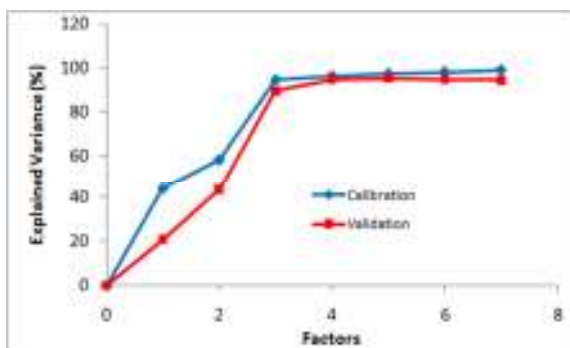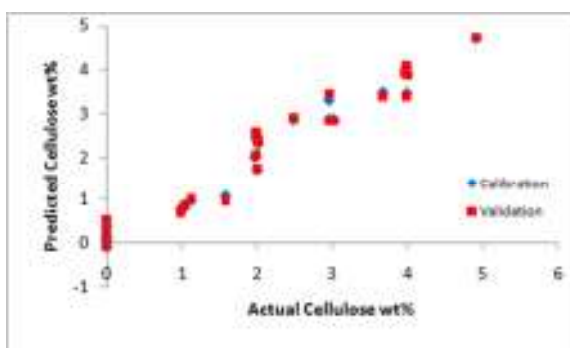
a)

b)

c)

d)

Figure B.8: Diagnostics for the normalized PLS model: a) explained variance (%), b) Hotelling T^2 statistic, c) predicted vs. actual cellulose wt%, d) Y-residuals vs. predicted Y.

a)

b)

c)

d)

Figure B.9: Diagnostics for the SNV-detrending PLS model: a) explained variance (%), b) Hotelling T^2 statistic, c) predicted vs. actual cellulose wt%, d) Y-residuals vs. predicted Y.
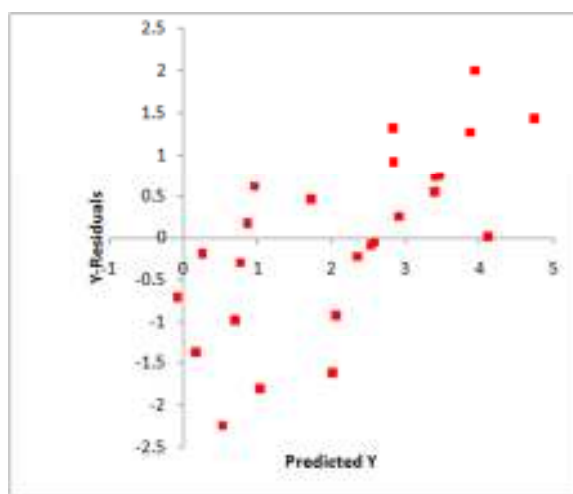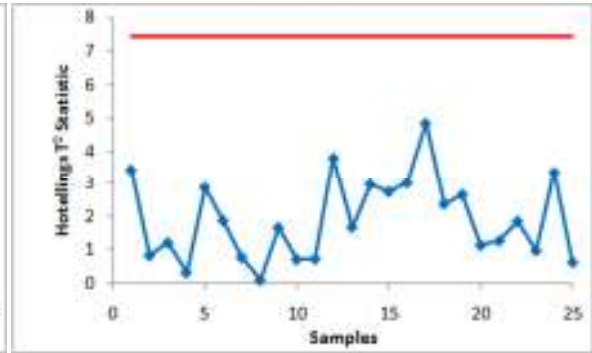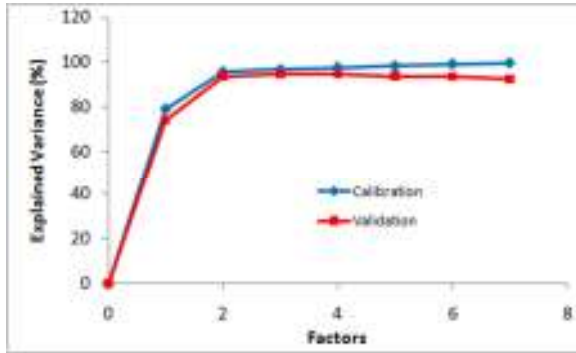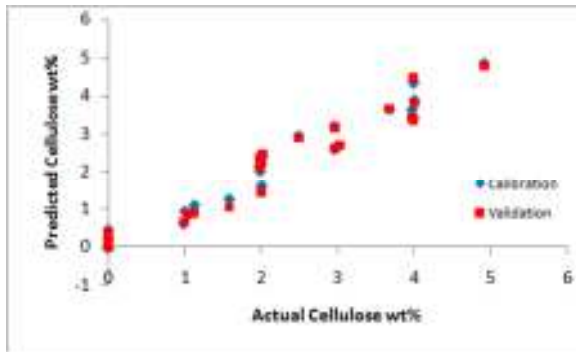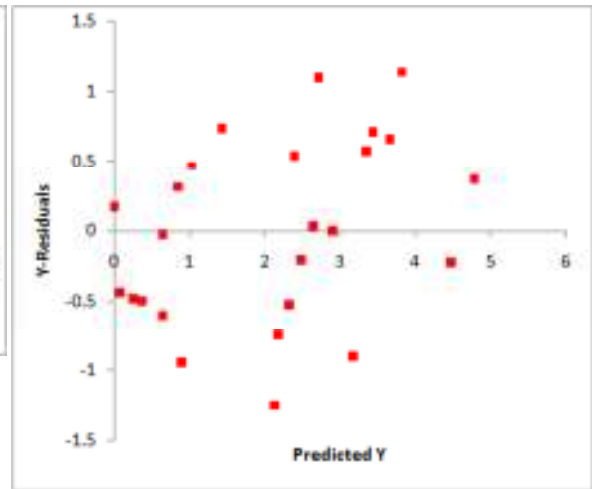
Appendix C - Cellulose Dissolution Experiments for the CO_2 Study

Table C.1: Cellulose dissolution experiments at 75°C for 3, 12, and 24 hours under either 20 psi N_2 or 50 psi CO_2.

Temp. (°C)	Environment	Time (hrs)	% Cellulose Dissolved
50	20 psi N_2	3	28.7
50	20 psi N_2	3	16.1
50	20 psi N_2	3	17.2
50	20 psi N_2	12	43.8
50	20 psi N_2	12	24.4
50	20 psi N_2	12	40.8
50	20 psi N_2	24	43.5
50	20 psi N_2	24	38.8
50	20 psi N_2	24	33.0
50	50 psi CO_2	3	19.1
50	50 psi CO_2	3	12.3
50	50 psi CO_2	3	10.0
50	50 psi CO_2	12	44.0
50	50 psi CO_2	12	28.6
50	50 psi CO_2	12	33.9
50	50 psi CO_2	24	68.0
50	50 psi CO_2	24	69.7
50	50 psi CO_2	24	62.4

Table C.2: Cellulose dissolution experiments at 75°C for 3, 12, and 24 hours under either 20 psi N_2 or 50 psi CO_2.

Temp. (°C)	Environment	Time (hrs)	% Cellulose Dissolved
75	20 psi N_2	0.5	11.7
75	20 psi N_2	0.5	12.2
75	20 psi N_2	0.5	9.4
75	20 psi N_2	3	46.0
75	20 psi N_2	3	46.0
75	20 psi N_2	3	39.8
75	20 psi N_2	12	81.0
75	20 psi N_2	12	67.3
75	20 psi N_2	12	89.3
75	20 psi N_2	24	91.1
75	20 psi N_2	24	92.6
75	20 psi N_2	24	91.8
75	50 psi CO_2	0.5	13.7
75	50 psi CO_2	0.5	20.1
75	50 psi CO_2	0.5	19.2
75	50 psi CO_2	3	51.1
75	50 psi CO_2	3	65.0
75	50 psi CO_2	3	58.3
75	50 psi CO_2	12	86.3
75	50 psi CO_2	12	98.3
75	50 psi CO_2	12	80.4
75	50 psi CO_2	24	104.7
75	50 psi CO_2	24	100.2
75	50 psi CO_2	24	98.5

Appendix D - Dinitrosalicylic Acid (DNS) Assay

D.1 Preparation

To prepare the 1% DNS assay solution the following were added to 1L of water:

- 10g dinitrosalicylic acid
- 2g phenol
- 0.5g sodium sulfite
- 10g sodium hydroxide

To prepare the 40% potassium sodium tartrate solution the following was added to 100mL of water:

- 40g potassium sodium tartrate

D.2 Procedure

1. The DNS assay was performed on the 10:1 (water:IL) solution, which was preserved after cellulose regeneration and initial filtration (Dilution A). 1mL of the 10:1 solution was diluted into 3mL distilled water (Dilution B) to ensure that if all the added cellulose had been hydrolyzed to glucose, the resulting concentration of glucose to be used in the DNS assay would not exceed 1g/L, the maximum concentration at which this assay will reliably work.

2. 3mL of the 1% DNS assay solution were added to 3mL of Dilution B. This solution was allowed to boil for 7 minutes. After 7 minutes, 1mL of the 40% potassium sodium tartrate solution was added and the solution was allowed to cool in room temperature water.

3. Once cooled, the absorbance at 540 nm was recorded with a UV spectrophotometer

D.3 Results

Table D.1: Summary of DNS assay results.

Sample	Absorbance (at 540 nm)	Glucose Concentration $(g/L)^{\dagger}$
0.5hrs - CO_2	0.142	<0.1
0.5hrs - N_2	0.143	<0.1
3hrs - CO_2	0.145	<0.1
3hrs - N_2	0.144	<0.1
24hrs - CO_2	0.149	<0.1
24hrs - N_2	0.149	<0.1

†The detection limits of the assay is 0.1g/L

Appendix E - Cellulose Dissolution Results for the CO_2 Study

Table E.1: Summary of 4 wt% cellulose dissolution experiments in [emim][OAc] under either 20 psi N2 or 50 psi CO2 environments.

Temperature (°C)	Environment	Time (hrs)	% Cellulose Dissolved
50	20 psi N_2	3	20.7 ±7.9
50	20 psi N_2	12	36.3 ±11.9
50	20 psi N_2	24	38.4 ±5.9
50	50 psi CO_2	3	13.8 ±5.4
50	50 psi CO_2	12	35.5 ±8.9
50	50 psi CO_2	24	66.7 ±4.3
75	20 psi N_2	0.5	11.1 ±1.7
75	20 psi N_2	3	44.0 ±4.1
75	20 psi N_2	12	79.2 ±12.6
75	20 psi N_2	24	91.9 ±1.3
75	50 psi CO_2	0.5	17.7 ±3.9
75	50 psi CO_2	3	58.1 ±7.9
75	50 psi CO_2	12	92.3 ±9.7
75	50 psi CO_2	24	100 (±3.6)